4th ISAMAP

4th International Symposium on Advanced Materials in Asia-Pacific Rim (Nihonkai Polymer Workshop)

Program & Abstracts

July 13-15, 2007

Niigata Convention Center (TOKI MESSE), Niigata, Japan

The 4th International Symposium on

Advanced Materials

in Asia-Pacific Rim

[4th ISAMAP]

July 13-15, 2007

TOKI MESSE, NIIGATA, JAPAN

Preface

Dear Distinguished Participants:

It is our great pleasure to welcome you to the 4th International Symposium on Advanced Materials in Asia-Pacific Rim(4th ISAMAP in Niigata). We believe that this 4th symposium will set the stage for successful continuation of ISAMAP.

The ISAMAP was founded in 2004 by Prof. Kawakami, the present president of the Society of Polymer Science, Japan, Hokuriku Branch. The aim is not only to discuss scientific results on advanced materials and technology, but also to expand and strengthen cooperation in research and education between scientists, especially young scientists and engineers including students in Asia-Pacific region. The 1st ISAMAP was held in 2004 at Japan Advanced Institute of Science and Technology (JAIST), Ishikawa, Japan, the 2nd ISAMAP was held in Hanoi by Prof. Nguyen Van Noi from Hanoi University of Science, Vietnam, in 2005, and the 3rd was held by Prof. Chang-Sik Ha from Pusan National University at Ulsan, Korea in 2006 where 22 oral and 69 poster presentations were given by around 90 scientists from Korea, Japan, Vietnam, China, and so on.

In this coming 4th symposium held in Niigata city which has recently been designated by government ordinance, 27 oral presentations including 13 lectures by scientists and students from overseas countries and 125 poster presentations will be delivered. More than 170 scientists (the number of pre-registered scientists is 170) will participate in this symposium from more than 11 countries such as Japan, Korea, China, Vietnam, Thailand, Egypt, Indonesia, Myanmar, Malaysia, Bangladesh, Mexico, and so on. The oral presentations contain a plenary lecture by President Yoshida from JSR Company, Japan. The 4th ISAMAP is co-organized by the Society of Polymer Science, Japan(SPSJ), Hokuriku Branch; Center for Education and Research on Environmental Technology, Materials Engineering, and Nanochemistry, Niigata University; Center for Transdisciplinary Research, Niigata University; the Advanced Nano Membrane of Niigata; and JAIST. The symposium venue of 4th ISAMAP is the Niigata convention center(Toki Messe) located at the mouth of Shinano River which is the longest one in Japan.

We wish you all have an enjoyable and productive stay in Niigata city and good opportunity to find or deepen friendship between scientists from different countries.

This symposium was given much financial supports from JAIST, SPSJ, Niigata University, the Uchida Energy Science Promotion Foundation, Niigata city, the Intelligent Cosmos Academic Foundation, Varian Inc, and so on. We would like to express our sincere appreciation and gratitude for the financial support to these organizations.

Thank you,

Professor Toshiki Aoki, Chairman of 4th ISAMAP
Niigata University

Organization / Sponsorship

International organizing committee

Prof. Toshiki Aoki, Niigata University, Japan: Chairman
Prof. Yusuke Kawakami, JAIST, Japan
Prof. Nguyen Van Noi, Hanoi University of Science, Vietnam National University, Vietnam
Prof. Chang-Sik Ha, Pusan National University, Korea
Prof. Tiesheng Li, Zhengzhou University, China
Prof. Supawan Tantayanon, Chulalongkorn University , Thailand

Local organizing committee

Prof. Toshiki Aoki, Niigata University: Chairman
Prof. Yusuke Kawakami, JAIST
Prof. Hiromi Kitano, University of Toyama
Prof. Norio Tsubokawa, Niigata University
Prof. Mineo Sato, Niigata University
Prof. Takaomi Kobayashi, Nagaoka University of Technology
Prof. Takashi Kaneko, Niigata University
Prof. Takeshi Yamauchi, Niigata University
Prof. Masayuki Yagi, Niigata University
Prof. Ken-ichi Shinohara, JAIST

General Secretary

Prof. Masahiro Teraguchi, Niigata University

Supporting Organizations

Center for Transdisciplinary Research, Niigata University
The Society of Polymer Science, Japan, Hokuriku Branch
The Society of Polymer Science, Japan
The Advanced Nano Membrane of Niigata
Japan Advanced Institute of Science and Technology (JAIST)

Scope / General Information

The following subjects are going to be the main topics in ISAMAP 2007.

1. Polymers as Advanced Materials
2. Nanostructured Materials
3. Advanced Metals or Inorganic Materials
4. Nanoparticles and Nanocomposites
5. Advanced Applications of Materials
6. Composites and Hybrids Materials; Interface and Processing
7. Special Topics

Presentations and Proceedings

Language

English is the official language for the symposium. No simultaneous translation facilities will be provided.

Oral Presentation

Plenary Lecture:	60 minutes including discussion
Invited Lecture	30 minutes including discussion
Oral Lecture	15 minutes including discussion

The oral session will be held at Room 1. The session room is equipped with LCD projector and personal computer as well as microphone and a laser pointer.

Poster Presentation

Poster session will be held at Room 2 and the 3rd floor Lobby on July 14 (Sat). The space available for each poster is 120 cm width and 240 cm height.

Poster Session Schedule

Set up: 8:00 – 11:30, Removal: 16:30 – 17:30

Obligation time:

Session A: 12:45 – 13:15, Session B: 13:15 – 13:45, Session C: 16:00 – 16:30

General Information

Venue

Toki Messe, Niigata Convention Center
Bandaijima 6-1, Niigata, Japan
Tel: +81-25-246-8400
Fax: +81-25-246-8411

Registration

Registration desk is open during the following hours:

July 13 (Fri) 18:30 – 20:00 (Hotel Nikko Niigata 30F)
July 14 (Sat) 8:00 –19:00 (Convention Center 3F Lobby)

		Until July 5, 2007	From July 6, 2007
Registration Fee	Regular Participants	JPY 10,000	JPY 15,000
	Student	JPY 3,000	JPY 4,500
	Accompanying Person	JPY 0	JPY 0
Welcome Reception		JPY 4,000	JPY -----
Banquet		JPY 6,000	JPY -----
Post-symposium Tour		JPY 8,500	JPY -----

Registration fee for regular participants and student includes admission to all oral and poster sessions; abstract book; coffee breaks.

Social Program

Welcome Reception

Date: July 13 (Fri)
Time: 19:30 – 20:30
Place: Hotel Nikko Niigata 30F

Banquet

Date: July 14(Sat)
Time: 19:00 – 21:00
Place Hotel Nikko Niigata 30F

Access Map to Toki Messe

Floor Guide (Toki Messe/Hotel Nikko)

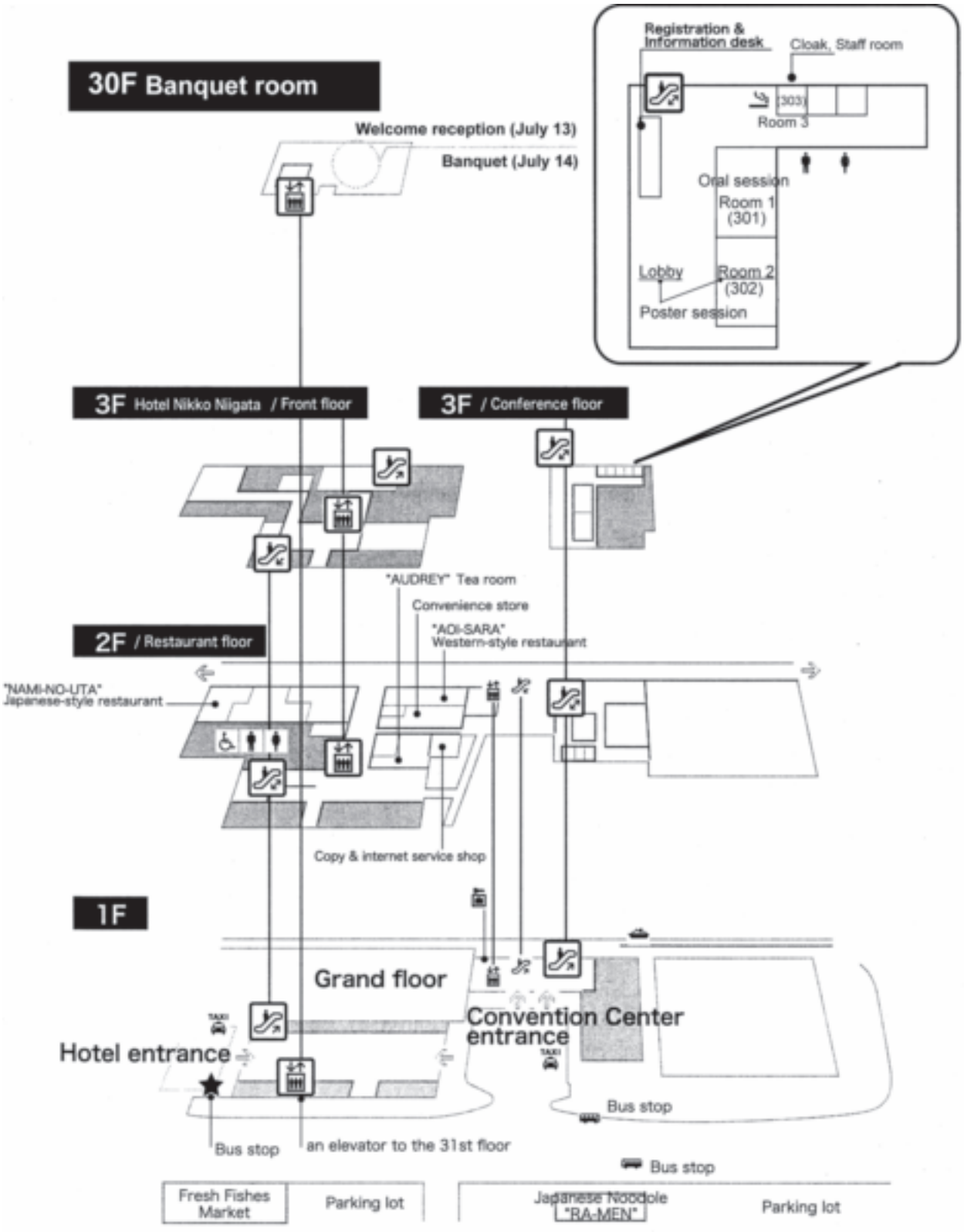

Program

PL: Plenary Lectures: 60 minutes including discussion

I L: Invited Lectures: 30 minutes including discussion

OL: Oral Lectures: 15 minutes including discussion

Poster Session Schedule on July 14(Sat), 2007

Set up: 8:00-11:30, Removal: 16:30-17:30

Obligation time * The end letter of the Poster codes means the Poster Session code.

Session A: 12:45 - 13:15, Session B: 13:15 - 13:45, Session C: 16:00 - 16:30

July 13 (Fri), 2007

18:30 - 20:00	**Registration** (Hotel Nikko Niigata 30F)
19:30 - 20:30	**Welcome Reception** (Hotel Nikko Niigata 30F)

July 14 (Sat), 2007

8:00 - 19:00		**Registration** (Convention Center 3F Lobby)	
8:45 - 09:00		**Opening Ceremony** (Convention Center 3F Room 1) Prof. Yusuke Kawakami (Founder of ISAMAP, JAIST, Japan) & Prof. Toshiki Aoki (Chairman of 4th ISAMAP, Niigata University, Japan)	
Plenary Lecture (Convention Center 3F Room 1) Chair: Prof. Yusuke Kawakami (Japan Advanced Institute of Science and Technology, Japan)			
9:00 - 10:00	PL01	**Globalization of JSR Advanced Materials Business** Yoshinori Yoshida (President of JSR Corporation, Japan)	1
Oral Session 1 10:00-11:30 (Convention Center 3F Room 1) Cochair: Prof. Chang-Sik Ha (Pusan National University, Korea) & Prof. Takashi Kaneko (Niigata University, Japan)			
10:00 - 10:30	IL01	**A Mechanistic Consideration on the Formation of Cage-type POSS Derivatives** Yusuke Kawakami (Japan Advanced Institute of Science and Technology, Japan)	3
10:30 - 11:00	IL02	**Synthesis of a Novel POSS-based Material Having Carbazole, and Its Thermal, Electrochemical and Optical Properties** Ichiro Imae (Hiroshima University, Japan)	4
11:00 - 11:15	OL01	**Effects of Dendritic Silsesquioxane on Performance of Holographic Gratings Based on Photopolymer Film** Hoque Md. Asadul, Yeong Hee CHO, and Yusuke Kawakami* (Japan Advanced Institute of Science and Technology, Japan)	5

11:15 - 11:30	OL02	**Novel Holographic Polymer Dispersed Liquid Crystals Formed with Accelarated Multifunctional Acrylates Containing Siloxane Network** Yeong Hee CHO, Go Suzuki, and Yusuke Kawakami* (Japan Advanced Institute of Science and Technology, Japan)	7
11:30 - 12:45	Lunch		
Poster Sessions 12:45-13:45 (Convention Center 3F Room 2 & Lobby)			
12:45 - 13:15	**Poster Session A**		
13:15 - 13:45	**Poster Session B**		
Oral Session 2 13:45-15:30 (Convention Center 3F Room 1) Cochair: Prof. Tiesheng Li (Zhengzhou University, China) & Prof. Toshiki Aoki (Niigata University, Japan)			
13:45 - 14:15	IL03	**Development of Catalytic Composites for Removal of Hazardous Compounds from Water** Nguyen Van Noi, Tran Thi Nhu Mai, and Bui Quynh Trang (Hanoi University of Science, Vietnam)	9
14:15 - 14:45	IL04	**Design and Synthesis of Fluoroionophores and Surface-based Sensors for the Detection of Lithium and Ammonium Ions** Nantanit Wanichacheva[1], Christopher R. Lambert[2], and W. Grant McGimpsey[2]* ([1]Silpakorn University, Thailand and [2]Worcester Polytechnic Institute, USA)	11
14:45 - 15:15	IL05	**Gas Transport Properties of Polyimide Ultrathin Membranes** Hiroyoshi Kawakami (Tokyo Metropolitan University, Japan)	15
15:15 - 15:30	OL03	**Synthesis and Gas Permeation Properties of Poly(diphenylacetylene) Derivatives** Toshikazu Sakaguchi[1],* Toshio Masuda[2], and Tamotsu Hashimoto[1] ([1]University of Fukui and [2]Kyoto University, Japan)	19
Coffee Break & Poster Session 15:30-16:30 (Convention Center 3F Room 2 & Lobby)			
15:30 – 16:00	**Coffee Break**		
16:00 - 16:30	**Poster Session C**		
Oral Session 3 16:30-18:45 (Convention Center 3F Room 1) Cochair: Prof. Nguyen Van Noi (Hanoi University of Science, Vietnam) & Prof. Masahiro Teraguchi (Niigata University, Japan)			
16:30 - 17:00	IL06	**Intramolecular Cyclisation of Enamide Derivatives and Synthesis of Pyrrolidine *trans*-Lactams** Anawat Ajavakom (Chulalongkorn University, Thailand)	21
17:00 - 17:30	IL07	**Development of Novel Polymer-supported Chiral Ligand for Asymmetric Reactions** Shinichi Itsuno,* Yukihiro Arakawa, Atsuko Chiba, Keiichi Tsuru, and Naoki Haraguchi (Toyohashi University of Technology, Japan)	23

17:30 - 18:00	IL08	**Synthesis and Applications of (Nitrilotriacetic Acid)- end-functionalized Polystyrene** Su-jeong Kim, Hyo Kyoung Lee, Ji-Yeon Lee, Hong Y. Cho, Yu Jin Kim, Sun-Gu Lee, and Hyun-jong Paik* (Pusan National University, Korea)	27
18:00 - 18:15	OL04	**Grafting of Vinyl Polymers onto Silica Nanoparticles Surface in Solvent-free Dry-system** Jun Ueda[1], Kazuhiro Fujiki[2], Takeshi Yamauchi[1], and Norio Tsubokawa[1]* ([1]Niigata University and [2]Joetsu University of Education, Japan)	28
18:15 - 18:30	OL05	**Colloidal Crystallization of Colloidal Silica Modified with Iron(0) Complex-grafted Polymer in Organic Solvent** Kohji Yoshinaga,* Mahiro Nakano, and Emiko Mouri (Kyushu Institute of Technology, Japan)	29
18:30 - 18:45	OL06	**Amphiphilic Dendron-modified Silica Particles: Synthesis, Characterization, and Application on Organic Dye Adsorption in Water** Chih-Chien Chu* and Toyoko Imae (Keio University, Japan)	30
Banquet 19:00 - 21:00 (Hotel Nikko Niigata 30F)			

July 15 (Sun), 2007

Oral Session 4 8:00-10:00 (Convention Center 3F Room 1) Cochair: Prof. Hyun-jong Paik (Pusan National University, Korea) & Prof. Takaomi Kobayashi(Nagaoka University of Technology, Japan)			
8:00 - 8:15	OL07	**Capacitively Coupled Air Plasma Etching of Polycarbonate** J. K. Kim, Y. W. Joo, Y. H. Park, G. S. Cho, H. J. Song, and J. W. Lee* (Inje University, Korea)	33
8:15 - 8:30	OL08	**Capacitively Coupled O_2/N_2 RF Plasma Etching of Polymethyl methacrylate (PMMA)** Y. H. Park, J. K. Kim, Y.W. Joo, J. H. Lee, G. S. Cho, and J. W. Lee* (Inje University, Korea)	34
8:30 - 8:45	OL09	**A Thermochemical Two-step Water Splitting Cycle with Magnetite-coated Ceramic Foam Device** Ayumi Nagasaki, Koichi Sakai, Nobuyuki Gokon, and Tatsuya Kodama* (Niigata University, Japan)	35
8:45 - 9:00	OL10	**Processing of High Temperature Superconducting Bulk Materials and Their Application to Strong Magnetic Field Generators** Tetsuo Oka,* Yutaka Hirose, Hayato Kanayama, Hokuto Kikuchi, Satoshi Fukui, Jun Ogawa, Takao Sato, and Mitsugi Yamaguchi (Niigata University, Japan)	36
9:00 - 9:30	IL09	**Synthesis of the Liquid Silicon and Its Application for a Thin Film Transistor** Tatsuya Shimoda (Japan Advanced Institute of Science and Technology, Japan)	37
9:30 - 10:00	IL10	**Studies and Application of Ultrathin Films** Tiesheng Li,* Wnjian Xu, Bing Mu, Luyan Mao, Suhua Zhang, and Yangjie Wu* (Zhengzhou University, China)	39

Coffee Break 10:00 - 10:30 (Convention Center 3F Lobby)			
Oral Session 5 10:30-12:30 (Convention Center 3F Room 1) Cochair: Prof. Ichiro Imae (Hiroshima University, Japan) & Prof. Masayuki Yagi (Niigata University, Japan)			
10:30 – 11:00	IL11	**Controlled Synthesis of Nanostructured ZnS by Soft-solution Processing and Its Application to Polymer Hybrid Materials** Md. Habib Ullah and Chang-Sik Ha* (Pusan National University, Korea)	41
11:00 - 11:30	IL12	**Effect of Silane-modification of Clay on the Mechanical Properties of Poly(L-lactide)/Clay Composites** Jin San Yoon (Inha University, Korea)	45
11:30 - 11:45	OL11	**Facil Synthesis of Free-standing PMO Films with Amorphous and Crystal-like Wall Structure** Sung Soo Park and Chang-Sik Ha* (Pusan National University, Korea)	47
11:45 - 12:00	OL12	**Preparation of Hybrid Material of Polymer-grafted Carbon Micro-coils and Thermo-sensitive Polymer Gel** Takeshi Yamauchi[1], Shigenori Sato[1], Norio Tsubokawa[1], Kenji Kawabe[2], Yukio Hishikawa[2], and Seiji Motojima[3] ([1]Niigata University, [2]CMC Technology Development Co. Ltd., [3]Gifu University, Japan)	49
12:00 - 12:15	OL13	**Dielectric Study of Miscibility in Polymer Blends** Kazunori Se* and Ryuusuke Shimaguchi (University of Fukui, Japan)	50
12:15 - 12:30	OL14	**Crosslinking Points of Natural Rubber Vulcanizates** Seiichi Kawahara,* Jinta Ukawa, and Yoshimasa Yamamoto (Nagaoka University of Technology, Japan)	51
Closing Remarks 12:30 - 12:45 (Convention Center 3F Room 1) Prof. Toshiki Aoki (Chairman of 4th ISAMAP, Niigata University, Japan) & Prof. Tiesheng Li (Chairman of 5th ISAMAP, Zhengzhou University, China)			

Organizing Committee Member ONLY

12:45 - 13:45	**Organizing Committee Meeting** (Convention Center 3F Room 3)

Poster Session

Poster Session Schedule on July 14(Sat), 2007

Set up: 8:00-11:30, Removal: 16:30-17:30

Obligation time

Session A: 12:45 - 13:15, Session B: 13:15 - 13:45, Session C: 16:00 - 16:30

↓ ***The end letters (A, B, C) of the Poster codes mean the Poster Session code.***

P001A pH-Sensitive Thin Films Containing Carboxyl-terminated Poly(amido amine) Dendrimer
Shigeru Tomita, Katsuhiko Sato, and Jun-ichi Anzai*(Tohoku University, Japan)*

P002B Preparation of Layer-by-Layer Assemblies Containing Insulin
Shigehiro Takahashi, Kentaro Yoshida, Hiroshi Sato, and Jun-ichi Anzai**(Tohoku University, Japan)*

P003C pH-Triggered Release of Insulin from Layer-by-Layer Assemblies
Kentaro Yoshida* and Jun-ichi Anzai*(Tohoku University, Japan)*

P004A Preparation of Novel Sulfonated Block Copolyimides for Proton Conductivity Membranes
Kouta Yamazaki, Shoji Nagaoka, and Hiroyoshi Kawakami *(Tokyo Metropolitan University, Japan)*

P005B Gas Transport Properties of a Novel Organic-inorganic Hybrid Membrane by Plasma Based Ion Implantation
D.Muraoka[1], T.Tezuka[1], S.Nagaoka[1], Y.Suzuki[2], T.Kobayashi[2], and H.Kawakami[1]
([1]Tokyo Metropolitan University, Japan; [2]The Institute of Physical and Chemical Research, Japan)

P006C Tocopherol Targeted-hybrid Moleculary Imprinting Applied as Membrane Adsorbents
Che Ku Mohammad Faizal and Takaomi Kobayashi**(Nagaoka University of Technology, Japan)*

P007A Effect of Supercritical Carbon Dioxide Upon Properties of Molecularly Imprinted Membranes with Selective Uracil Binding
Quanqiu Zhang and Takaomi Kobayashi* *(Nagaoka University of Technology, Japan)*

P008B Novel Membrane Adsorbents Made of Hybrid Molecularly Imprinted Polymer for Indole Derivatives
Kohei Takeda, Kohei Uemura, and Takaomi Kobayashi**(Nagaoka University of Technology, Japan)*

P009C Molecularly Imprinted Polymer Spheres Having Adsorption Selectivity of Bisphenol Derivatives
Kaori Katagawa, Masaya Kozuka, and Takaomi Kobayashi**(Nagaoka University of Technology, Japan)*

P010A Preparation and Thermosensitive Properties of PolyNIPAM Sphere Microgels Containing Itaconic Acid Segments

Takashi Onozuka and Takaomi Kobayashi* *(Nagaoka University of Technology, Japan)*

P011B Preparation and Characterization of Environmentally Sensitive Microgel Particles with Fluorescence Probe
Yoshihiko Sato, Y. Xin, and Takaomi Kobayashi**(Nagaoka University of Technology, Japan)*

P012C Molecular Imprinting Microparticles Having Inosine Recognition in Binding Behavior
Takayuki Kusunoki and Takaomi Kobayashi**(Nagaoka University of Technology, Japan)*

P013A Synthesis and Gas Permeability of Polyphenylacetylene Membranes Having Amino Groups
Yuki Sato, Masahiro Teraguchi, Takeshi Namikoshi, Edy Marwanta, Takashi Kaneko, and Toshiki Aoki**(Niigata University, Japan)*

P014B Air Humidification by Triethylene Glycol Membrane Supported on a Hydrophobic Microporous Membrane
Jinlong Li* and Akira Ito*(Niigata University, Japan)*

P015C Preparation of Hydroxyapatite Composite Gel by Biomineralization and Application to Medical Material
Sachiko Obara, Hiroshi Saito, Takeshi Yamauchi,* and Norio Tsubokawa *(Niigata University, Japan)*

P016A Preparation of Poly(*N*-isopropylacrylamide) Gel Containing Polymer-grafted Carbon Micro-coils and Its Application to Drug Carrier
Shigenori Sato[1], Takeshi Yamauchi[1],* Norio Tsubokawa[1], Kenji Kawabe, Yukio Hishikawa[2], and Seiji Motojima[3]*([1]Niigata University, Japan; [2]CMC Technology Development Co. Ltd., Japan; [3]Gifu University, Japan)*

P017B LSPR for Applications to Biosensing Element
Yasutaka Anraku[1]* and Hiromi Kitano[2]*([1]The University of Tokyo, Japan; [2]University of Toyama, Japan)*

P018C Effect of Zwitterionic Polymers on Wound Healing
Shigeto Fujishita[1,2], Chika Inaba[1], Susumu Tada[1], Makoto Gemmei-Ide[1], Hiromi Kitano[1],* and Yoshiyuki Saruwatari[3]*([1]University of Toyama, Japan; [2]Teika Pharmaceutical Co., Ltd., Japan; [3]Osaka Organic Chemical Ind., Ltd., Japan)*

P019A Study on the Bio-compatibility of Polymers with A Carboxybetaine Moiety
Makoto Gemmei-Ide[1], Chika Inaba[1], Susumu Tada[1], Hiromi Kitano[1],* Takayuki Matsunaga[2], Akira Mochizuki[3], Masaru Tanaka[4], and Yoshiyuki Saruwatari[5]
([1]University of Toyama, Japan; [2]Toyama Prefectural Institute for Pharmaceutical Research, Japan; [3]Tokai University, Japan; [4]Tohoku University, Japan; [5]Osaka Organic Chemical Industry Ltd., Japan)

P020B Glucose Fuel Cell with an Anode of Polythiophene Derivative Bearing Glucose Oxidase
Takashi Kuwahara, Mizuki Kondo, Rie Yamazaki, and Masato Shimomura**(Nagaoka University of Technology, Japan)*

P021C DNA Sensing with a Quartz Crystal Microbalance for Determination of *Esherichia coli*
K. Kon[1], M.Shimomura[1], and K.Kaneko[2]*([1]Nagaoka University of Technology, Japan; [2]Niigata Environment Hygiene Central Laboratory Co., Japan)*

P022A Separation of Serine Proteases Using a Thermoresponsive Polymer Bearing Diphenyl 1-Amino-2-phenylethylphosphonate
Shin Ono[1],* Shigenori Yoshikawa[1], Atsushi Yamamoto[1], Kazuki Yasue[1], Fumie Manzaki[1], Takeshi Terashima[1], and Hirofumi Kuroda[2] *([1]University of Toyama, Japan; [2]Toyama National College of Technology, Japan)*

P023B Isolation of Microorganisms that Preferentially Degrade Crystal and Amorphous Region of Biodegradable Polymers
Naoya Kitamura and Satoshi Osawa*(Kanazawa Institute of Technology, Japan)*

P024C Gelation Behavior and Aggregate Morphology of Cholesterol Derivatives
Rie Yamazaki,* Mizuki Kondo, Masato Shimomura, and Noritaka Kimura *(Nagaoka University of Technology, Japan)*

P025A Structure and Shrinking Kinetics of Polymer Hydrogels
Hiroshi Sasaki, Keita Tamura, Masamitsu Miya, Hiroki Takeshita,* Katsuhiko Takenaka, and Tomoo Shiomi*(Nagaoka University of Technology, Japan)*

P026B Preparation and Characterization of Interpenetrating Polymer Networks (IPNs) with Good Optical Transparency and Flexibility for Substrates of Flexible Displays
Myeon-Cheon Choi and Chang-Sik Ha**(Pusan National University, Korea)*

P027C Compatibility and Ionic Conductivity of Nitrile Rubber/Ionic Liquid Composites
Edy Marwanta,[1] Tomonobu Mizumo,[2] and Hiroyuki Ohno[2]*([1]Niigata University, Japan; [2]Tokyo University of Agriculture and Technology, Japan)*

P028A Reactive Mixing of Epoxidized Natural Rubber with Poly(L-lactide)
Takayuki Saito, Warunee Klinklai, Niti Sripitakchai, and Seiichi Kawahara* *(Nagaoka University of Technology, Japan)*

P029B Removal of Proteins from Natural Rubber with Urea and Its Application to Continuous Process
Yoshimasa Yamamoto, Warunee Klinklai, Takayuki Saito, and Seiichi Kawahara* *(Nagaoka University of Technology, Japan)*

P030C Molecular Weight of Grafted Polystyrene of PS-g-DPNR Copolymer
Nanthaporn Pukkate and Seiichi Kawahara**(Nagaoka University of Technology, Japan)*

P031A Preparation and Characterization of Poly(styrene-g-natural rubber) Copolymer
Patjaree Suksawad and Seiichi Kawahara**(Nagaoka University of Technology, Japan)*

P032B Hydrogenation of Natural Rubber Having Epoxy Group
Phan Trung Nghia, Agata Oshio, Yoshimasa Yamamoto, and Seiichi Kawahara* *(Nagaoka University of Technology, Japan)*

P033C Half Width and Relaxation Time of Latex State NMR Spectroscopy for Polyalkylacrylate
Jun Minowa, Seiichi Kawahara,* and Yoshimasa Yamamoto*(Nagaoka University of Technology, Japan)*

P034A Filler Network Characterization by Differential Dynamic Modulus in Reversing Double-Step Large Compression
Yukitoshi Yamaguchi, Kohji Suda, Shuji Fujii, and Yoshinobu Isono**(Nagaoka University of Technology, Japan)*

P035B Recovery of Filler Network Ruptured in Carbon Black Filled Rubber
Yoshitomo Sato, Shuji Fujii, and Yoshinobu Isono**(Nagaoka University of Technology, Japan)*

P036C Nonlinear Viscoelasticity and Change in Filler Network of Filled Rubber
H. Kondo, Y. Satoh, S. Fujii, and Y. Isono*(Nagaoka University of Technology, Japan)*

P037A Viscoelastic Properties of Spatially Confined Multilamellar Vesicles
S. Fujii* and Y. Isono*(Nagaoka University of Technology, Japan)*

P038B Structural Analysis of Microbial Poly(ε-lysine)/Poly(acrylic acid) Blend by Using Solid-state NMR
Shiro Maeda*[1], Yasuhiro Fujiwara[1], Chizuru Sasaki[2], and Ko-Ki Kunimoto[3]*([1]University of Fukui, Japan; [2]The University of Tokushima, Japan; [3]Kanazawa University, Japan)*

P039C Characterization of Microbial Poly(ε-L-lysine)/Carboxy Methyl Cellulose Blends by IR and Solid State ^{13}C and ^{15}N NMR Spectroscopies
Shiro Maeda[1],* Kumiko Kato[1], Chizuru Sasaki[2], and Ko-Ki Kunimoto[3]*([1]University of Fukui, Japan; [2]The University of Tokushima, Japan; [3]Kanazawa University, Japan)*

P040A *In situ* Analysis *Using* FT-IR Spectroscopy for Polymers-ozone Reaction
Makoto Arisawa, Wingky Kurniawan, and Takaomi Kobayashi**(Nagaoka University of Technology, Japan)*

P041B Phase Structure and Crystallization of Ethylene-Isoprene Block Copolymers and Their Blends with Corresponding Homopolymers
Yuanji Gao, Yusuke Takata, Hiroki Takeshita, Katsuhiko Takenaka, and Tomoo Shiomi**(Nagaoka University of Technology, Japan)*

P042C Synthesis of Styrene-Diene Block Copolymer Containing Chiral Amide Function and Its Application to Optical Resolution of Amino Acids
Shino Nakagawa, Masamitsu Miya, Hiroki Takeshita, Katsuhiko Takenaka,* and Tomoo Shiomi*(Nagaoka University of Technology, Japan)*

P043A Adhesive Bonding of Metal Nanowires
Takaaki Toriyama and Tsutomu Ishiwatari***(Shinshu University, Japan)*

P044B Construction of Cyclodextrin-Carbon Nanotube Hybrids
Tomoki Ogoshi[1], Tada-aki Yamagishi[1], Yoshiaki Nakamoto[1], and Akira Harada[2]*
([1]Kanazawa University, Japan, [2]Osaka University, Japan)*

P045C Postgraft Polymerization of Styrene from Poly(ethylene glycol)-grafted C_{60}

Fullerene by Grafting-from Method
H. Wakai, T. Momoi, T. Shinno, T. Yamauchi, and N. Tsubokawa**(Niigata University, Japan)*

P046A Grafting of Polymers onto Carbon Microcoil by Use of Carboxyl Groups on the Surface and Dispersibility of the Polymer-grafted Carbon Microcoil
Yuji Nishida[1], Kazuhiro Hujiki[2], Takeshi Yamauchi[1], Norio Tsubokawa[1],* Kenji Kawabe[3], Yukio Hishikawa[3], and Seiji Motojima[4]*([1]Niigata University, Japan; [2]Joetsu University of Education, Japan; [3]CMC Technology Development Co. Ltd., Japan; [4]Gifu University, Japan)*

P047B Immobilization of Capsaicin onto Hyperbranched Poly(amidoamine)-grafted Silica Nanoparticle and its Biorepellent Property
Tomoya Saito, Wei Gang, Kumi Shirai, Takeshi Yamauchi, and Norio Tsubokawa* *(Niigata University, Japan)*

P048C Preparation and Properties of Flame Retardant-immobilized Silica Nanoparticle
Akira Yuki**,** Takeshi Yamauchi, and Norio Tsubokawa**(Niigata University, Japan)*

P049A Grafting of Polybutadiene onto Silica Nanoparticle and Carbon Black Surface in the Presence of $Sc(OTf)_3$
Masaaki Takamura**,** Takeshi Yamauchi, and Norio Tsubokawa* *(Niigata University, Japan)*

P050B Grafting of Antibacterial Polymers onto Silica Nanoparticle and Their Properties
Yoko Takeuchi, Wei Gang**,** Kumi Shirai, Takeshi Yamauchi, and Norio Tsubokawa*
(Niigata University, Japan)

P051C Surface Grafting of Poly(amidoamine) onto Silica Nanoparticles in Solvent-Free Dry-System
Norio Tsubokawa, Jun Ueda, and Takeshi Yamauchi *(Niigata University, Japan)*

P052A Preparation of Polymer Gels with Ionic Liquids as Solvent and Its Functional Evaluation
Yoshihide Ito, Takeshi Yamauchi,* and Norio Tsubokawa*(Niigata University, Japan)*

P053B Electrical Properties of Polypyrrole/Calcium Alginate Composite Gel
Shotaro Kon, Takeshi Yamauchi,* and Norio Tsubokawa*(Niigata University, Japan)*

P054C Preparation of High Molecular Weight Phenolic Resins
Wang Pengfei, Tada-Aki Yamagishi,* Tomoki Ogoshi, and Yoshiaki Nakamoto
(Kanazawa University, Japan)

P055A Preparation of Poly(arylenemethylene)s Derived from Multi-substituted Aromatic Series and Evaluation of Their Properties
Tadamasa Nemoto, Ataru Kobayashi, and Gen-ichi Konishi**(Tokyo Institute of Technology, Japan)*

P056B Copolymerization of Vinyl Ether with a Tricyclodecane Unit and n-Butyl Vinyl Ether: Synthesis of New Polymeric Materials Consisting of Poly(vinyl ether) Backbones
Takeshi Namikoshi[1] and Tamotsu Hashimoto[2]**([1]Niigata University, Japan; [2]University of Fukui, Japan)*

P057C Preparation of $(A)_1$-*star*-$(B)_1$ Star Block Copolymers *via* Anionic Living Polymerization of Macromonomers
Teppei Yamazaki, Yasunari Hayashino, and Kazunori Se*(*University of Fukui, Japan*)

P058A RAFT Polymerization of *N,N*-Diethyl-2-methylene-3-butenamide
Masahito Matsui, Masamitsu Miya, Hiroki Takeshita, Katsuhiko Takenaka,* and Tomoo Shiomi *(Nagaoka University of Technology, Japan)*

P059B Phase Structure of Block Copolymers Consisting of Two Liquid Crystalline Components
Shin-ichi Taniguchi, Takebumi Abe, Masamitsu Miya, Hiroki Takeshita, Katsuhiko Takenaka, and Tomoo Shiomi* (*Nagaoka University of Technology, Japan)*

P060C Phase Structure of Liquid Crystalline Block Copolymers Having a Rubbery Amorphous Component
Noriaki Okumura, Shin-ichi Taniguchi, Masamitsu Miya, Hiroki Takeshita, Katsuhiko Takenaka and Tomoo Shiomi* *(Nagaoka University of Technology, Japan)*

P061A Asymmetric Induced Copolymerization of Achiral Phenylacetylene with a Chiral Amino Group
Mohammed Hoda, Masahiro Teraguchi, Masayuki Sato, Takeshi Namikoshi, Edy Marwanta, Takashi Kaneko, and Toshiki Aoki* *(Niigata University, Japan)*

P062B Application of Chiral Helical Poly(phenylacetylene)s for Optical Resolution
S. Hadano[1, 2], M. Teraguchi[1], T. Kaneko[1], and T. Aoki[1]* *([1]Niigata University, Japan, [2]Kyoto University, Japan)*

P063C Synthesis and Attempts of Helix-sense-selective Polymerization of Achiral Phenylacetylenes Having Two Alkylamido Groups
Chen Chen Liu, Masahiro Teraguchi, Takeshi Namikoshi, Edy Marwanta, Takashi Kaneko, and Toshiki Aoki* *(Niigata University, Japan)*

P064A The Control of the Helix Sense in the Copolymerization of (4-Ethynylphenyl)galvinoxyl by the Composition of Comonomer
Yasuhiro Umeda, Takashi Kaneko,* Takeshi Namikoshi, Edy Marwanta, Masahiro Teraguchi, and Toshiki Aoki *(Niigata University, Japan)*

P065B Synthesis of One−handed Helical Polyphenylacetylenes Stable in Solution by Removing the Chiral Groups from Poly(phenylacetylene having chiral groups) in Membrane State
Yunosuke Abe, Masahiro Teraguchi, Takeshi Namikoshi, Edy Marwanta, Takashi Kaneko, and Toshiki Aoki**(Niigata University, Japan)*

P066C Synthesis of Chiral Polyphenylacetylenes Bearing a One-handed Helical Backbone and Photo-responsive Side Chains
Ippei Suzuki, Masahiro Teraguchi, Takeshi Namikoshi, Edy Marwanta, Takashi Kaneko, and Toshiki Aoki* *(Niigata University, Japan)*

P067A Helix-sense-selective Polymerization of Phenylacetylene Having Two Aminoalcohol Residues
Kazuki Matsumoto, Masahiro Teraguchi, Takeshi Namikoshi, Edy Marwanta, Takashi Kaneko, and Toshiki Aoki* *(Niigata University, Japan)*

P068B Helix-sense-selective Polymerization of 3,5-Bis(hydroxymethyl)-4-benzyloxyphenylacetylene Bearing Galvinoxyl, and Chiroptical and Magnetic Properties
Hiroo Katagiri, Takashi Kaneko,* Takeshi Namikoshi, Edy Marwanta, Masahiro Teraguchi, and Toshiki Aoki *(Niigata University, Japan)*

P069C Asymmetric-induced Polymerization of Phenylacetylene Having Two Hydroxyl Groups and a Chiral Pinanylsilyl Group
Jia Hongge, Kazuomi Mottate, Masahiro Teraguchi, Takeshi Namikoshi, Edy Marwanta, Takashi Kaneko, and Toshiki Aoki* *(Niigata University, Japan)*

P070A Attempt to Living Helix-sense-selective Polymerization of Achiral Phenylacetylenes by $MoOCl_4$ or $WOCl_4$ -alkylating agent-chiral alcohol
Motohiro Kiuchi, Masahiro Teraguchi, Takeshi Namikoshi, Edy Marwanta, Takashi Kaneko, and Toshiki Aoki**(Niigata University, Japan)*

P071B Synthesis of TEMPO-pendant Poly(phenylacetylene)s, and Their Chiroptical and Magnetic Properties
Atsuko Kawami, Takashi Kaneko,* Takeshi Namikoshi, Edy Marwanta, Masahiro Teraguchi, and Toshiki Aoki *(Niigata University, Japan)*

P072C Magnetic Properties of TEMPO Radicals Included in a Supramolecular Anthracene Derivative
Masayuki Sato, Takashi Kaneko,* Takeshi Namikoshi, Edy Marwanta, Masahiro Teraguchi, and Toshiki Aoki *(Niigata University, Japan)*

P073A Synthesis of Poly(binaphthyl-6,6'-diylethynylene-1,3-phenyleneethynylene)-based Chiral Polyradical Bearing Galvinoxyl, and Its Chiroptical and Magnetic Properties
Hiromasa Abe, Takashi Kaneko,* Takeshi Namikoshi, Edy Marwanta, Masahiro Teraguchi, and Toshiki Aoki *(Niigata University, Japan)*

P074B Synthesis of Oligo(anthryleneethynylene)-based Foldamers Containing Stable Radicals
Kensuke Ochiai, Takashi Kaneko,* Takeshi Namikoshi, Edy Marwanta, Masahiro Teraguchi, and Toshiki Aoki *(Niigata University, Japan)*

P075C Synthesis of Chiral Helical Poly(phenyleneethynylene) Membranes by Desubstitution of Chiral Group
Makoto Inoue, Masahiro Teraguchi, Takeshi Namikoshi, Edy Marwanta, Takashi Kaneko, and Toshiki Aoki* *(Niigata University, Japan)*

P076A Synthesis of Poly(*p*-benzamide)s Bearing *α*-Branched Chiral Alkyl Side Chain and Investigation of Their Chiral Conformation
Tomoaki Saiki, Akihiro Yokoyama, and Tsutomu Yokozawa**(Kanagawa University, Japan)*

P077B Investigation of Catalyst-transfer Condensation Polymerization for the Synthesis of Well-defined Polypyridine
Yutaka Nanashima, Akihiro Yokoyama, and Tsutomu Yokozawa* *(Kanagawa University, Japan)*

P078C Synthesis of a Variety of Well-defined *N*-Alkyl Poly(*m*-benzamide)s and Their

Block Copolymers by Chain-growth Condensation Polymerization
Tomoyuki Ohishi, Akihiro Yokoyama, and Tsutomu Yokozawa *(Kanagawa University, Japan)*

P079A Development of Chain-growth Condensation Polymerization of Monomer Immobilized on Solid-support: Model Reaction and Polymerization
Ryota Negishi, Yoshio Kabe, Kazuo Yamaguchi, Akihiro Yokoyama, and Tsutomu Yokozawa* *(*Kanagawa University, Japan*)*

P080B Knoevenagel Reactions in Water Catalyzed by Immobilized Organomolecular Catalyst
Hisahiro Hagiwara,* Kohei Isobe, Ayuko Numamae, Takashi Hoshi, Toshio Suzuki *(Niigata University, Japan)*

P081C Biphenylene-containing Ruthenocenylphosphine Designed as a Novel Phosphine-arene Ligand: Application to Pd-Catalyzed Suzuki-Miyaura Reaction
Takashi Hoshi,* Ippei Saitoh, Taichi Nakazawa, Toshio Suzuki, and Hisahiro Hagiwara* *(Niigata University, Japan)*

P082A Framework-rearrangement Reaction of Completely-condensed Octa(aryl) octasilsequioxane (ARYL-T8)
Ze Li and Yusuke Kawakami**(Japan Advanced Institute of Science and Technology, Japan)*

P083B Synthesis and Chemical Properties of Polyfluorinated Porphyrins
Yusuke Hoshina[1], Akihiro Suzuki[2]**(*[1]Nagaoka University of Technology, Japan; [2]Nagaoka National College of Technology, Japan)*

P084C Bioactive Cardenolides from the Stems and Twings of *Nwrium Oleander*
Liyan Wang[1], Ming Zhao[1], Liming Bai[1,5], Asami Toki[1], Toshiaki Hasegawa[2], Midori Kikuchi[2], Mariko Abe[2], Jun-ichi Sakai[1], Ryo Hasegawa[1], Yuhua Bai[1,7], Tomokazu Mitsui[3], Hirotsugu Ogura[3], Takao Kataoka[3], Seiko Oka[4], Hiroko Tsushima[4], Miwa Kiuchi[4], Katutoshi Hirose[5], Akihiro Tomida[6], Takashi Tsuruo[6], and Masayoshi Ando[1,7]
([1]Niigata University, Japan; [2]Mitsubishi Gas Chemical Company, Inc., Japan; [3]Tokyo Institute of Technology, Japan; [4]Hokkaido University, Japan; [5]KNC Laboratories Co. Ltd., Japan; [6]Japanese Foundation for Cancer Research, Japan; [7]Qiqihar University, China)

P085A Photolithographic Properties of Ultrathin Polymer Langmuir-Blodgett Films Containing Naphthyl Group
Wenjian Xu, Tiesheng Li,* Gouliang Zeng, Suhua Zhang, Wei Shang, and Yangjie Wu**(Zhengzhou University,China)*

P086B Polymer Langmuir-Blodgett Films Using for Pattern Transformation
Guoliang Zeng, Tiesheng Li,* Wei Shang, Wenjian Xu, Jun Wang, Suhua Zhang, and Yangjie Wu**(Zhengzhou University, China)*

P087C Atomic Force Microscopy Studies on Langmuire-Blodgett Films of "Tailed" Porphyrin
Wei Shang, Pingping Liu, Jun Wang, Wenjian Xu, Tiesheng Li,* Luyuan Mao, Suhua Zhang, Guoliang Zeng Bing Mu, and Yangjie Wu*(Zhengzhou University, China)*

P088A Studies on the Characteristics of Langmuir-Blodgett Films of Amphiphilic

Cyclopalladated Ferrocenylimines
Bing Mu, Tiesheng Li,* Pingping Liu, Wei Shang, Wenjian Xu, and Yangjie Wu* *(Zhengzhou University, China)*

P089B Synthesis and Solid-stated Polymerization Behavior of Diacetylene Derivative
Lei Zhang, Tiesheng Li,* Shengli Gao, and Yangjie Wu**(Zhengzhou University, China)*

P090C Molecular Ordering of 1-TNATA Thin Films and Organic Electroluminescence Device Properties
Dosoon Kang , So Hyun Park, Phuong Thanh Vu, Young-Rae Cho, Dae-Won Park, and Youngson Choe *(Pusan National University, Korea)*

P091A Sensitization Reaction of the Oxime Type Photoacid Generator for Photo-lithography
Tomoaki Tsumita, Shota Suzuki, and Shigeru Takahara**(Chiba University, Japan)*

P092B Multiple Electrochromic Performance of an All-solid Electrochromic Device Using A WO_3 / Tris(2,2'-bipyridine)ruthenium(II) / Polymer Hybrid Film
Koji Sone, Satomi Iijima, and Masayuki Yagi**(Niigata University, Japan)*

P093C Different Effects Due to Shape Configuration in Three-layer Electroactive Polymers
Josue F. Guzman L., Jorge A. Cortes R., Sergio Gallegos C., Lucio Florez C., and Manuel Martinez M. *(Instituto Tecnologico y de Estudios Superiores de Monterrey (ITESM), Mexico)*

P094A Visible Light Induced Pohotocurrent Generation by Perylene Derivatives Adsorved on Metal Oxide Semiconductor Films in an Aqueous Solution
Takeo Takahashi, Satoru Sasagawa, Syou Maruyama, and Masayuki Yagi* *(Niigata University, Japan)*

P095B Catalytic Activity for Water Oxidation of Dipyridyl Pyrazole-bridged Dinuclear Ruthenium Complex in a Heterogeneous System
Shouhei Tajima and Masayuki Yagi**(Niigata University, Japan)*

P096C Substituent Effects on Catalytic Activity for Water Oxidation by Di-μ-oxo Manganese Complex Supported by Clay Compounds
Hirosato Yamazaki and Masayuki Yagi**(Niigata University, Japan)*

P097A Water Oxidation Catalysis by $[Ru(TERPY)LOH_2]^{2+}$ (L = Bidentate Ligand) Complexes Adsorbed in Layer Compounds
Manabu Komi and Masayuki Yagi**(Niigata University, Japan)*

P098B Artifical Model of Photosynthetic PS II: Photochemical Production of O_2 from Water by an Di-μ-oxo Manganese Complex in a Heterogeneous System
Satoshi Yamada, Mayuu Toda, and Masayuki Yagi**(Niigata University, Japan)*

P099C Inverted Bulk-heterojunction Organic Solar Cells Using a Sol-gel-derived Titanium Oxide Thin Film as an Electron Injection Electrode Inserted into ITO/Organic Solid Layer Interface
Takayuki Kuwabara, Yasunori Sigeyama, Takahiro Yamaguchi, and Kohshin Takahashi**(Kanazawa University, Japan)*

P100A Inverted Bulk-heterojunction Organic Solar Cells Using an Electrodeposited Zinc Oxide Thin Film as Electron Injection Electrode
Yoshitaka Kawahara, Takayuki Kuwabara, Takahiro Yamaguchi, and Kohshin Takahashi* *(Kanazawa University, Japan)*

P101B Inverted Bulk-heterojunction Organic Solar Cells Using an Electrodeposited Titanium Oxide Thin Film
Hirokazu Sugiyama, Takayuki Kuwabara, Takahiro Yamaguchi, and Kohshin Takahashi* *(Kanazawa University, Japan)*

P102C Inverted Bulk-heterojunction Organic Solar Cells Using a Self-assembled Zinc Sulfide Thin Film as an Electron Injection Electrode Inserted into ITO/Organic Solid Layer Interface
Masayuki Nakamoto, Takayuki Kuwabara, Takahiro Yamaguchi, and Kohshin Takahashi* *(Kanazawa University, Japan)*

P103A Anodic Oxidation of Methanol on Hydrophobic Nickel Electrode
Masaki Igarashi and Yasushi Ono *(Niigata University, Japan)*

P104B Preparation of Electroconductive Polymer Film by Dip Coating Method and Its Characterization
Atsushi Tamura and Yasushi Ono**(Niigata University, Japan)*

P105C Electropolymerization of Pyrrole in Ionic Liquid Diluted by the Organic Solvent
Daichi Mori and Yasushi Ono *(Niigata University, Japan)*

P106A Indirect Electroorganic Reaction with Oxygen Reduction on Hydrophobic Silver Granules Cathode
Tomohiro Shiota and Yasushi Ono *(Niigata University, Japan)*

P107B Application of Layered Tantalum Oxides Nanosheet to Photocatalytic Reaction
Yoshiyuki Mori, Hidetoshi Kibe, Kazuyoshi Uematsu, Kenji Toda,* and Mineo Sato *(Niigata University, Japan)*

P108C Melt Synthesis and Morphology Control of Phosphor Materials
Kenji Toda[1],* Masafumi Hosoume[1], Kazuyoshi Uematsu[1], Mineo Sato[1], Tadashi Ishigaki[2], and Masahiro Yoshimura[2] *([1]Niigata University, Japan; [2]Tokyo Institute of Technology, Japan)*

P109A Removal of Fluorine from Waste Water by Ettringite
Kenji Sato, Hiroko Morinaga, Toshiaki Tokumitsu, Kazuyoshi Uematsu, Kenji Toda, and Mineo Sato*(Niigata University, Japan)*

P110B Preparation of $KNbO_3$ Thin Film at Room Temperature
Toshinari Takahashi , Kazuyoshi Uematsu , Kenji Toda,* and Mineo Sato *(Niigata University, Japan)*

P111C Development of Novel Phosphor for a White LED
Yoshitaka Kawakami, Akira Komeno, Kazuyoshi Uematsu, Kenji Toda,* and Mineo Sato *(Niigata University, Japan)*

P112A New Photocatalyst of Metal Oxides with d^{10} Configuration
Hironori Ishikawa, Kazuyoshi Uematsu, Kenji Toda,* and Mineo Sato*(Niigata University, Japan)*

P113B Low Temperature Growth of Potassium Niobate Single Crystal
Akihiro Iida, Kazuyoshi Uematsu, Kenji Toda,* and Mineo Sato *(Niigata University, Japan)*

P114C Photocatalytic Activity of Bismuth Layered Perovskite Treated with Acid
Yousuke Narumi, Kenji Toda,* Kazuyoshi Uematsu, and Mineo Sato *(Niigata University, Japan)*

P115A Synthesis of Novel Molybdate Phosphor
Satomi Seki, Yutaka Ito, Kazuyoshi Uematsu, Kenji Toda, and Mineo Sato *(Niigata University, Japan)*

P116B Low Temperature Synthesis of TiO_2
Sae Nakajima, Yoshiomi Yamanaka, Kazuyoshi Uematsu, Kenji Toda,* and Mineo Sato *(Niigata University, Japan)*

P117C Double-walled Tubular Reactor with Molten Salt Thermal Storage for Solar Reforming of Methane
Shin-ichi Inuta, Daisuke Nakano, Yoshinori Hara Nobuyuki Gokon, and Tatsuya Kodama* *(Niigata University, Japan)*

P118A Thermochemical Two-step Water-splitting Cycle by ZrO_2-supported Fe_3O_4 for Solar Hydrogen Production
Hiroko Murayama, Shingo Takahashi, Nobuyuki Gokon, and Tatsuya Kodama* *(Niigata University, Japan)*

P119B Removal of Manganese in Wastewater Accompanied by the Precipitation of Fine Ferrite Particles
Kenji Miyamura, Yoji Taguchi, and Isao Kimura* *(Niigata University, Japan)*

P120C Release and Control of Alkaline Earth Metal Ions from Methylcellulose Hydrogel
Masashi Nakagawa and Isao Kimura* *(Niigata University, Japan)*

P121A Effects of Oil Phase Media on the Preparation of Hydroxyapatite Microspheres in a Multiple Dispersion
Tatsuro Honma and Isao Kimura**(Niigata University, Japan)*

P122B Comparison of O_2/N_2 and N_2O/N_2 Plasma Etching of Polymer
Y.W. Joo, J. K. Kim, Y. H. Park, G. S. Cho, H. J. Song, and J. W. Lee**(Inje University, Korea)*

P123C A Mechanism of Ablation of Metals by Sub-femto Second Laser Pulses
Guan Sik Cho*, Eun Mi Ko, Myung Hoon Kang, and Jewon Lee (*Inje University, Korea; University of Alberta at Edmonton, Canada)*

P124A Ultrasound Effect on Hydrogen Bonding Formation Appeared in Alumina-polyacrylic acid Slurry
Ngo Le Ngoc and Takaomi Kobayashi * *(Nagaoka University of Technology, Japan)*

P125B Effect of Reflected Ultrasounds Having Different Frequency on Preparation of Nano-sized Sol-gel TiO_2 Powders

Kyaing Kyaing Latt and Takaomi Kobayashi* *(Nagaoka University of Technology, Japan)*

Plenary Lecture
&
Oral Session 1

July 14 (Sat)

[9:00 –11:30]

PL01

GLOBALIZATION OF JSR ADVANCED MATERIALS BUSINESS

Yoshinori Yoshida

JSR Corporation

1. About JSR

JSR Corporation was established in 1957 by the Special Measures Law for Synthetic Rubber Production to produce domestic synthetic rubbers. In 1969, JSR became a purely publicly-owned company and has continued to strive to expand its business, and reinforce stabilization of its management, from general purpose synthetic rubbers for the tire industry to specialized rubbers for auto parts to complement with the rapid growth of automobile industry. Furthermore, JSR expanded its business field into other areas such as paper coatings and home and office appliances through application of its proprietary polymer technologies, such as emulsion and synthetic resins. Due to volatility in the oil and gas industry and the burst of our bubble economy, the commodity business has weakened, which has the potential to affect our company's position. Under these circumstances, JSR has decided to shift direction and focus more intently on the opto-electronic materials business and begin working to enter into the fast-growing information and communication industries through the application of its polymer technologies, resulting in more R&D resources being put into this new field. JSR has shifted its resources, like R&D, to focus more on the functional chemical business than commodity business.

2. Functional Chemicals Business

Industries were grown during the 20th century through innovations in materials technologies, energy technologies and information technologies and polymer chemistry has played an important role in that growth. In addition, shifting from general purpose polymer technology to functional polymers has taken place rapidly. JSR is focused on three strategies – to be the de facto standard in materials business, to synergize a clustered business, and expand its business as a global leader, especially in the area of opto-electronic materials. It is understood that functional chemicals will be crucial for several major sectors, Information network and electronics, medical, environment and energy. These are areas that Japan has specialized in and are recognized as industries on which chemical companies are focusing.

JSR's globalization will be explained here through an explanation of the current and future situation of lithography materials for semiconductor manufacturing and LCD materials.

3. RD and New Business Development

The importance of MOT (Management of Technology) is well-recognized by manufacturing companies where R&D strategies take a crucial role in management strategies. Objectives of the MOT are to create value-added materials and products in broad meaning and to maximize usage of the R&D function

within that defined meaning. In order to be successful, the following three items are necessary; 1) Integrate a corporate management strategy, a business strategy and a R&D strategy, 2) Strong commitment to R&D activities from senior management, and 3) Innovative methods to tie R&D results to next-stage business opportunities.

JSR aims to expand its business and technologies in not only the existing materials and technologies, but also new materials business in the next stage and growing businesses, such as next generation electronics, displays, opto-functional, environmental energy, medical care and others.

IL01

A MECHANISTIC CONSIDRATION ON THE FORMATION OF Cage – type POSS DERIVATIVES

Yusuke KAWAKAMI
School of Materials Science, Japan Advanced Institute of Science and Technology
Asahidai 1-1, Nomi, Ishikawa 9231292 Japan: kawakami@jaist.ac.jp

Although, completely condensed "cubic" octameric silsesquioxane, [POSS, $(RSiO_{1.5})_8$, T_8] has been paid a lot of attention by many researchers, they are not always convenient for further functionalization. Some functional groups are desired for further practical use. The products in the hydrolysis of tri-functional silane compounds depend on the reaction conditions such as concentration of the compound, amount of water, temperature, reaction time, etc.

By changing the reaction conditions, even incompletely condensed products can be obtained, which will find high applicability in designing new nano-composite materials. Under basic condition with Si : Na ratio; 2 : 1, incompletely condensed Si-7 triol derivative, whose MS and NMR are shown in Figure 1, was firstly formed, and converted into Si-8 compound. This Si-8 compound was elucidated as so-called double decker silsesquioxane by its MS and NMR. When cubic T8 was treated with sodium hydroxide in an alcohol, T7 and double decker silsesquioxane were produced. When the double decker silsesquioxane was treated with an acid, it was converted into completely condensed T8. Some higher condensed products were also seen. These compounds are inter-convertible under suitable condition.

In any cases, formation of cyclic tetramer seems essential to give higher condensed products. In many cases, the selectivity of the formation of the *cis* isomer is very high. This might be caused by template effect of sodium ion.

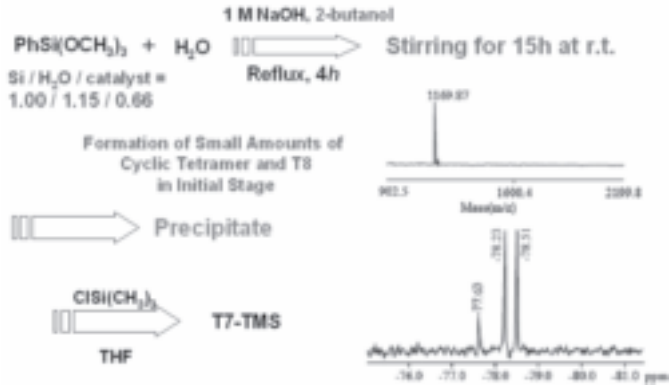

Figure 1. Product after 15 hr stirring

References

1. C. Pakjamsai, Y. Kawakami, *Polym J.* **36**, 455 (2004).
2. C. Pakjamsai, N. Kobayashi, M. Koyano, S. Sasaki, Y. Kawakami, *J. Polym. Sci., Part A: Polym. Chem.* **42**, 4587 (2004).
3. C. Pakjamsai, Y. Kawakami, *Design. Monom. Polym.* **8**, 423(2005).
4. D. W. Lee, Y. Kawakami, Polymer J., **39**(3), 230(2007).

IL02

SYNTHESIS OF A NOVEL POSS-BASED MATERIAL HAVING CARBAZOLE, AND ITS THERMAL, ELECTROCHEMICAL AND OPTICAL PROPERTIES

Ichiro Imae
Department of Applied Chemistry, Faculty of Engineering, Hiroshima University

Cubic polyhedral oligomeric silsesquioxane (POSS) is well-known as a novel class of organic-inorganic hybrid component. Each silicon atom at the corner of cubic POSS can possess an organic substitutent, and they are directed radially. Thus, when the photo- and electroactive chromophores are introduced onto the silicon atom of POSS, these chromophores should be isolated due to both steric and electronic effects, originated from the chemical structure as above-mentioned and from the nature of nonconjugation of siloxane bond, respectively. The isolation is expected to solve the problem about the aggregation of chromophores in solid state. We report here the first synthesis of POSS having carbazole as one of photo- and electroactive chromophores (**POSS-Cz**) and the investigation of photoluminescence properties in both solution and solid states.

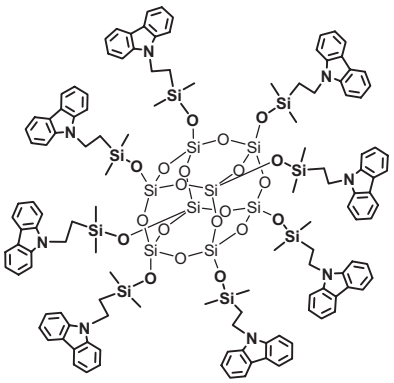

Chemical Structure of **POSS-Cz**

Carbazole could be easily introduced by hydrosilylation reaction between octakis(dimethylsiloxy)-silsesquioxane and 9-vinylcarbazole in the presence of platinum catalyst. The product is soluble in common organic solvents, such as toluene, THF, and chloroform, and could be purified by column chromatography and reprecipitation. The product was characterized by ^{1}H, ^{13}C, ^{29}Si NMR and MALDI-TOF MS spectroscopies, and the results suggested that the product has a perfectly uniform structure. From the thermogravimetry, it was found that **POSS-Cz** is stable until around 400°C even in air. DSC and XRD results showed that **POSS-Cz** as prepared is crystalline, but it becomes amorphous glass after the melt sample was cooled to room temperature.

Photoluminescence properties in dilute solution and solid film of **POSS-Cz** were investigated. **POSS-Cz** showed monomeric emission peak in dilute solution, which is similar result of 9-ethylcarbazole. Unlikely, poly(9-vinylcarbazole) showed broad and weak emission peak due to the formation of excimer of pendant carbazole unit. Interestingly, **POSS-Cz** showed mainly monomeric peak even in solid state film, while 9-ethylcarbazole showed complicated peak because of the aggregation due to the crystallinity.

References

1. Ichiro Imae and Yusuke Kawakami, *Journal of Materials Chemistry*, **15**(43), 4581–4583 (2005).
2. Ichiro Imae, Yusuke Kawakami, Yousuke Ooyama, and Yutaka Harima, *Macromolecular Symposia*, **249–250**(1), 50–55 (2007).

OL01

EFFECTS OF DENDRITIC SILSESQUIOXANE ON PERFORMANCE OF HOLOGRAPHIC GRATINGS BASED ON PHOTOPOLYMER FILM

Hoque Md. Asadul (*Materials Science, JAIST*), Yeong Hee CHO (*JAIST*), and Yusuke KAWAKAMI* (*JAIST*)

Abstract

A transparent photopolymer film was prepared by embedding the epoxy cured octaaminophenylsilsesquioxane (dendritic-POSS) into poly (vinyl chloride) (PVC) matrix containing acrylate monomers. Holographic gratings were successfully generated in that films by irradiation of laser light with 532 nm wavelength.The diffraction efficiency was increased with increasing the dendritic-POSS concentration up to 15 wt% and started to decrease beyond that limit due to the back ward migration of monomers in PVC matrix. This can be considered that the dendritic-POSS plays an important role in formation of holographic gratings. Because the photopolymer film based on PVC matrix became softer as the dendritic-POSS molecules loosen the polymer matrix which was supported by DSC and TG analysis. This plasticizing effect made the monomer diffusion much more effective providing higher diffraction efficiency (D.E ~80%) compared to the film without dendritic-POSS (D.E~50%). Some improvement of volume shrinkage could be obtained for the photopolymer films containing dendritic-POSS molecules in recording of slanted holographic gratings.

Results and Discussions

The higher diffraction efficiency and first grating formation were found in case of the photopolymer film comprised of 15% dendritic-POSS in PVC matrix as compared to the film made of with only PVC as the matrix component. From the fig-1, it is seen that with the identical additives composition and irradiation conditions, about 80% diffraction efficiency was found for the photopolymer film containing dendritic-POSS whereas, only ~50% diffraction efficiency was found for the photopolymer film containing only PVC. T_g analysis showed that POSS played as an effective plasticizer to loosen the polymer packing and increased the free volume in films which made the film softer. As a result the monomer diffusion was

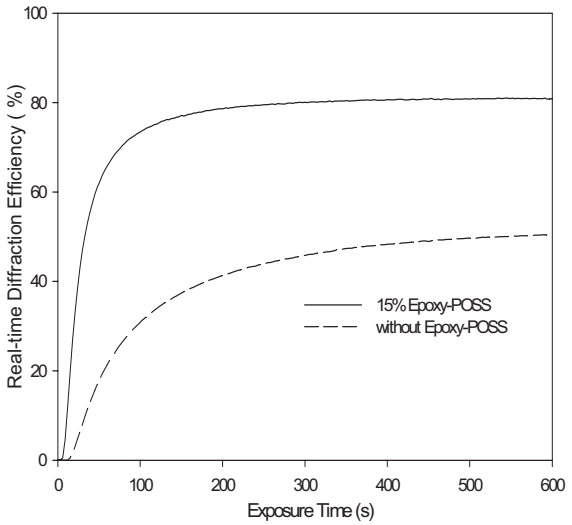

Fig 1 Real-time diffraction efficiency of holographic gratings formed at 3% PI, 0.5% PS and 28.9 mW/cm^2 with Epoxy-POSS and without epoxy-POSS (PVC:Epoxy-POSS:TPGDA:NVP=(70-X):X:20:10).

facilitated to increase the concentration of the polymerizable monomers in the bright region. The silicon based dendritic-POSS also provided the incompatibility with carbon based polymer matrix resulted in very fast phase separation. However, the lower (10%) and higher (20%) loading of dendritic-POSS provided lower diffraction efficiency. It may be considered that 10 wt% loading of dendritic-POSS can not provide sufficient plasticizing effect for good phase separation whereas higher loading of dendritic-POSS (20 wt%) provides higher plasticizing effect and can not hold the created gratings intact resulting backward migration of polymer chain.

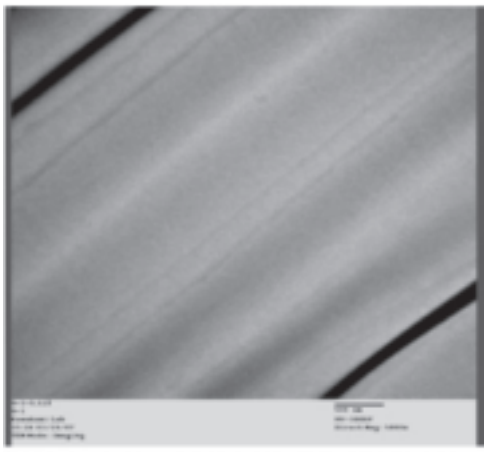

Figure 2. TEM image of the holographic gratings for the film containing dendritic-POSS

Conclusion

Organically modified silsesquioxane (dendritic-POSS) was prepared and used in the photopolymer formulation for holographic recording. The incorporation of dendritic-POSS in PVC based photopolymer film decreased the brittleness of the film. It also played a role as plasticizer for lowering $T_{g.}$ The measurement of real-time diffraction efficiency showed the increased rate of photoreaction with efficient monomers diffusion. Our results showed that dendrictic-POSS could be useful matrix supporting material to improve photopolymers for holographic recording.

OL02

NOVEL HOLOGRAPHIC POLYMER DISPERSED LIQUID CRYSTALS FORMED WITH ACCELARATED MULTIFUNCTIONAL ACRYLATES CONTAINING SILOXANE NETWORK

Yeong Hee CHO, Go SUZUKI, and Yusuke KAWAKAMI*

School of Materials Science, Japan Advanced Institute of Science and Technology, 1-1 Asahidai, Nomi, Ishikawa 923-1292, Japan

1. Introduction

Recently our research was focused on the novel process for fabrication of holographic gratings via simultaneous photopolymerization and siloxane network formation. In previous report, we demonstrated the effectiveness of siloxane network formation in polymer matrix on performance of holographic gratings by using trialkoxysilyl (meth)acrylates[4]. By loading high concentration of trimethoxysilyl-containing derivatives, higher diffraction efficiency, lower volume shrinkage, and the well-constructed morphology of the gratings were obtained. In this research, novel materials with trialkoxysilane derivatives capable of hydrolysis and condensation were introduced into recording solution to form denser siloxane cross-linking resulting in the further improvement of performance of holographic gratings.

2. Experimental

To tune the reaction rate and cross-linking density, multi-functional acrylate, trimethylolpropane triacrylate (**TMPTA**), purchased from Aldrich Chemical Co., was used as radically polymerizable cross-linking monomer. Various trialkoxysilane derivatives of methacryloxypropyl trimethoxysilane (Ma-TMS), methacryloxypropyl-triethoxysilane (Ma-TES), *O*-(methacryloxyethyl)-*N*-(triethoxysilylpropyl)urethane (Ma-U), and N-(3-methacryloxy-2-hydroxypropyl)-3-aminopropyltriethoxysilane (Ma-H) were used as monomers to be incorporated in the matrix by radical polymerization with hydrolyzable silyl functional groups. 1-Vinyl-2-pyrrolidone (**NVP**) was used as a radically polymerizable reactive diluent. Photoinitiation solution with diphenyliodoniumhexafluorophosphate and 3,3'-carbonylbis(7-diethylamino coumarin) was selected to have a sensitivity to Nd-YAG laser (λ=532 nm). Liquid crystal, TL203 was used. Recording solution was prepared by mixing the photo-polymerizable compounds and TL203, and injected into a glass cell with a gap of 20 μm controlled by bead spacer.

Real-time diffraction efficiency was measured by monitoring the intensity of diffracted beam and diffraction efficiency is defined as the ratio of diffraction intensity after recording to transmmitted beam intensity before recording. To determine the angular selectivity, diffraction efficiency was measured by rotating the hologram precisely by constant angle. The optimum condition was established to obtain the high diffraction efficiency, high resolution, and excellent long-term stability after recording.

3. Results and Discussion

To study the effectiveness of trialkoxysilane derivatives on the performance of gratings, chemical structures of alkoxysilane derivatives were modified. **Figure 1** shows the real-time diffraction efficiency of holographic gratings formed with various trialkoxysilane derivatives with methacrylate capable of radical photopolymerization. The ratio of **TMPTA**: trialkoxysilane derivatives: **NVP** was 10: 80: 10 wt% to induce the large effects of trialkoxysilane derivatives on formation of gratings.

Firstly, by varying the trialkoxysilyl function group as trimethoxy and triethoxy of **Ma-TMS** and **Ma-TES**, respectively, at same chain length of linker, higher diffraction efficiency was shown in gratings formed with **Ma-TMS** than **Ma-TES,** which resulted from the fast network formation in polymer matrix induced fast phase separation of **TL203**. This can be considered that trimethoxysilyl group induce faster hydrolysis-condensation

reaction than triethoxysilyl function as reported in sol-gel systems.

Secondly, when the chemical structures of linkage of trialkoxysilane derivatives as **Ma-TMS**, **Ma-TES**, **Ma-U**, and **Ma-H**, the highest diffraction efficiency of about 75% and the shortest induction period of about 15s were observed in gratings formed with **Ma-U** having urethane moiety and **Ma-H** having hydroxy moiety, respectively even though with triethoxysilyl group. It can be considered that the linkage structures of trialkoxysilane derivatives plays an important role on the formation of gratings, especially in sol-gel systems hydrophilic moiety of urethane and hydroxyl affected strongly on the rates of cross-linking network formation of siloxane network and radical polymerization induced network. Gratings formed with **Ma-H** having the strongest hydrophilic property had the lowest diffraction efficiency of 20 % even the shortest induction period due to the fastest matrix formation resulted in the restriction of diffusion **TL203** to high intensity regions of interference fringes. However, if the formulation of recording solution with **Ma-H** is optimized, and the chemical structures of trialkoxysilane derivatives with **Ma-H** are modified, their gratings should be high diffraction efficiency, which study is under.

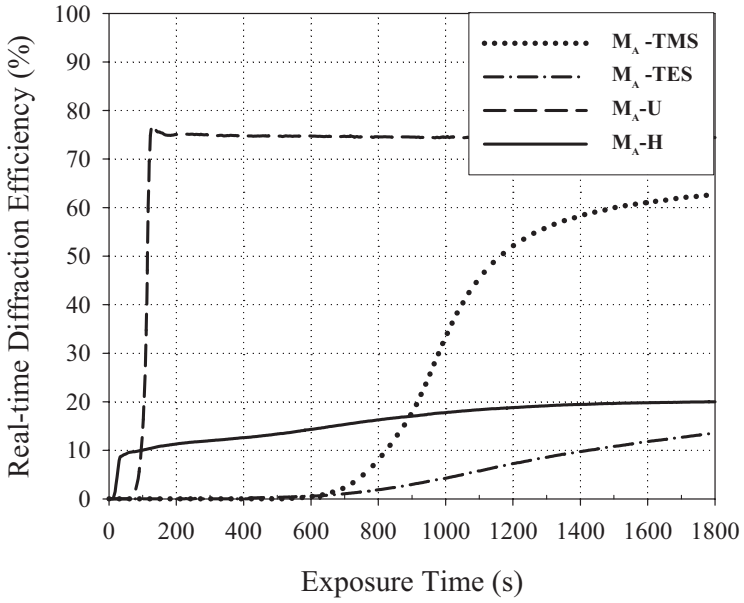

Figure 1. Real-time diffraction efficiency of the gratings formed with various alkoxysilane derivatives in the ratio of **TMPTA** : **trialkoxysilane derivatives**: **NVP**= 10 : 80 : 10 wt%, **TL203** (35 wt% to matrix compounds), and **KC-DPI** (0.2 wt% - 2 wt%).

References

[1] Y. H. Cho, C. W. Shin, N. Kim, B. K. Kim, and Y. Kawakami, "High-perfromance holographic gratings via different polymerization rates of dipentaerythritol acrylates and siloxane-containing epoxides", *Chemistry of Materials*, **17**,6263 (2005).

[2] Y. H. Cho and Y. Kawakami, "High performance holographic polymer dispersed liquid crystal systems using multi-functional acrylates and siloxane-containing epoxides as matrix components", *Applied Physics A*, **83**, 365 (2006).

[3] Y. H. Cho and Y. Kawakami, "A novel process for holographic polymer dispersed liquid crystal system via simultaneous photopolymerization and siloxane network formation", *Silicon Chemistry*, **3,** 219 (2007).

Oral Sessions 2 & 3

July 14 (Sat)

[13:45 –15:30,

16:30 – 18:45]

IL03

DEVELOPMENT OF CATALYTIC COMPOSITES FOR REMOVAL OF HAZARDOUS COMPOUNDS FROM WATER

Nguyen Van Noi, Tran Thi Nhu Mai, Bui Quynh Trang

Faculty of Chemistry, Hanoi University of Science, 19 Le Thanh Tong St., Hanoi

Introduction

Heterogeneous photocatalysis using TiO_2 semiconductor has been found very effective for the achievement of complete mineralization of many organic molecules dissolved in water by advanced oxidation processes (AOPs). Conventional oxidation treatment has found difficulty to oxidize dyestuffs and complex structure of organic compounds at low concentration or if they are especially refractory to the oxidants. AOPs are considered to be an alternative water treatment technology for treating textile wastewater. The textile industry's dyeing operations are of primary environmental concern, due to the variety of toxic chemicals used in the dyeing of garments. The removal of colour from textile industry and dyestuff manufacturing industry wastewaters represents a major environmental concern. Color itself is increasingly being regulated, as there have been links to aquatic toxicity and lower DO (dissolved oxygen) values in receiving streams.

There is a strong synergy between silica and titania as a combined oxide. For substances that are easily adsorbed to the silica surface, a higher decomposition rate was found with TiO_2 - SiO_2 composites versus a plain TiO_2 slurry. The presence of an adsorbent was considered to promote efficiency by increasing the concentration of the substrate near the TiO_2 sites relative to the solution concentration.

Silica gels play the basic role of dispersion and support for TiO_2. Silica gels have many advantages over other materials as catalyst supports. The transparency of silica allows the penetration of photons to the catalyst surface. This is extremely beneficial and allows for a fixed-bed reactor design that can be highly efficient in relation to input energy. Silica also has high mechanical strength, thermal stability, and can be synthetically formed into any shape, such as cylindrical pellets. Furthermore, TiO_2 and SiO_2 can be chemically combined, enabling the formation of highly efficient photocatalysts. These TiO_2 - SiO_2 photocatalysts allow the placement of the catalyst on both external surfaces and internal surfaces within the porous silica matrix where pollutants are adsorbed.

The goal of any AOPs design is to generate and use hydroxyl free radical (HO•) as strong oxidant to destroy compound that can not be oxidized by conventional oxidant. While UV use or an oxidant alone may yield partial degradation of a compound, the combined use of UV with an oxidant and a photocatalyst has been shown to yield complete mineralization of organic contaminants to carbon dioxide. When the surface of the photocatalyst absorbs a specific amount of energy, an electron from the valence band jumps to the conduction band, thereby leaving a positive "hole" in the valence band. These electrons (e^-) and holes (h^+) may either recombine, releasing heat, or migrate to the surface of the catalyst. The reactive oxidative species are then generated from reactions with the electrons or holes on the surface.

Experimental

Silica-titania composites were made using a sol-gel method that allows the doping of titania during gelation. Gels were prepared by the acid-catalyzed hydrolysis of tetraisopropyl orthotitanate (TIOT) and tetraethoxysilane (TEOS). The gelation rate was increased by use of acid catalysts and allowed the composites to be made into pellets with sufficient dispersion of TiO_2 within the silica matrix. The solution of TIOT/TEOS mixture with the desired Ti/Si ratio was added dropwise to a solution of anhydrous 2-propanol and concentrated HC1 at 0^0C. The resulting solution was stirred in an ice bath. The mixture was allowed to age at room temperature in a covered beaker for ten days after gelling. Solvent was then removed under vacuum, and while still under vacuum, the catalysts were heated to 103^0C for 18 hours and then to 180^0C for 6 hours. The resulting glassy material was ground in a mixer mill.

The prepared titania/silica particles were analyzed by X-ray diffraction patterns on D8/Advance X-ray diffractometer (Bruker). The major phase of the photocatalyst is pure anatase without brookite and rutile.

Results and Discussion

The photocatalytic ability of a TiO_2 catalyst is foremost affected by the anatase content and by the size of the crystal. This could be due to the larger migration distance of the holes and electrons to the surface of the catalyst, thereby decreasing the possibility of recombination. Modifications in the catalyst surface have also been investigated for prevention of electron-hole recombination.

The photoreactor consists of a 500 ml cylindrical glass body with sampling port, gas outlet port and gas inlet at the bottom of the glass body. A 300W UV lamp was located in the center of the reactor. The photocatalytic activity of a catalyst was evaluated by measuring the loss of red reactive azo dye RR. The UV exposure time was 90 minutes, and the percentage of decomposed RR was calculated by comparing the absorption (ABS) of initial and final solutions at RR's absorption peak of 525 nm. Experiments with 50 ppm and 100 ppm solutions of RR were prepared in similar ways. The results showed that more than 99 percents of RR was decomposed after 120 minutes of irradiation in two solutions above.

Conclusions

AOPs represent a powerful treatment for refractory and/or toxic pollutants in textile wastewaters. The silica-titania composites produced by sol-gel methods are a very efficient photocatalyst for AOPs in the destruction of some azo dyes in textile wastewater. These materials combine the photocatalytic properties of TiO_2 and the adsorptive properties of SiO_2. These results confirm and reinforce that photodegradation of dyes is closely related to the adsorption of dyes on the surface of the TiO_2 particles, and the degradation takes place at or near to the TiO_2 particle surface, rather than in the bulk solution.

Acknowledgment

This work was supported by the National Fundamental Research Program (Project 5.079.06).

References

1. Hu Chun, Wang Yizhong, Tang Hongxiao, Preparation and characterization of surface bond-conjugated TiO2/SiO2 and photocatalysis for azo dyes, Applied Catalysis B: Environmental 30 (2001) 277–285.
2. Carl Anderson and Allen J. Bard, Improved Photocatalytic Activity and Characterization of Mixed TiO2/SiO2 and TiO2/Al2O3 Materials, J. Phys. Chem. B (1997), 101, 2611-2616.

IL04

DESIGN AND SYNTHESIS OF FLUOROIONOPHORES AND SURFACE-BASED SENSORS FOR THE DETECTION OF LITHIUM AND AMMONIUM IONS

Nantanit Wanichacheva[1], Christopher R. Lambert,[2] W. Grant McGimpsey[2*]
[1] *Department of Chemistry, Faculty of Science, Silpakorn University, 6 Rachamankanai Road, Nakorn Pathom 73000, Thailand*
[2] *Department of Chemistry and Biochemistry, Worcester Polytechnic Institute, 100 Institute Road, Worcester, Massachusetts 01609, USA*

New ionophores and a fluoroionophore were designed based on the fundamental requirements for ion-ionophore complexation, such as size fit requirements and electrostatic interactions. Ionophores and a fluoroionophore in this work were used in two different formats; bulk organic solution and gold surface modified electrodes.

Monitoring of lithium ion in blood is necessary for patients who suffer from manic depressive and hyperthyroidism illnesses and who are treated with lithium salts. In this lithium fluoroionophore work[1], a major motivation was to design of a fluoroionophore with a high sensitivity and selectivity with a significantly reduced synthetic effort. 21-(9-Anthrylmethyl)-4,17,13,16-tetraoxa-1,10,21-triazabicycle [8.8.5]tricosane-19,23-dione (**I**) was synthesized and characterized as a fluoroionophore for the selective, optical detection of lithium ions. The compound was prepared in a conventional four step synthesis. In this synthetic strategy, the cyclization step was the most difficult step. The concentration of reagents in this reaction played an important role because the reactants needed to be dilute to avoid dimerization and polymerization; however, the reaction needed an appropriate concentration to provide a good yield. The concentration found to be optimum for this reaction was 2 mmole solute per 100 mL solvent, providing 70 % yield product.[1]

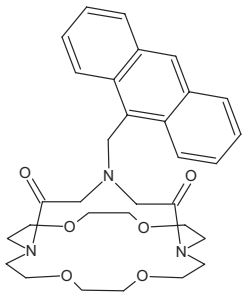

I

I is based on a bridged diazacrown structure, which provides a semi-rigid binding framework. The molecular dynamics calculations predict high selectivity of **I** for lithium ions over sodium and potassium ions. In bulk organic solution, **I** can be used to selectively complex with lithium ions in organic solutions and act as a fluoroionophore. In the absence of ion, the fluorescence of the anthryl group is substantially quenched by intramolecular photo induced electron transfer from the free electron pair of the nitrogen atom at the amine bridge and/or in the amide groups to the anthryl group. In the presence of a complexed ion, the electric field of the ion disrupts the PET process, causing a substantial increase in anthryl fluorescence emission in which the magnitude of sensitivity is relative to the type and concentration of the ions. The lithium–fluoroionophore complexation illustrates very high sensitivity. In a 3:1 dichloromethane/tetrahydrofuran solvent mixture, **I** acts as an intramolecular electron transfer "off-on" fluorescence switch, exhibiting a greater than 190-fold enhancement in fluorescence emission intensity in the presence of lithium ions over the non-complexed fluoroionophore. This enhancement in sensitivity could due to efficient PET from the amine bridge and/or amide groups, as well as the location of the ion relative to the electron lone pair on the amine nitrogen atom and to the anthryl fluorophore. The effect of

charge density on the electrostatic interaction between the metal ion and the nitrogen lone pair is strongly distance dependent. The shorter distance between the bound ion and the lone pair of the nitrogen atom leads to a stronger electrostatic interaction and results in more effective interference with the electron transfer quenching process, providing the enhancement in the fluorescence response. In addition to distance effects, the enhancement in sensitivity of **I** compared to other systems[2,3], such as 9-anthryl-calix[4]arene-azacrown-3 which have aromatic moieties is due to elimination of the interaction between the ion and the π–system. The interaction between the ion and the π–system of the phenyl ring results in a reduction in the fluorescence response. The magnitude of sensitivity of the metal ion-fluoroionophore complex in **I** is governed by electrostatic interaction, particularly with the azacrown oxygen atoms and the oxygen atoms of carbonyl groups in the molecule.

The relative selectivity is expressed as log K, where more negative values indicate higher selectivity. Based on the observed fluorescence behavior, the selectivity was calculated to be $\log K_{Li+,Na+} = -3.36$ and $\log K_{Li+,K+} = -1.77$. These values are regarded as lower limits due to the limited solubility of the sodium and potassium salts used in the experiments. Compound **I** also exhibits selectivity for ammonium ions over sodium and potassium ions ($\log K_{NH4+,Na+} = -1.59$, $\log K_{NH4+,K+} = -1.34$). The selectivity of this compound is due to the size fit approach where the cavity of compound provides appropriate size fit to lithium ion and too small for sodium, potassium and ammonium ions.

According to the design and the experimental results of this fluoroionophore, it can lead us to design a future system which can be achieved by conventional synthesis, provide high sensitivity and selectivity for cations. For example, the bicyclic-diazacrown can be easy synthesized by conventional approach as well as the absence of aromatic ring in the bicyclic-diazacrown structure can eliminate the cation-π interaction and will result in the high sensitivity. The size of the diazacrown ring can be changed to provide appropriate size fit for bigger ions such as potassium; therefore, it can provide the enhancement in the selectivity.

Ultimately, our goal is to build a sensor that can be used in aqueous environments and to do this, the ionophore moiety was synthesized in such a way to attach the moiety to the gold surface in order to monitor the transduction mechanism in aqueous media. Self-assembled monolayers (SAMs) can provide the potential applications in sensor technology; specifically in our work are microfluidic sensor applications. This technology is focused on the use of SAMs for the selective recognition of guests, and the transduction of the binding into a detectable signal, such as an electrochemical signal.[4] We had reported the successful work of a lithium fluoroionophore (**I**) which provide the high selectivity for lithium against the interfering ions. Here, we also presented the further work and the results for a lithium sensor fabricated as a self-assembled monolayers (SAM) electrode on a gold surface.[5] The SAM comprises a single molecular layer of a bicyclic structure shown in figure below.

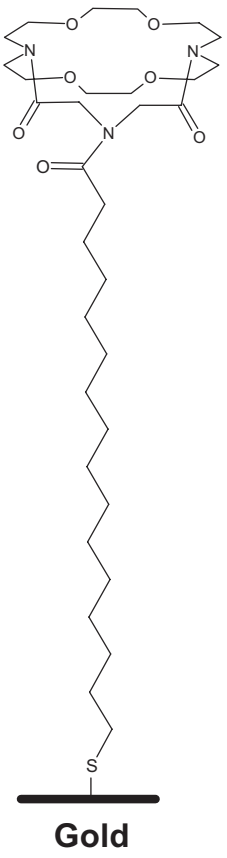

21-(16-Mercaptohexadecan-1-oyl)-4,7,13,16-tetraoxa-1,10,21-triazabicyclo-[8.8.5]tricosane-19,23-dione (**II**) was synthesized in six steps using conventional methods. This compound was used to prepare as a self-assembled monolayer (SAM) on gold. Characterization of a gold surface modified with **II** was carried out by sessile drop contact angle goniometry, ellipsometry, and grazing angle FT-IR spectroscopy. Self-assembled monolayers of hexadecanethiol coupled to a bicyclic molecule (**II**) are able to bind cations from aqueous solutions. The binding of cations affects the dielectric constant of the layer, resulting in an increase of the monolayer capacitance. The ability of these monolayers to function as sensors was observed by cyclic voltammetry and impedance spectroscopy techniques. Impedance experiments in the absence of a redox probe (i.e., only supporting electrolyte) provides reproducible data that shows a change in monolayer capacitance upon ion complexation. The films of **II** show selectivity for complexation of lithium ions over sodium and potassium ions, with log $K_{Li+,Na+}$ = -1.30 and log $K_{Li+,K+}$ = -0.92. To the best of our knowledge, this is the first demonstrations of lithium sensors fabricated using self-assembled monolayer technology.

Ammonium ions are the metabolite from urea and creatinine from blood sample, which used as an important disease indicator; therefore, continuous monitoring of ammonium ion is sometimes required. In a previous works, we had the successful design of ammonium ionophore based on a cyclic depsi-peptide structure.[6] This ionophore was incorporated into a plannar ion-selective electrode sensor format, which provide selectivity for ammonium ion against the interfering ions, sodium and potassium ions, log $K_{NH4+,Na+}$ ~ -2.1 and log $K_{NH4+,K+}$ ~ -0.6.[6] Here is the report of a ammonium sensor fabricated from a self assembled monolayer on gold. The SAM comprises a single molecular layer of a cyclic depsi-peptide structure shown in the figure below.

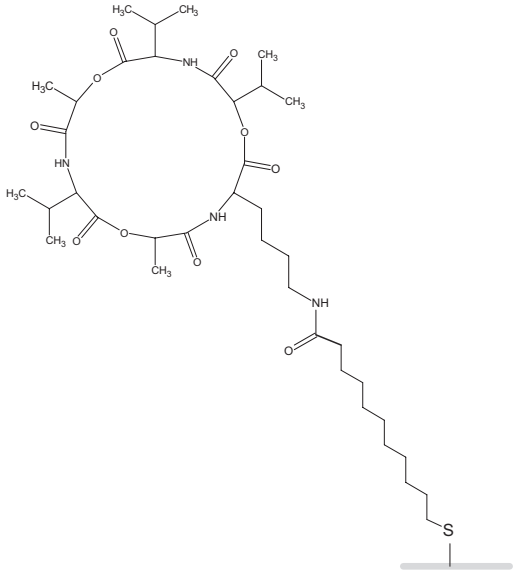

11-Mercapto-*N*-(4-(9,15,18-triisopropyl-6,12-dimethyl-2,5,8,11,14,17-hexaoxo-1,7,13-trioxa-4,10,16-triazacyclooctadecan-3yl)butyl)undecanamide (**III**) was synthesized in fifteen steps with an orthogonal protecting group strategy. The several steps in the synthesis are partly due to the many protection and de-protection steps required to build the structure. SAMs of **III** were prepared on gold and the characterization of the SAMs was carried out by sessile drop contact angle, ellipsometry, grazing angle FT-IR spectroscopy and electrochemical techniques. The cation recognition properties of the SAM were studied by impedance spectroscopy. The films show moderate selectivity for detection of ammonium ions in aqueous solution over potassium and sodium ions, with selectivity values calculated to be log $K_{NH4+,Na+}$ ~ -1.23 and log $K_{NH4+,K+}$ ~ -1.17. The selectivity of this sensor for ammonium ions over potassium ions was somewhat higher for this compound than for nonactin (log $K_{NH4+,K+}$ ~ -0.9), a compound used for detection of ammonium ions in commercial ion selective electrodes. To the best of our knowledge, this is the first demonstration of an ammonium sensor fabricated using self-assembled monolayer technology.

References:

1. Wanichecheva, N.; Benco, J. S.; Lambert, C. R.; McGimpsey, W. G. *Photochem. Photobiol.* **2006**, *82*, 268-273.
2. Benco, J. S.; Nienaber, H. A.; McGimpsey, W. G. *J. Photochem. Photobiol., A.* **2004**, *162*, 289-296.
3. Benco, J. S.; Nienaber, H. A.; Dennen, K.; McGimpsey, W. G. *J. Photochem. Photobiol., A.* **2002**, *152*, 33-40.
4. Flink, S.; Van Veggel, F. C. J. M.; Reinhoudt, D. N. *Sensors Update* **2001**, *8*, 3-9.
5. Wanichacheva, N.; Soto, E. R.; Lambert, C. R.; McGimpsey, W. G. *Anal. Chem.* **2006**, *78*, 7132-7137.
6. Benco, J. S.; Nienaber, H. A.; McGimpsey, W. G. *Anal. Chem.* **2003**, *75*, 152-156.

IL05

GAS TRANSPORT PROPERTIES OF POLYIMIDE ULTRATHIN MEMBRANES

H. Kawakami

Dept. of Applied Chemistry, Tokyo Metropolitan University, Hachioji, Tokyo 192-0397, Japan
Phone: +81-426-77-1111 (Ext) 4972, Fax: +81-426-77-2821, E-mail: kawakami-hiroyoshi @c.metro-u.ac.jp

Introduction

The gas separation process using polymer membranes has received much attention, because the membrane systems provide better energy efficiency than conventional separation methods. Many polymers have been synthesized to control the gas permeability and selectivity of the polymer membranes, because the ability to achieve such control provides a good understanding of the relationships between the chemical structure of polymers and the gas permeation property. However, many studies of the structure/permeability relationships of polymer membranes have led to the trade-off correlations between the gas permeability and selectivity, which have become a major problem in realizing a gas separation process using polymer materials. Therefore, an important objective for the gas separation membrane is the development of new polymer membranes combining high gas permeability and selectivity.

Recently, we reported the gas permeability through an asymmetric polyimide membrane with a thin and defect-free skin layer prepared by a dry-wet phase inversion process.[1-5] We succeeded in preparing an asymmetric polyimide membrane with an ultrathin and defect-free skin layer (10nm) having a significantly high gas permeance. Additionally, we reported that the gas selectivities of an asymmetric polyimide membrane with a defect-free skin surface oriented by shear stress without a coating process increased with an increase in the molecular orientation of the polyimide. This result indicates that an asymmetric membrane with a modified ultrathin and defect-free skin layer would enhance both the gas permeability and selectivity.

This presentation focuses on an organic-inorganic hybrid membrane, which exhibits an asymmetric structure consisting of a carbonized skin layer and a polymeric porous substructure, used to synthesize a novel gas separation membrane combining high gas permeability and selectivity. It is well known that ion-beam irradiation can directly modify the surface of a membrane and that the polymer surface irradiated with high ion fluence is carbonized.[6,7] This means that the ion irradiation can only carbonize a thin surface skin layer, while the pyrolysis of a polymer at high temperature degrades the entire volume. We prepared an asymmetric polyimide membrane with a thin skin layer carbonized by the ion-beam irradiation. The asymmetric membrane with the carbonized skin layer was characterized by being tough and having a good mechanical property, and the ultrathin and defect-free carbonized skin layer realized both a high gas permeability and selectivity.

Experimental Section

The polyimide, 6FDA-6FAP, was synthesized by chemical imidization of the poly(amic acid) precursors as reported in the literature.[8,9] The structures of 6FDA-6FAP are shown in Scheme 1. The synthesized 6FDA-6FAP had an Mw of 3.2×10^5 with a polydispersity index of 2.1.

To investigate the effects of the skin layer thickness on the gas permeation properties of the asymmetric polyimide membrane, membranes with a different skin layer, approximately 100 nm and 4mm, were prepared by a dry/wet phase inversion process.[1,2,10]

Ion-beam irradiation is a physico-chemical surface-modification process resulting from the impingement of a high-energy ion beam (Riken ion implanter, Riken, Saitama, Japan). The ion depth through the top skin layer was regulated by changing the ion specie and its energy. In this study, ion irradiation was performed on polyimide membranes and He^+ was used. Ion irradiation was carried out on a 2 x 2 cm^2 surface area at an energy of 50 keV with a fluence ranging from 1×10^{12} to 3×10^{15} ions/cm^2.

Gas permeances of carbon dioxide, oxygen, methane, and nitrogen were measured with a high vacuum apparatus (Rika Seiki, Inc., K-315-H, Tokyo, Japan). The gas permeation measurements of the membranes were carried out at 35°C and 76cmHg. The apparent skin layer thickness of the asymmetric polyimide membranes was calculated from

$$L = \frac{P}{Q} \qquad (1)$$

where L [cm] is the apparent skin layer thickness, P [cm^3 (STP)cm/(cm^2 sec cmHg)] is the gas permeability coefficient measured from the dense polyimide flat membrane, and Q [cm^3 (STP)/(cm^2 sec cmHg)] is the gas permeance of the asymmetric polyimide membranes. L was determined from the oxygen permeability coefficient.

Results and Discussion

The changes in the chemical structures of the H^+-irradiated polyimide surface were analyzed by attenuated total reflection. Figure 1 shows the ATR-FTIR spectra of the asymmetric polyimide membranes before and after ion irradiation. The He^+ irradiation was carried out on the polyimide surface at 50 keV with a fluence of 3×10^{15} ions/cm^2. The normal line represents the spectrum of the virgin asymmetric membrane, and the bold line represents the spectrum of the irradiated asymmetric membrane. There was a significant difference in the absorbance between the virgin and irradiated membranes. Ion-beam irradiation induced changes in the chemical structure of the polyimide surface, and the changes strongly depended on the ion fluence. The spectra show the changes in the characteristic absorbance of the carbonyl (1720 cm^{-1}), CF_3 (1200-1250 cm^{-1}), imide (1376 cm^{-1}), and aromatic (1500 cm^{-1}) groups. The absorbance intensities were significantly reduced.

Figure 2 shows the Raman spectra of the asymmetric polyimide membranes irradiated by a 50 keV He^+ with 1×10^{15} and 3×10^{15} ions/cm^2. The peaks at 1240, 1380, 1620, and 1780 cm^{-1} correspond to C-F_3, C-N, and C=C in the aromatic ring, and C=O, respectively. After the irradiation of a 50 keV He^+ at

a fluence of 1 x 10^{15} ions/cm^2, these peaks on the polyimide surface disappeared. However, two broad peaks on the polyimide surface irradiated at a fluence of 3 x 10^{15} ions/cm^2 appeared at around 1360 and 1580 cm^{-1}. These peaks correspond, respectively, to the well-known D and G broad bands of disordered graphitic materials, indicating that the surface on the membrane changed to a carbon-enriched material.

Both the gas permeance and selectivity of the asymmetric polyimide membranes strongly depended on the He^+ fluence, as shown in Table 1. The O_2 and CO_2 permeances of the asymmetric membranes irradiated at the fluence of less than $1x10^{13}$ (ions/cm^2) increased when compared with the asymmetric membrane before the ion irradiation. In contrast, the permeances of the asymmetric membranes irradiated at the fluence of more than $1x10^{14}$ (ions/cm^2) decreased with an increase in the He^+ fluence. In particular, the asymmetric membrane irradiated at $3x10^{15}$ (He^+/cm^2) indicated significantly decreased gas permeances, and the O_2 and CO_2 permeances in the membrane showed 59 % and 48 % reductions, respectively, when compared with those of the asymmetric membrane before ion irradiation. On the other hand, the (O_2/N_2) and (CO_2/CH_4) selectivities in the asymmetric membrane irradiated at the fluence of more than $1x10^{14}$ (ions/cm^2) increased with an increase in the He^+ fluence. It should be noted that the (O_2/N_2) and (CO_2/CH_4) selectivities in the asymmetric membrane irradiated at $3x10^{15}$ (He^+/cm^2) resulted in 63 % and 163 % increases, respectively, when compared with those of the asymmetric membrane before ion irradiation.

Generally, the more common polymer membranes show a decreasing trend of polymer selectivity with increasing permeability. CMS membranes also lead to the trade-off correlations between the gas permeability and selectivity. Singh-Ghosal reported that the partially carbonized polyimide membranes during pyrolysis showed a significantly high gas permeability compared with the virgin polyimide membrane and that the finally pyrolyzed membrane did a large increase in the gas selectivity with the low gas permeability. The behaviors of the gas permeability and selectivity of the He^+-irradiated asymmetric

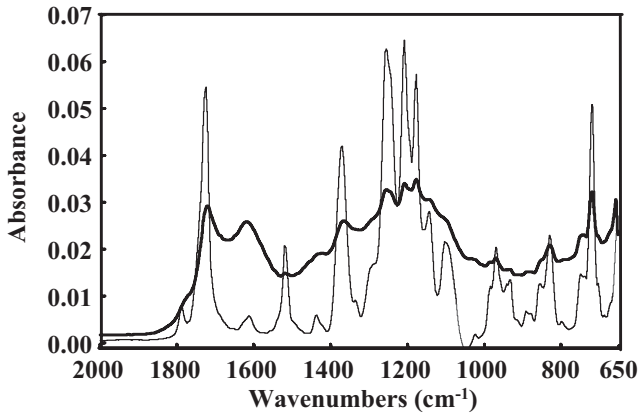

Fig. 1 ATR-FTIR spectra of asymmetric polyimide membranes. (—) Virgin; (▬) He^+-irradiation at $3x10^{15}$ions/cm^2.

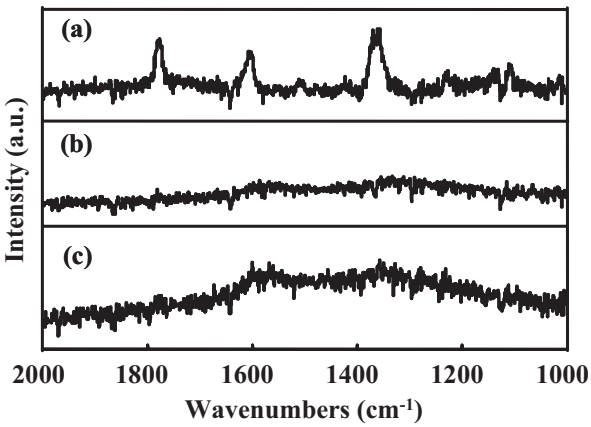

Fig. 2 Raman spectra of asymmetric polyimide membranes:
(a) Virgin
(b) He^+-irradiation at $1x10^{15}$ ions/cm^2
(c) He^+-irradiation at $3x10^{15}$ ions/cm^2.

polyimide membranes were also similar to those of the CMS membranes.

It is desirable to prepare a polymer membrane with both a high gas permeability and selectivity for gas separation. The ion-irradiated asymmetric polyimide membrane prepared in this study showed interesting gas permeation results, and we consider that the ion irradiation would be one of the important membrane fabrication techniques for realizing a high gas permeability and selectivity.

Table 1 Effect of He^+ fluence on gas permeance and selectivity of He^+-irradiated asymmetric polyimide membranes at 35℃ and 76cmHg.

He^+ fluence ($ions/cm^2$)	QO_2	QCO_2	QO_2/QN_2	QCO_2/QCH_4
Virgin	**8.0**	**28**	**4.8**	**30**
$1x10^{12}$	**10.0**	**35**	**4.8**	**32**
$1x10^{13}$	**10.0**	**37**	**4.6**	**32**
$1x10^{14}$	**7.4**	**27**	**4.6**	**30**
$1x10^{15}$	**5.4**	**22**	**6.7**	**59**
$3x10^{15}$	**3.3**	**15**	**7.8**	**79**

Apparent skin layer thickness is 80±3.7nm.
Q: 10^{-5} [cm^3(STP)/(cm^2 • sec • cmHg)]

References

[1] Kawakami, H.; Mikawa, M.; Nagaoka, S. *J. Appl. Polym. Sci.,* 1996, 62, 965.

[2] Kawakami, H.; Mikawa, M.; Nagaoka, S. *Macromolecules*, 1998, 31, 6636.

[3] Niwa, M.; Kawakami, H.; Nagaoka, S.; Kanamori, T.; Shinbo, T. *J. Membr. Sci.,* 2000, 171, 253.

[4] Niwa, M.; Kawakami, H.; Kanamori, T.; Shinbo, T.; Kaito, A.; Nagaoka, S. *Macromolecules*, 2001, 34, 9039.

[5] Niwa, M.; Kawakami, H.; Kanamori, T.; Shinbo, T.; Kaito, A.; Nagaoka, S. *J. Membr. Sci.,* 2004, 230, 141.

[6] Ektessabi, A. M.; Hakamata, S. *Thin Solid Films,* 2000, 377-378, 621.

[7] Svorcik, V.; Arenholz, E.; Rybka, V.; Hnatowicz, V. *Nucl. Instr. and Meth. in Phys. Res. B,* 1997, 122, 663.

[8] Kawakami, H.; Anzai, J.; Nagaoka, S. *J. Appl. Poly. Sci.,* 1995, 57, 789.

[9] Kawakami, H.; Mikawa, M.; Nagaoka, S. *J. Membr. Sci.,* 1996, 118, 223.

[10] Pinnau, I.; Wind, J. W.; Peinemann, K.-V. *Ind. Eng. Chem. Res.,* 1990, 29, 2028.

OL03

Synthesis and Gas Permeation Properties of Poly(diphenylacetylene) Derivatives

Toshikazu Sakaguchi[1,*], Toshio Masuda[2], Tamotsu Hashimoto[1]

[1]*Graduate School of Engineering, University of Fukui*

[2]*Graduate School of Engineering, Kyoto University*

Introduction

Polyacetylenes having various substituents have been synthesized by using transition metal catalysts [1]. Among those polymers, poly[1-(trimethylsilyl)-1-propyne] [poly(TMSP)] is the most permeable polymer. Its oxygen permeability coefficient (PO_2) is ca. 10,000 barrers at 25 °C [2]. The extremely high gas permeability of poly(TMSP) is due to possessing large free volume in its membrane. Poly[1-(*p*-trimethylsilyl)phenyl-2-phenylacetylene] [poly(TMSDPA)], which obtained by the polymerization with $TaCl_5$–*n*-Bu_4Sn, shows high gas permeability; its PO_2 value reaches 1500 barrers at 25 °C [3].

The PO_2 value of poly[2,4,5-tris(trifluoromethyl)phenylacetylene] [poly(TTFMPA)] is 780 barrers [4], from which it can be said that this polymer is the most gas-permeable among poly(phenylacetylene) derivatives. In general, the gas permeability of mono substituted acetylene polymers such as poly(phenylacetylene)s is appreciably lower than that of disubstituted acetylene counterparts such as poly(diphenylacetylene)s. Therefore, fluorine-containing poly(diphenylacetylene)s are expected to show high gas permeability.

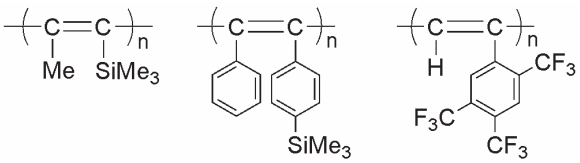

Poly(TMSP) Poly(TMSDPA) Poly(TTFMPA)

Results and Discussion

Poly[1-(*p*-trimethylsilyl)phenyl-2-phenylacetylene]s [poly(TMSDPA)] having fluorines (F), chlorines (Cl), bromines (Br), and methyl groups (Me) (**2a**–**d**) and studied their properties including gas permeability (Scheme 1). High-molecular-weight polymers were obtained in good yields by the polymerization of corresponding

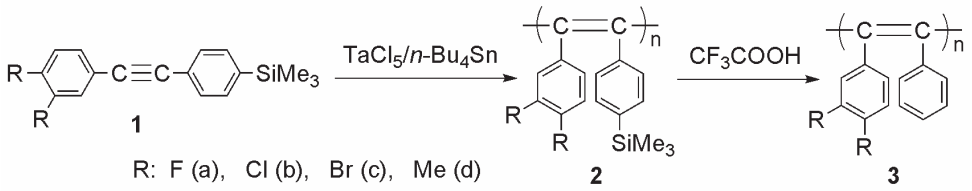

Scheme 1. Synthesis of poly(diphenylacetylene) derivatives

acetylene monomers (**1a**–**d**) with $TaCl_5$–*n*-Bu_4Sn (Table 1). These polymers dissolved in common organic solvents such as toluene and $CHCl_3$, and afforded free-standing membranes by casting them from toluene solution. Membranes of Si-containing polymers (**2a**–**d**) were desilylated with trifluoroacetic acid to afford membranes of poly(diphenylacetylene)s [poly(DPA)] having F, Cl, Br, and Me (**3a**–**d**).

The densities of F-, Cl-, and Br-containing polymers were larger than those of Me-containing polymers. The FFVs of membranes of **2a**–**c** were extremely large (0.29–0.31), which are obvious larger than that of poly(TMSDPA) [FFV = 0.26] [5], while the FFV of membrane of **2d** was somewhat smaller than those of **2a**–**c**. The FFVs of halogen-containing desilylated polymer membranes (**3a**–**c**) were also larger than that of **3d**. These results indicate that incorporation of halogen atoms in poly(TMSDPA) leads to high FFVs of the membranes. The oxygen permeability coefficients (P_{O_2}) of membranes of F-containing poly(TMSDPA) and poly(DPA) were 3600 and 3800 barrers, respectively, which are larger than that of poly(TMSDPA) [P_{O_2} = 1500 barrers]. Membranes of Cl- and Br-containing polymers (**2b**, **2c**, **3b**, and **3c**) also showed high oxygen permeability compared to poly(TMSDPA), and their P_{O_2} values are 2100–5400 barrers. On the other hand, the P_{O_2} value of membranes of Me-containing polymers (**2d** and **3d**) were smaller than that of poly(TMSDPA). It was found that polymer membranes having halogen atoms such as F, Cl, and Br exhibited high gas permeability. High gas permeability of halogen-containing polymers should originate from the large free volume of membranes.

Table 1. Polymerization of Monomers [a]

	polymer [b]		
monomer	yield, %	$M_w \times 10^{-6}$ [c]	M_w/M_n [c]
1a	58	1.1	3.1
1b	70	3.8	1.9
1c	69	1.2	3.3
1d	68	4.1	9.0

[a] In toluene at 80 °C for 24 h; $[M]_0$ = 0.20 M, $[TaCl_5]$ = 20 mM, [*n*-Bu_4Sn] = 40 mM. [b] Methanol-insoluble product. [c] Measured by GPC (polystyrene standard).

Table 2. Densities, FFV, and Gas Permeability coefficients (*P*) [a] of Membranes

	2				**3**			
membrane	density	FFV	P_{O_2}	P_{N_2}	density	FFV	P_{O_2}	P_{N_2}
a	0.94	0.31	3600	2400	1.07	0.31	3800	3000
b	1.01	0.29	5400	3700	1.10	0.31	3000	2000
c	1.21	0.31	2700	1800	1.40	0.32	2100	1300
d	0.874	0.28	1300	730	0.980	0.24	530	290

[a] At 25 °C in the units of 1×10^{-10} cm^3 (STP) cm / (cm^2 s cmHg) (= 1 barrer).

References

[1] T. Masuda, F. Sanda in *Handbook of Metathesis*, R. H. Grubbs, Ed.; Wiley-VCH, Weinheim, 2003; Vol. 3 Chap. 3.11.

[2] K. Nagai, T. Masuda, T. Nakagawa, B. D. Freeman, I. Pinnau *Prog. Polym. Sci.* 2001, 26, 721.

[3] K. Tsuchihara, T. Masuda, T. Higashimura *J. Am. Chem. Soc.* 1991, 113, 8548.

[4] Y. Hayakawa, M. Nishida, T. Aoki, H. Muramatsu *J. Polym. Sci. Part A: Polym. Chem.* 1992, 30, 873.

[5] L. G. Toy, K. Nagai, B. D. Freeman, I. Pinnau, Z. He, T. Masuda, M. Teraguchi, Y. P. Yampolskii Macromolecules 2000, 33, 2516.

IL06

Intramolecular Cyclisation of Enamide Derivatives and Synthesis of Pyrrolidine *trans*-Lactams

I. Novel Radical Based Routes to Pyyrolidine *trans*-Lactams

Anawat Ajavakom[a], Ian Baldwin[b], Jeremy D. Kilburn[c]
[a]Department of chemistry, Faculty of Science, Chulalongkorn University, Bangkok, Thailand
[b]GlaxoSmithKline, Stevenage, UK
[c]Department of chemistry, Faculty of Science, University of Southampton, UK

Pyyrolidine *trans*-lactams **1 (Fig. 1)**, which proved to be HNE inhibitors[1], based on a radical cyclisation mediated by either samarium diiodide or tributyltin hydride were successfully synthesized.

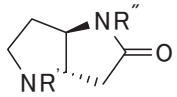

Pyrrolidine *trans*-lactams **1**

Fig. 1

Novel synthetic route towards the target pyyrolidine *trans*-lactams starts from the radical cyclisation of α-aza radicals derived from *N*-(benzotriazolylalkyl) alkenylamines[2] **3** mediated by samarium diiodide to access the *trans*-2,3-disubstituted pyrrolidines **4**. The cyclisation of the pyyrolidine derivatives **4** successfully gave pyyrolidine *trans*-lactam **5**.

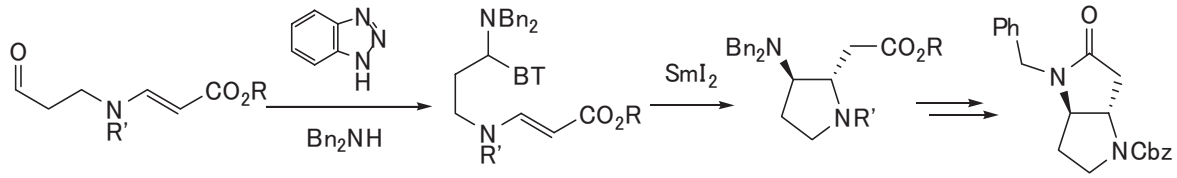

2 **3** **4** **5**

The other strategy to make an α-aza radical, using radical translocation[3]. Efforts were focused on the synthesis of 2,4-dinitrophenyl sulfonamide precursors **6** and **7** and their cyclisations, which failed to give cyclopentyl derivative but only the dehalogenated compound **8**.

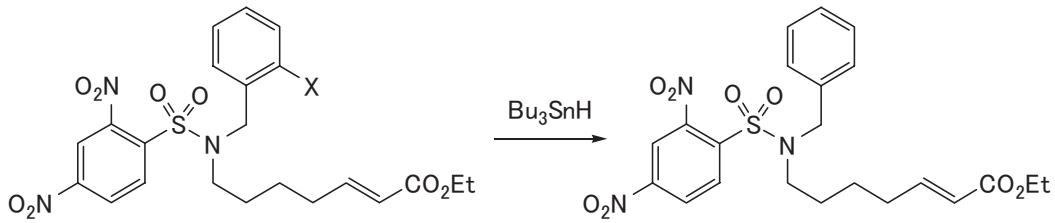

6, X = I
7, X = Br

8

Reference: [1] S. J. F. Macdonald, J. G. Montana, D. M. Buckley, and M. D. Dowle, *Synlett.*, **1998**, 1378.
[2] M. Aurrecoechea, B. Lopez, A. Fernandez, A. Arrieta, and F. P. Cossio, *J. Org. Chem.,* **1997**, *62*, 1125.
[3] D. P. Curran, D. Kim, H. T. Liu, and W. J. Shen, *J. Am. Chem. Soc.*, **1988**, *110*, 5900.

II. Acid-promoted intramolecular cyclisation of enamide derivatives

Kulyanee Hansuthirakul, Thirawat Sirijindalert, Anawat Ajavakom
Department of chemistry, Faculty of Science, Chulalongkorn University, Bangkok, Thailand

In general, oxazolidinones **9 (Fig. 2)** are used as valuable intermediates of natural products and medicines such as antianaerobic agents[1], antibacterials[2], and antibiotics[3], and pyridines are ubiquitous in agrochemicals[4].

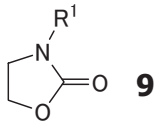

9

Fig. 2

Herein the novel methodology of oxazolidinone synthesis will be presented. The synthesis started from the coupling of **10** and **11**[5] followed by the protection of enamine nitrogen by Boc-group to donate substrate **13** in good yields. The acid-promoted intramolecular cyclisation of enamide substrates gave heterocyclic oxazolidinones **15** and pyridines **16** in moderate yields**,** while the cyclisation of compounds **12** could produce the dihydropyrrole **14**.

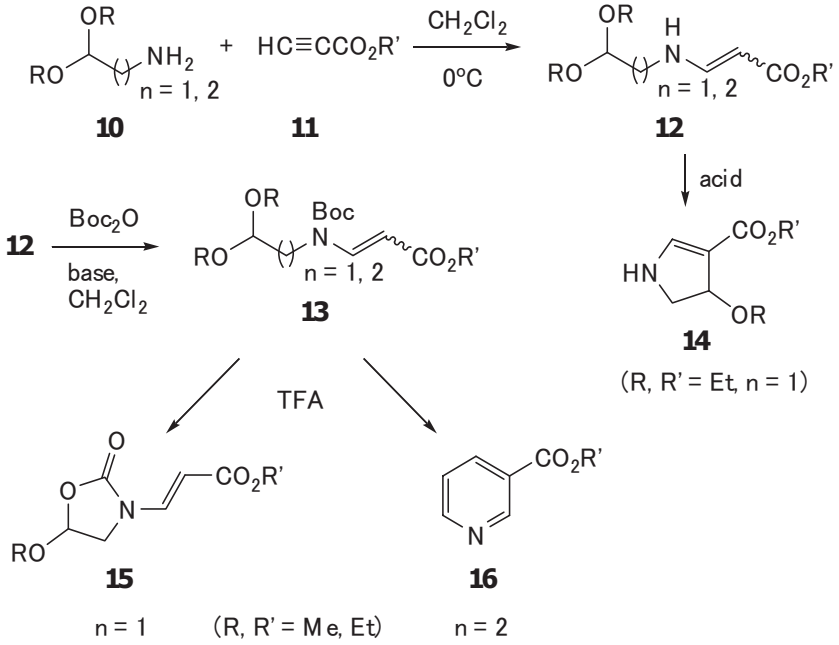

Reference: [1] L. M. Ednie, M. R. Jacobs, and P. C. Appelbaum, *J. Antimicrob Chemother*, **2002**, *50 (1)*, 101-105.
[2] A. Ammazzalorso, R. Amoroso, G. Bettoni, M. Fantacuzzi, B. D. Filippis, L. Giampietro, C. Maccallini, D. Paludi, and M. L. Trica, *IL Framaco*, **2004**, *59*, 685-690.
[3] S. J. Brickner, *Curr.Pharm. Design* **1996**, *2*, 175-194.
[4] G. Matolcsy, Pesticide Chemistry; *Elseviier Scientific*: Amsterdam, Oxford, **1988**, 427-430.
[5] S. J. F. Macdonald, K. Mills, J. E. Spooner, and M. D. Dowel, *J. Chem. Soc. Perkin Trans.1*, **1998**, 3931.

IL07

Development of Novel Polymer-supported Chiral Ligand for Asymmetric Reactions

Shinichi Itsuno,* Yukihiro Arakawa, Atsuko Chiba, Keiichi Tsuru, Naoki Haraguchi

Department of Materials Science, Toyohashi University of Technology

The use of polymer-supported reagent and catalyst always facilitates the reaction process and has become a standard technique in modern organic synthesis. Polymeric species can be easily separated and removed from the reaction mixture by simple filtration. Usually the polymeric catalyst can be recycled many times. In some cases continuous flow reaction system can be operated by means of polymer-supported catalyst. The polymer-support technique is especially useful in asymmetric reactions mainly due to easy recycle use of precious chiral catalyst.[1] We have developed novel polymer-supported chiral ligand for asymmetric reactions including transfer hydrogenation of ketones and imines. Optically active secondary alcohols and amines were easily obtained by using the polymeric chiral catalyst.

Asymmetric transfer hydrogenation of aromatic ketones by means of polymer-supported chiral catalyst in aqueous media

One of powerful enantioselective synthesis of secondary alcohol is asymmetric transfer hydrogenation of ketones. Compared to hydrogenation reactions high pressure of hydrogen gas is not necessary in case of transfer hydrogenation. Hydrogen source in the transfer hydrogenation reaction is 2-propanol or formic acid derivatives. Monosulfonamide of enantiopure 1,2-diphenylethylenediamine is known to be an efficient chiral ligand of the chiral Ru complex, which has been used for the asymmetric transfer hydrogenation of ketones.[2] Excellent enantioselectivities with high yields were obtained in the asymmetric transfer hydrogenation of ketones. We have prepared the polymer-supported version of the Ru complex **P-1** – **P-5**. Since this reaction can be carried out in aqueous media hydrophilic pendant groups such as sulfonate, phosphonate and carboxylate were introduced into the polymer-support. In the presence of **P-1** only a low conversion was attained in water as expected from the highly hydrophobic character of the polystyrene support. On the other hand, the use of sulfonated polymers and phosphonated polymers resulted in remarkable improvement in the reactivity.[3,4] Especially the quaternary ammonium salt of sulfonate effectively enhanced not only the reactivity but also the enantioselectivity. In the case of qurternary ammonium salt of sulfonate as pendant group very high reactivity and enantioselectivity was attained (98% ee). This enantioselectivity is even higher than that obtained using low-molecular-weight catalyst derived from TsDPEN in water. Not only acetophenone

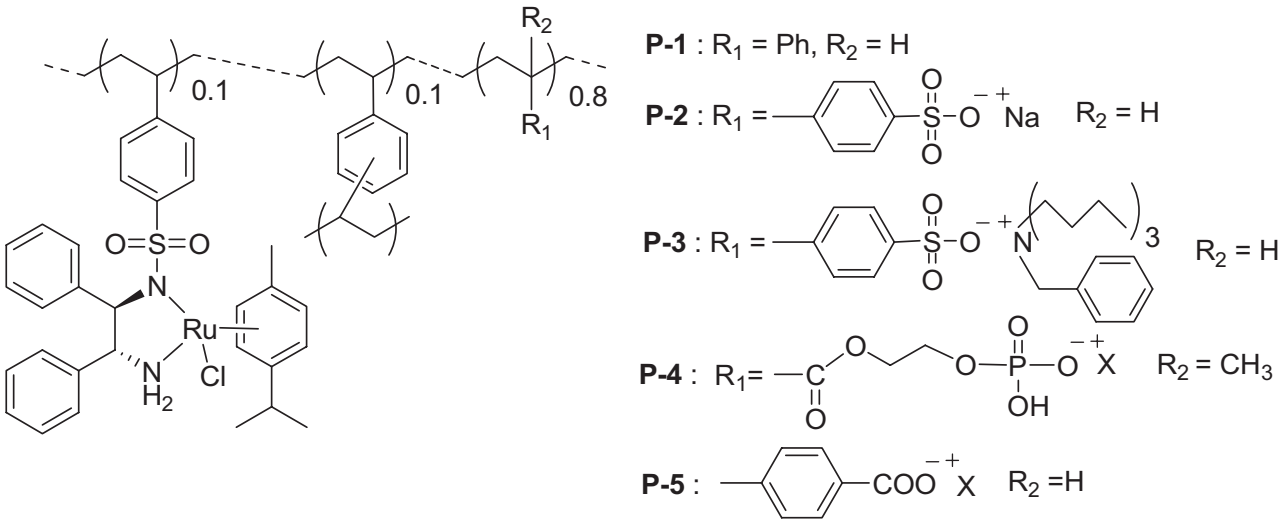

some other aromatic ketones were efficiently reduced to give the alcohols in higher enantioselectivities using polymeric catalyst compared to low-molecular-weight catalyst in solution system. To our knowledge this is the first example of the higher enantioselectivity using the polymeric catalyst in water. No organic solvent is necessary to perform the reaction with these polymeric catalysts. Recycle use of these polymeric catalysts is also possible at least 5 times without decrease of the enantioselectivity.

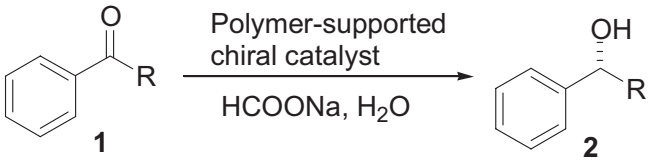

Table 1 Asymmetric transfer hydrogenation of acetophenone with polymer-supported chiral Ru complex

Catalyst	Time, h	Conv. %	Ee %	*Config.*
(*R*,*R*)-**TsDPEN**[1)]	1	52	94	*R*
P-1	17	7	86	*R*
P-2	15	92	91	*R*
P-3	3	100	98	*R*
P-4 (X=H)	22	63	89	*R*
P-4 (X=BTBA)[2)]	3	92	95	*R*
P-5 (X=Na)	20	2	82	*R*
P-5 (X=BTBA)[2)]	20	50	96	*R*

1) Catalyst prepared from (*R*,*R*)-*N*-(*p*-toluenesulfonyl)-1,2-diphenylethylendiamine and $[RuCl_2(p\text{-cymene})]_2$.
2) Benzyltributylammonium salt.

Asymmetric transfer hydrogenation of imines using polymer-supported chiral catalyst

Although optically active amines have been considerably important compounds especially in the synthesis of chiral drugs and naturally occurring compounds, relatively less numbers of researches have been reported on the asymmetric transfer hydrogenation of C=N double bond compounds. We have tested the reaction of *N*-benzylimine **3** under the same reaction condition used for ketone reduction. Unfortunately no reaction occurred by using the polymer-supported catalyst **P-3** having quaternary ammonium sulfonate pendant groups in water. However when the polystyrene-supported catalyst **P-1** was used in organic solvent the same reaction proceeded smoothly to give the corresponding chiral secondary amine **4** in high yield with high enantioselectivity.

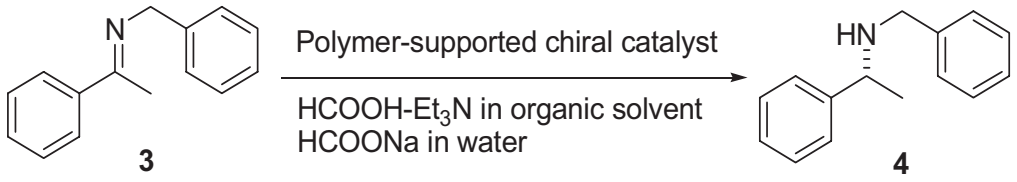

3 **4**

These imines are susceptible to be hydrolyzed to give the parent ketone and benzyl amine. Another *N*-benylimine **5** prepared from tetralone was also reduced to give the corresponding secondary amine. When *p*-methoxy derivative **6** was used its decomposition occurred during the reaction. In the case of the reaction with *N*-phenyl imine **7** derived from acetophenone no reaction occurred under the same reaction condition. In contrast to these imines, cyclic imines are quite stable even in water. For example cyclic imine **8** was treated with sodium formate in water in the presence of polymeric catalyst. The asymmetric transfer hydrogenation by using polymer-supported catalyst occurred smoothly in water using **P-3**. High level of enantioselectivity was successfully obtained. The same reaction also occurred in organic solvent (CH_2Cl_2) if the polystyrene-supported catalyst **P-1** was employed as catalyst.

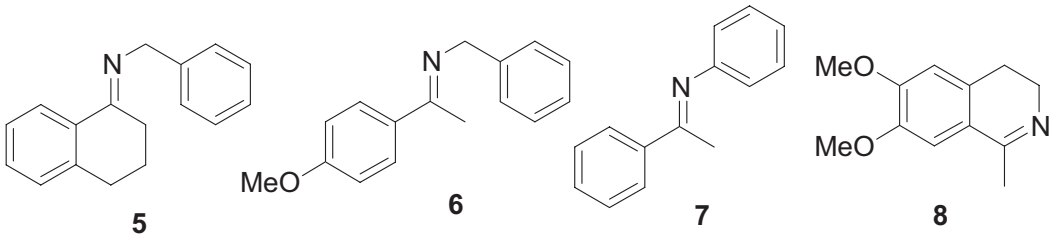

5 **6** **7** **8**

Table 2 Asymmetric transfer hydrogenation of imines by means of polymeric chiral catalyst

Catalyst	Imine	Solvent	Time, h	Conv. %	Ee %	*Config.*
(*R*,*R*)-**TsDPEN**[1)]	**3**	CH_2Cl_2	36	72	77	*R*
P-1	**3**	CH_3CN	36	96	86	*R*
P-2	**3**	CH_2Cl_2	114	3	-	-
P-3	**3**	CH_2Cl_2	24	3	-	-
P-1	**5**	CH_2Cl_2	138	86	49	*R*
P-1	**6**	CH_2Cl_2	24	dec.	-	-
P-1	**7**	CH_2Cl_2	163	0	-	-
P-1	**8**	CH_2Cl_2	24	99	92	*S*
P-1	**3**	H_2O	24	0	-	-
P-3	**8**	H_2O	48	83	91	*S*

1) Catalyst prepared from (*R*,*R*)-*N*-(*p*-toluenesulfonyl)-1,2-diphenylethylendiamine and $[RuCl_2(p\text{-cymene})]_2$.

In summary we have synthesized novel polymer-supported chiral ligand of *N*-sulfonated 1,2-diamine. Complexation with Ru-*p*-cymene smoothly occurred on the polymeric chiral ligand to give the polymeric chiral complex, which could be applied to the asymmetric transfer hydrogenation of ketones and imines. The corresponding enantioenriched alcohol and amines have been obtained with high level of enantioselectivities. Polymer-support containing quaternary ammonium sulfonate pendant groups provided a suitable microenvironment for the asymmetric reaction in aqueous phase mainly due to its hydrophilic character of the polymer. By using the polymeric catalyst developed in this study higher enantioselectivties compared to the low-molecular-weight counter part in solution system were usually obtained.

References

1. Itsuno, S.; Haraguchi, N.; Arakawa, Y. *Recent Res. Devel. Organic Chem.*, **2005**, *9*, 27-47. El-Shehawy, A. A.; Itsuno, S. in "*Current Topics in Polymer Research"* Bregg, R. K. ed. Nova Science Publisher, New York, pp.1-69 (2005).
2. Uematsu, N.; Fujii, A.; Hashiguchi, S.; Ikariya, T.; Noyori, R. *J. Am. Chem. Soc.* **1996**, *118*, 4916-4917.
3. Arakawa, Y.; Haraguchi, N.; Itsuno, S. *Tetrahedron Lett*., **2006**, *47*, 3239-3243.
4. Itsuno, S.; Takahashi, M.; Arakawa, Y.; Haraguchi, N. *Pure Appl. Chem.* **2007**, in press.

IL08

Synthesis and Applications of (Nitrilotriacetic Acid)-End-Functionalized Polystyrene

Su-jeong Kim[1], Hyo Kyoung Lee[1], Ji-Yeon Lee[1], Hong Y. Cho[1], Yu Jin Kim[2],

Sun-Gu Lee[2], Hyun-jong Paik[1*]

[1]Department of Polymer Science & Engineering, Pusan National University,
[2]Department of Chemical Engineering, Pusan National University,
San 30 Jangjundong Kumjunggu, Busan 609-735, Korea

Email: hpaik@pusan.ac.kr

Conjugation of proteins with polymers has been extensively studied because of its wide uses in medicine and biotechnology. One method to bio-conjugate proteins with polymers is to use end-functionalized polymers which have specific reactivity or interaction with targeted proteins. In my presentation, a new approach to bio-conjugate proteins and polymers will be discussed. The developed method is based on the strong interaction with a sequence of histidine residues (His-tag) in genetically engineered proteins and Ni^{2+} complexed nitrilotriacetic acid (NTA) group at the polymer chain end. In our study, green fluorescent protein (GFP) with His-tag was conjugated with Ni^{2+}-NTA end-functionalized polystyrene. His-tagged GFP was expressed in recombinant E. coli BL21 (DE3) and end-functionalized polystyrene was prepared by Atom Transfer Radical Polymerization using NTA containing initiator.

OL04

Grafting of Vinyl Polymers onto Silica Nanoparticles Surface in Solvent-free Dry-system

J. Ueda[1], K. Fujiki[2], T. Yamauchi[1,3,4] and N. Tsubokawa[3,4,5]
[1]*Graduate School of Science and Technology, Niigata University;* [2]*Joetsu University of Education;* [3]*Center for Transdisciplinary Research, Niigata University;* [4]*Center for Education and Research on Environmental Technology, Materials Engineering, and Nanochemistry;* [5]*Faculty of Engineering, Niigata University*

Introduction

Recently the surface modification and the application of surface-modified silica nanoparticles have become of major interest. The scale-up synthesis of polymer-grafted nano-sized particles, however, was hardly achieved in solvent, because the complicated operations are necessary for the isolation of these nanoparticles from the reaction mixture. Therefore, we have designed a solvent-free dry-system for the purpose of the prevention of the environmental pollution and the simplification of reaction process. In this paper, the radical and cationic grafting of several polymers onto the surface of silica nanoparticles in a solvent-free dry-system was investigated.

Experimental

Silica nanoparticle used was Aerosil 200, obtained from Nippon Aerosil Co., Ltd. The introduction of azo groups onto the silica nanoparticle surface was achieved by the reaction of surface amino groups with 4,4'-azobis(4-cyanopentanoic chloride) in the presence of pyridine. The introduction of methoxysulfonyl and iodopropyl groups onto the silica nanoparticle surface was achieved by the treatment of surface silanol groups with 2-(4-methoxysulfonylphenyl)ethyltrimethoxysilane and 3-iodopropyltrimethoxysilane, respectively, in a solvent-free dry-system.

Results and Discussion

In a solvent-free dry-system, monomer was splayed onto silica nanoparticle surface and the reaction was conducted in powder fluid system under nitrogen. After the reaction, unreacted monomer was removed under high vacuum. Table 1 shows the result of the radical graft polymerization of styrene (St) and methyl methacrylate (MMA) initiated by azo groups introduced onto silica surface in a solvent-free dry-system. In the presence of untreated silica and silica-NH_2, PSt and PMMA were scarcely grafted onto surface. On the contrary, it was found that the radical graft polymerization of St and MMA were successfully initiated by azo groups introduced onto the silica surface in solvent-free dry-system. The grafting of PSt and PMMA onto the silica surface was identified by TGA, thermal decomposition GC-MS, and FT-IR.

It is interesting to note that the grafting efficiency (percentage of grafted polymer to total polymer formed) of PSt and PMMA was extremely high, 90~95 %, indicating the depression of formation of ungrafted polymers by the fragment radicals. This may be due to that the graft polymerization precedes only the silica surface.

In addition, it became apparent that the cationic ring-opening polymerization of 2-methyl-2-oxazoline was initiated by methoxysulfonyl and iodopropyl groups introduced onto silica nanoparticles in a solvent-free dry-system to give the corresponding polymer-grafted silica. The grafting efficiency of the cationic grafting in solvent-free dry-system was also high in comparison with that in solvent system.

Table 1 Radical graft polymerization of vinyl monomers initiated by azo groups introduced onto silica nanoparticles surface in solvent-free dry-system

Silica	Monomer	Time (h)	Grafting (%)	Grafting efficiency (%)
Untreated	Styrene	4	Trace	-
Silica-NH_2		4	Trace	-
Silica-Azo		1	8.5	36.0
		2	11.5	55.0
		3	11.6	48.5
		4	11.5	50.0
Silica-Azo	MMA	1	6.0	92.3
		2	6.8	98.6
		3	6.6	93.0
		4	7.0	77.8

Silica-Azo, 8.8 g; monomer 2.5 g; temp., 75 ºC.

OL05

Colloidal Crystallization of Colloidal Silica Modified with Iron(0) Complex-Grafted Polymer in Organic Solvent

Kohji Yoshinaga*, Mahiro Nakano, and Emiko Mouri

Department of Applied Chemistry, Faculty of Engineering, Kyushu Institute of Technology

Sensui, Tobata, Kitakyushu 804-8550, Japan

Recently, periodic particle-arrayed structure is received much attention for application to new devices, i.e. photonic crystal. One of promising approaches to fabrication of the periodic structure is immobilization of colloidal crystals, which are originated by electrostatic repulsion between particles. In this work, colloidal crystallization of silica particles grafted with polymer having a chromophore, ferrocenyl or diene-Fe(0)tricarbonyl complex group, were studied.

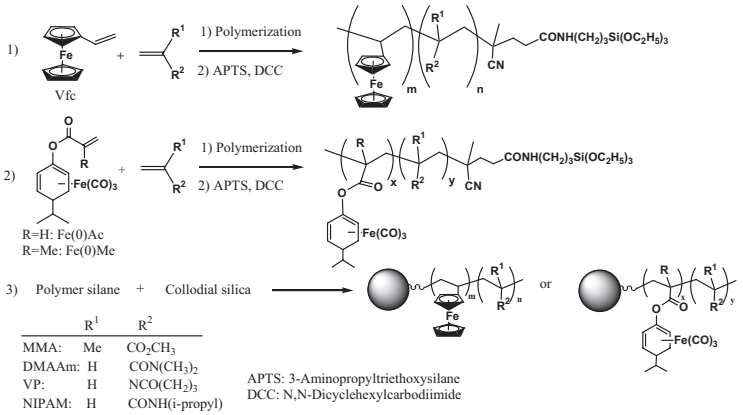

	R^1	R^2
MMA:	Me	CO_2CH_3
DMAAm:	H	$CON(CH_3)_2$
VP:	H	$NCO(CH_2)_3$
NIPAM:	H	CONH(i-propyl)

Scheme 1. Copolymerization and polymer grafting to colloidal silic

Colloidal silica, of 135 nm in diameter, was offered by Catalysts & Chemicals Co. Ltd., Japan. Synthesis of copolymer silane of vinyl ferrocene (Vfc) or iron(0)tricarbonyl(4,4-dimethyl-1,2-cyclohexadienyl) acrylate (FeAc) or methacrylate (FeMc) and vinyl monomer, and grafting to colloidal silica were carried out by the procedure as shown in Scheme 1. Colloidal crystallization was observed by naked eyes or reflection spectrum.

Copolymerization afforded the polymer contained Vfc moiety in molar ratio range of Vfc to vinyl group from 1/3 to 1/25. Although poly(MMA-co-Vfc)- grafted silica never crystallized in organic solvents, poly(DMMAm-co-Vfc)-, poly(VP-co-Vfc)- and poly(NIPAM-co-Vfc)-grafted silica formed colloidal crystals in ethanol, DMF or acetonitrile. Critical volume fractions for the crystallization are listed in Table 1. In the case of poly(NIPAM-co-Vfc)-grafted silica, the silica particles with relatively high fraction of Vfc moiety (Vfc/NIPAM=1/3) resulted in colloidal crystallization in ethanol or DMF. We observed a sharp reflection peak of poly(NIPAM-co-Vfc)/SiO_2 colloidal crystals in ethanol, suggesting formation of stable particle array structure. On the other hand, copolymerization of FeAc or FeMe gave the polymer contained the complex moiety in molar ratio of iron(0) component to vinyl monomer from 1/1 to 1/33. An increase of iron(0) complex fraction in the copolymer resulted in colloidal crystallization in polar solvents, such as DMF (Table 1). Copolymerization of a polar monomer, such as NIPAM or DMAAm, and FeAc gave copolymer having relatively high mole fraction of the complex. The polar copolymer-grafted silica made colloidal crystals in relatively low polar solvents, such as ethanol or acetone. In these cases, it was observed that the suspension containing colloidal crystals exhibited characteristic color; the solution and crystals were colored due to absorption of 300~500 nm bands by the iron(0) complex and Bragg diffraction, respectively.

Table 1. Critical volume fraction in colloidal crystallization of colloidal silica grafted with copolymer composed of Vfc, FeAc or FeMe

Copolymer-modified silica	x/y	Critical volume fraction (ϕ_o)			
		DMF	CH_3CN	Ethanol	Acetone
Poly(MMA-*co*-FeAc)/SiO_2	1/6	0.077	–	–	0.080
Poly(MMA-*co*-FeMe)/SiO_2	1/1	0.104	–	–	–
Poly(NIPAM-*co*-Vfc)/SiO_2	1/3	0.113	–	0.053	–
	1/8	0.073	–	0.046	–
Poly(NIPAM-*co*-FeAc)/SiO_2	1/3	0.100	0.052	–	0.100
Poly(MAAm-*co*-Vfc)/SiO_2	1/13	0.048	–	0.078	–
Poly(DMAAm-*co*-FeAc)/SiO_2	1/5	0.094	–	0.113	–

OL06

Amphiphilic dendron-modified silica particles: synthesis, characterization, and application on organic dye adsorption in water

Chih-Chien Chu,* and Toyoko Imae

Graduate school of science and technology, Keio University, Hiyoshi 3-14-1, kohoku-ku, Yokohama 223-8522, Japan

A successful preparation of novel amphiphilic dendron-modified silica particles composed of lipophilic aliphatic terminals and hydrophilic poly(amido amine) (PAMAM) dendritic backbone has been demonstrated. The synthetic strategy involved: 1) the successive propagation of PAMAM dednrons from inorganic initiator, aminopropyl-terminated silica particles (APS); 2) end-group-functionalization of amino terminals on PAMAM dendrons with n-octadecyl (C18) chains through urea formation. The FT-IR spectra of C18G1, C18G2, and C18G3 dendron-modified silica particles clearly showed the characteristic bands of amide stretching on PAMAM dendrons at 1650 and 1560 cm^{-1} and of methylene stretching on C18 chains at 2930, 2850 cm^{-1}. Moreover, the elemental analyses and thermalgravimetric analyses also confirmed the successful modification on silica surface due to the increasing grafted amounts of organic moieties.

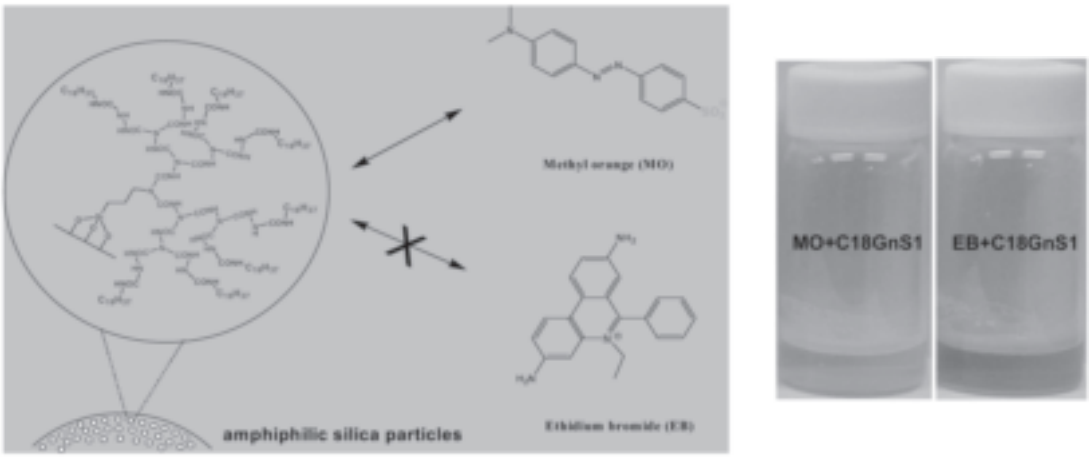

Figure 1. Novel amphiphilic dendron-modified silica particles as solid phase extractor toward organic dyes.

Porous silica and amphiphilic dendrimers can be the efficient adsorbents to remove organic compounds in water. Therefore, the amphiphilic dendron-modified silica particle (C18GnS), potentially combining high loading capacities and host-guest affinity, are regarded as the solid phase extractor for

water purification. Besides, after adsorbing organic compounds, amphiphilic silica particles can be easily separated from aqueous medium by filtration or centrifugation. For the extraction of water-soluble organic dyes, either amphiphilic dendron-modified or bare silica particles (controlled experiment) were added into Methyl orange (MO, anionic dye) and Ethidium bromide (EB, cationic dye) aqueous solution, respectively, and the mixture were allowed to equilibrate for overnight. Surprisingly, as shown in Figure 1, the remaining mixture of MO and C18GnS turned colorless in contrast with that of MO and bare silica mixture. Moreover, the spectroscopic analyses detected no MO in the residual solution, which suggested the C18GnS can be the effective dye adsorbents for water purification. In addition, no extraction was observed in EB and C18GnS mixture, which indicated the specific affinity of C18GnS toward the anionic dye rather than cationic dye due to the basic nature of the tertiary amines on PAMAM backbone.

The adsorption isotherm described the variation of the quantity (q) of the adsorbed MO per gram of C18GnS versus the concentration (C) of MO remaining in solution after overnight. Figure 2 shows analy sis plots of the ratio C/q versus C, deriving from Langmuir equation. The good linear relation between C/q and C indicates that the adsorption obeys Langmuir adsorption isotherm. Then the binding constant K_L is obtained from eq 1:

$$C/q = 1/NK_L + C/N \quad (1)$$

where N is total number of adsorption sites per unit weight of adsorbent. For C18G1S and C18G3S toward MO, the K_L was 6.56 and 9.54 cm^3/mg respectively. The value was comparable with that of the organically modified mesoporous silica toward organic pollutants and of ureasil gels toward organic molecules in water.

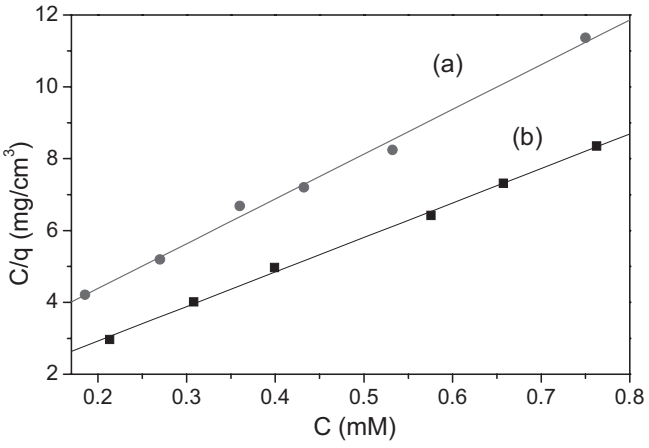

Figure 2. Adsorption isotherms of (a) C18G1S and (b) C18G3S follow Langmuir equation. C represents the concentration of MO remaining in water; q represents the quantity of adsorbed MO per gram of C18GnS.

Oral Sessions 4 & 5

July 15 (Sun)

[8:00 –10:00,

10:30 – 12:30]

OL07

CAPACITIVELY COUPLED AIR PLASMA ETCHING OF POLYCARBONATE

J.K.Kim, Y.W.Joo, Y.H.Park, G.S.Cho, H.J. Song and J.W.Lee*

School of Nano Engineering, Center for Nano Manufacturing, INJE University

621-749, Obang-dong, Gimhae, Gyeongnam, Korea(ROK)

**e-mail : jwlee@inje.ac.kr*

Abstract

Polycarbonate is an excellent material as a substrate for MEMS devices and Liquid Crystal Displays due to its high transparency, light weight and low material cost. We investigated dry etching of polycarbonate in air plasmas using a capacitively coupled reactive ion etching system. Reactive ion etching system has provided simple design, easy handling and consistent etch performance. Air was used for this research since we thought that oxygen and nitrogen in air could be a good gas sources for dry etching of polycarbonate. The etch process parameters included RIE chuck power, air flow rate and photo resist baking time. The RIE chuck power was controlled from 75 to 150W. The air flow rate was varied from 5 to 40sccm. Baking Time was changed from 60 to 180seconds at 70˚C. The process results were characterized in terms of etch rate, etch selectivity of polycarbonate to photoresist and surface roughness. Surface morphology was also studied using scanning electron microscopy. Etch rate of polycarbonate increased with RIE chuck power. We found that air plasma could etch polycarbonate at etch rates of 0.15~0.2um/min with 1:1 etch selectivity to photoresist. Surface roughness after etching of polycarbonate in 20sccm air and 100W RIE chuck power was ~7.62 nm, which was somewhat rough. We will discuss experimental results in detail in the presentation.

Keywords : polycarbonate, plasma etching, air plasma, polymer etching

OL08

Capacitively Coupled O_2/N_2 RF Plasma Etching of Polymethyl methacrylate (PMMA)

Y. H. Park, J. K. Kim, Y.W. Joo, J. H. Lee, G. S. Cho and J. W. Lee*

School of Nano Engineering, Inje Univ., Gimhae, GY, 621-749, Korea (ROK)

** e-mail : jwlee@inje.ac.kr*

Polymer substrates are continuously using for plastic semiconductors, MEMS, bio-chips and sensors. It is important to develop dry etching process for polymer device. We studied dry etching of PMMA, so called acrylic. The PMMA samples were coated with a photo resist and patterned using lithography method. After uv exposure, a KOH-based developing solution was used to remove the unexposed photo resist on PMMA. In the reactive ion etching runs, experimental variables were RF chuck power, % gas composition of O_2 and N_2. We characterized the results using surface profilometry, Optical Emission Spectroscopy, Atomic Force Microscopy(AFM) and Field Emission-Scanning Emission Microscopy(FESEM).

Etch rates of the PMMA was linearly increased from 0.2um/min to 0.6um/min with 75W and 200W RF chuck power, respectively. Etch selectivity of PMMA to photoresist was 1.5~3:1 in those conditions. PMMA etch rate was also a strong function of % gas composition of N_2 and O_2. Etch rate of PMMA was increased with $\%O_2$ in the mixed O_2/N_2 plasmas. Surface roughness of the etched PMMA substrates was about 7.2, which seemed to be somewhat rough. We will also discuss about the results of optical intensity of the plasma discharge during RIE etching.

OL09

A THERMOCHEMICAL TWO-STEP WATER SPLITTING CYCLE WITH MAGNETITE-COATED CERAMIC FOAM DEVICE

Ayumi Nagasaki[1], Koichi Sakai[2], Nobuyuki Gokon[1], Tatsuya Kodama[2,*]
[1]*Graduate School of Science and Technology, Niigata University, Center for Education and Research on Environmental Technology, Materials Engineering, and Nanochemistry*
[2]*Depertment of Chemistry & Chemical Engineering, Niigata University,*

A conversion of solar high-temperature heat to chemical fuels has the advantage of producing long-term storable and transportable energy carriers from solar energy. Hydrogen production from water is an important long-term goal in solar fuel production. Various processes for hydrogen production by multi-step thermochemical water splitting, such as UT-3, IS and Mark processes, have been proposed and demonstrated. However, most of the processes with more than three steps are too complicated for practical solar applications and, they use very corrosive reactant and/or product gases with steam at high temperatures. This results in difficulties with reactor construction materials. Another promising solar thermochemical water splitting process is a two-step water splitting cycle by a Fe_3O_4/FeO redox pair originally proposed by Nakamura.

In pararell with the basic research with respect to the redox working materials described above, many solar chemical receiver/absorbers or reactors have been proposed, developed and demonstrated to realize two-step water splitting by direct irradiation with high fluxes of concentrated solar radiation. The solar chemical reactors are equipped with transparent quartz window to pass concentrated solar radiation through the window and directly heat the redox working materials of unsupported ferrites, ZrO_2- or YSZ-supported ferrites. It was reported that solar hydrogen production was feasible by this reactor demonstrating that multi cycling of the process was possible in principle[1]. In the present work, a novel magnetite-coated ceramic foam device for a thermochemical two-step water splitting cycle is proposed, prepared and tested on the reactivity in a laboratory scale using a sun-simulator.

MPSZ (Mg-partially-stabilized zirconia) was used as a matrix foam. The magnetite-coated ceramic foam device was prepared by wash-coating with Fe_3O_4/YSZ particles and the subsequent $Fe(NO_3)_3$ impregnation method. The Fe_3O_4/YSZ/MPSZ-foam device was placed at a quartz tube reactor and then directly irradiated by the sun-simulator of a 6-kW Xe-arc lamp and heated up to temperatures above 1400ºC under an inert atomosphere (T-R step, Fig.1). That thermally-reduced ceramic foam was then transferred to another quartz tube reactor and heated to 1100ºC with an infrared furnace while passing an H_2O-N_2 gas mixture into the reactor (W-D step). Fig. 2 shows the amounts of the evolved hydrogen per gram of the device in the W-D steps of the repetition test. As can be seen in Fig. 2, the amount of hydrogen evolved per gram of device was 88-149μmol after 6 cycles while the amount of hydrogen evolved was 37-137μmol through the 1^{st}-5^{th} cycles. Unfortunately, the Fe_3O_4/YSZ/MPSZ-foam device had cracks and broken after 13^{th} cycle of the repetition test. This will be due to the fact that the thermal shock resistance of the foam is not high enough for the heat cycles. Ceramic foams with a higher thermal shock resistance, such as SiC foam, should be used as a matrix of ceramic foam device for thermochemical water-splitting cycle.

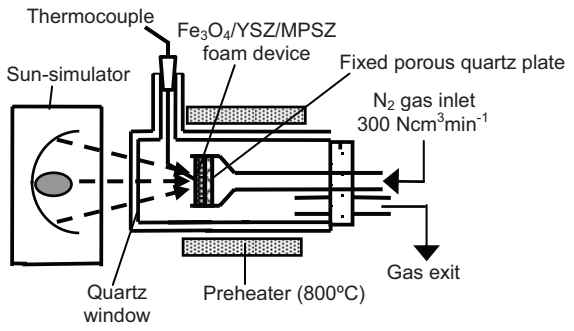

Fig.1. Experimental setups for the T-R steps

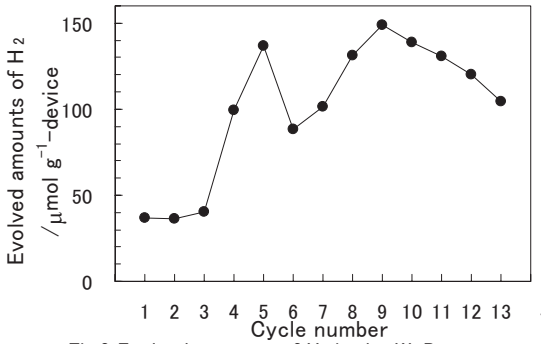

Fig.2 Evolved amounts of H_2 in the W-D steps

[1]: C. Agrafiotes, et al., 2005, "Solar water splitting for hydrogen production with monolithic reactors", Solar Energy, vol. 79, pp. 409-421.

OL10

PROCESSING OF HIGH TEMPERATURE SUPERCONDUCTING BULK MATERIALS AND THEIR APPLICATION TO STRONG MAGNETIC FIELD GENERATORS

Tetsuo Oka*, Yutaka Hirose, Hayato Kanayama, Hokuto Kikuchi, Satoshi Fukui,
Jun Ogawa, Takao Sato and Mitsugi Yamaguchi

Faculty of Engineering, Niigata University

The recent performances of trapping magnetic fields of the melt-textured high temperature bulk superconductors have been greatly improved by the fabrication techniques to obtain large size single domain bulks which have been established in so-called rare earth 123 systems that consist of REBa2Cu3Oy (RE is an abbreviation of Y, Sm, Gd, Eu, Yb), as shown in Fig. 1. The maximum trapped flux density of c-axis oriented single-domain Sm123 bulk superconductors has reached near 2 T at 77 K and 9 T at 25 K measured at the center of sample surface. This has led stable supply of bulk superconducting materials in the commercial market. The authors have been emphasizing the importance of using refrigerators to keep the superconductivity instead of liquid nitrogen, since all the superconducting properties are greatly enhanced when the materials are cooled below 77 K. A compact superconducting permanent magnet system activated by the field cooling FC technique has been constructed to apply the bulk magnets to various industries, which is capable of generating the magnetic fields up to 2 T in the open space outside the magnetic pole, as shown in Fig. 2. In addition to that, various types of superconducting bulk magnet systems capable of generating strong magnetic fields will be referred in the report, which have been constructed by using the superconducting bulk magnets in conjunction with compact refrigerators. Furthermore, the specific features and positions in the practical markets of the trapped field magnets among other field generators have been clarified from the industrial point of view, as shown in Fig. 3. A number of development projects for the practical applications have already started to carry out to realize the industries.

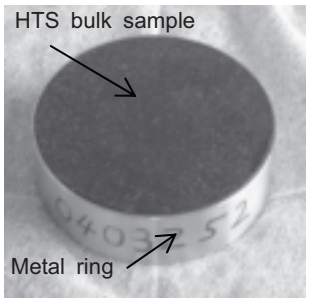

Fig. 1. High Tc bulk sample

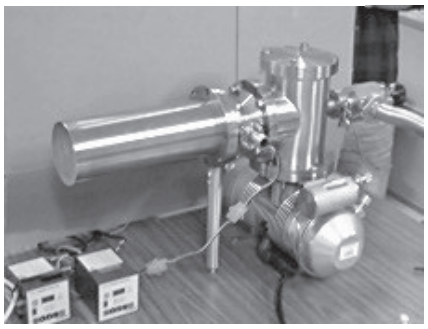

Fig. 2. A compact field generator with use of ST pulse tube cryocooler

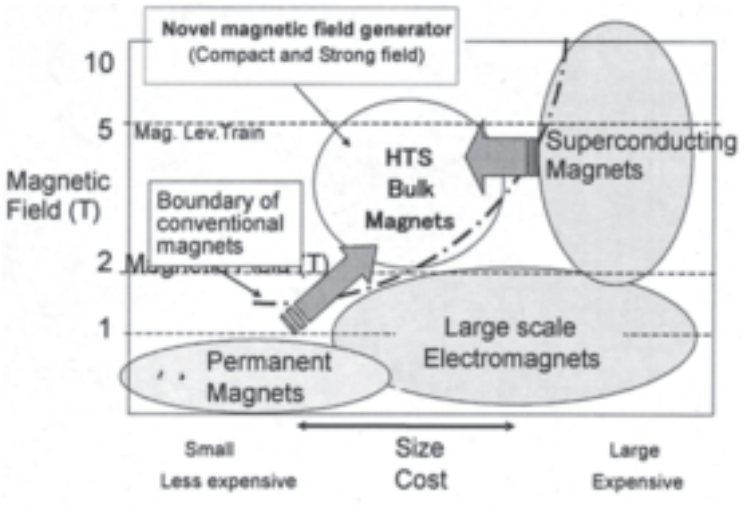

Fig. 3. Positions of various types of magnets

IL09

Synthesis of the liquid silicon and its application for a thin film transistor

Tatsuya Shimoda

Center for Nano Material and Technology, Japan Advanced Institute of Science and Technology
1-1 Asahidai, Nomi,Ishikawa 923-1292, JAPAN

Abstract

By applying photo-induced ring-opening polymerization for CPS (cyclopentasilane, Si_5H_{10}), a novel liquid precursor (liquid silicon material) was developed. Although the polymer made up of a mixture of hydrogenerated polysilanes is insoluble in all common organic solvents, it was found dissolved in a mixture of CPS and an organic solvent. The liquid silicon is coated and converted to an amorphous thin film by heating and then crystallized by an eximer laser irradiation. The poly -silicon film thus formed was used for fabrication of TFTs. The TFT having mobility of 108 cm^2/Vs was achieved using the spin-coated Si-film. TFTs were also fabricated using the inkjet printed Si-film.

Formation of liquid silicon material

Using the method developed by Hengge et al., CPS monomer (a clear and colourless liquid under ambient conditions) was synthesized. It has a boiling point of 194 degree C and is soluble in most organic solvents. After purification, the CPS was exposed to 405nm UV light to induce photo-polymerization. During exposure, the CPS gradually became cloudy and viscous. After sufficient exposure to the UV source, the liquid was transformed into a white solid, presumably made up of a mixture of hydrogenated polysilanes. Although this solid is insoluble in all common organic solvents, it proved to be soluble in the CPS monomer precursor. The hydrogenated polysilane was also found to dissolve in a mixture of CPS and an organic solvent. This solvent mixture plays an important role in controlling the wettability, coating properties, and thickness of the resulting silicon films, all of which are difficult to control when CPS is used alone. In the actual process, UV irradiation is halted before the CPS completely polymerizes such that polysilanes of various molecular weights are dissolved in unreacted CPS. By diluting the solution with an organic solvent and then filtering out those insoluble polysilanes that precipitated as a result of dilution, we obtained the solution that we refer to as liquid silicon material.

Fabrication of TFTs by spin-coating

The n-channel TFTs, whose structure is schematically illustrated in Fig. 1d, were fabricated as follows. First, an SiO_2 underlayer was formed by plasma CVD on a quartz substrate. After cleaning the substrate surface by 172nm UV-irradiation at 10mW/cm^2 for 10 min, the liquid silicon material—12 vol.% toluene solution of UV-irradiated CPS—was spin-coated in a nitrogen-filled dry box. The spin-coated substrate was immediately placed on a hot plate heated to 200 degree C and the temperature was raised to 400 degree C within 10 min. After maintaining a temperature of 400 degree C for 30 min, it was further increased to 540 degree C over another 10 min period and held for 2 h to form a 50-nm-thick a-Si film. Next, the amorphous film was converted to a polycrystalline one by irradiating it with 308 nm wavelength excimer laser light at 345 mJ/cm^2. After the poly-Si had been etched to create islands, a 120-nm-thick SiO_2 gate insulator (Gox in Fig.1d) was formed by plasma CVD, followed by tantalum sputtering and etching to form gate electrodes. The source and drain regions were formed by the self-aligned ion implantation of phosphorous ions using the gate electrodes as a mask. Finally, we made the TFTs accessible for measurement by forming an interlayer insulator, opening contact holes in the insulator to reveal the source and drain regions, and then sputtering aluminium to form electrodes. The channel width and length of the TFTs were both 10 um. The coating-formed silicon film did not present any notable problems or difficulties during the above fabrication steps, as the silicon film was of semiconductor-grade purity and the film processing conditions— etching rate, laser conditions and so on—were nearly the same as those used for CVD-produced

silicon film. For comparison, conventional TFTs were fabricated by the same process except that the silicon film was formed by CVD. As shown in Fig. 1a, these TFTs exhibit good electrical characteristics with field-effect mobility (calculated from the transconductance in the saturation region) ranging from 74 to 108 cm^2/Vs in 15 transistors randomly selected among a 4-inch substrate. The transistor of mobility 108 cm^2/Vs, whose output characteristics are shown in Fig. 1b, also possesses an on/off ratio of seven digits, 5.0 V in threshold voltage Vth and 0.83V per decade in s-factor (the gate voltage that induces a tenfold increase of drain current in the sub-threshold region).

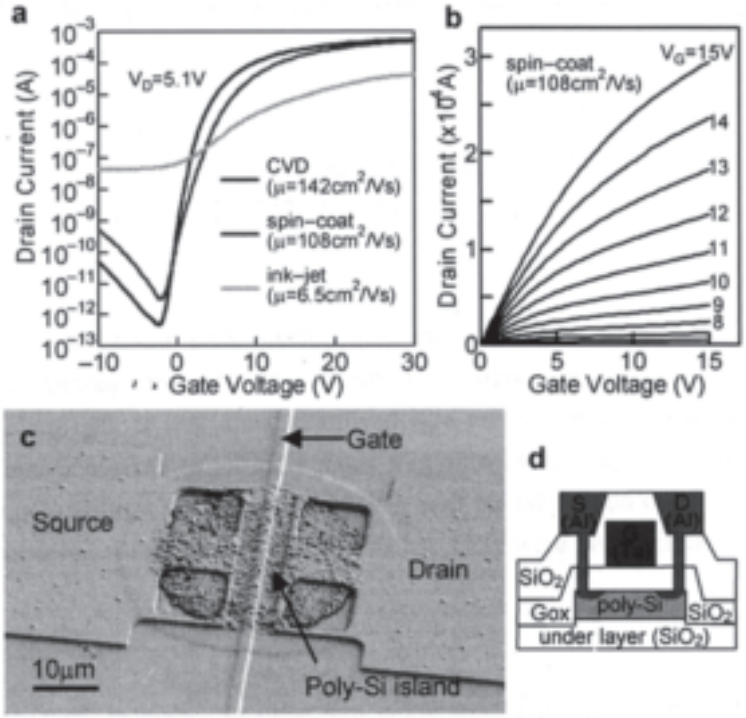

Figure 1. **The structure and characteristics of solution-processed LTPS TFTs. a,** The transfer characteristics of LTPS TFTs, whose silicon film was formed by CVD (blue), spin-coating (magenta) and ink-jet printing (green), respectively. The drain current of the ink-jetted TFT is normalized to have the same channel width and length as the CVD-formed and spin-coated TFTs, for comparison. **b,** The output characteristics of the TFT using spin-coated silicon film whose transfer properties are shown in a. **c,** An SEM image of the TFT made from ink-jetted silicon film, whose transfer characteristics are shown in a. **d,** A cross-sectional schematic of a fabricated TFT. Gox, SiO2 gate insulator.

Fabrication of TFTs by ink-jet printing

TFTs with the same structure as above were formed using ink-jet printing to form the channel silicon island. A 10 vol.% toluene solution of UV-irradiated CPS was ink-jet printed on a glass substrate in a nitrogen- filled dry box. This solution was suitable for ejection from a piezo-driven print head. Because, the ejection of the solution from the print head was stable and reproducible. Three droplets, each of weight 10 ng, were deposited in the location where the channel island was to be formed. The droplets were converted into a poly-Si island of diameter 30–40 um by baking at 540 degree C followed by 308nm excimer laser crystallization at 450 mJ/cm^2. The island was 300nm thick at the center and became thinner towards the periphery of the sample. After the gate insulator had been formed, the same steps were applied as for the spin-coated TFTs. The channel width and length of the resulting TFTs were 36 um and 2um. The ink-jet-printed TFT operated with a mobility of 6.5 cm^2/Vs and an on/off ratio of three digits (Fig. 1a). This low mobility is attributed to the poor crystallinity and rough surface, while the large off current, which was confirmed to be the current between source and drain rather than a leak current through the gate insulator, is also attributed to the thick silicon film. The formation of thin, uniform a-Si film using an ink-jet process would improve the surface morphology and electrical properties of the poly-Si films. However, the wettability and behaviour of microdroplets are known to differ significantly from those of macroscopic droplets. A thorough understanding of microdroplets will be needed to realize the ink-jet printing of liquid silicon material for practical applications.

Acknowledgements This work was done in the collaboration between JSR Corporation and Seiko Epson Corporation which the author belonged to. The author thank to Dr. Y. Matsuki, Mr. H. Iwasawa and Mr. D. Wang in JSR Corporation and Dr. M. Furusawa, Dr. H. Tanaka, Mr. I. Yudasaka and Mr.M. Miyasaka in Seiko Epson Corporation. This work is partially supported by a grant from the New Energy and Industrial Technology Development Organization (NEDO).

Reference

T. Shimoda, Y. Matsuki, M. Furusawa, T. Aoki, I. Yudasaka, H. Tanaka, H. Iwasawa, D. Wang, M. Miyasaka and Y. Takeuchi, “Solution-processed silicon films and transistors”, Nature, Vol.440, No.7085(2006)pp.783-786.

IL10

Studies and Application of Ultrathin Films

Tiesheng Li[1,2,3]*, Wnjian Xu[1,2,3], Bing Mu[1,2,3], Luyan Mao[4], Suhua Zhang[4] and Yangjie Wu[1,2,3]*

[1]*Department of Chemistry,The Key Lab of Chemical Biology and Oganic Chemistry of Henan Province,Zhengzhou 450052,China*

[3]*Advanced Nano-information Materials of Zhengzhou,Zhengzhou 450052,China*

[4]*College of Materials Science and Engineering,Zhengzhou University,Zhengzhou 450052,China*

*Cosponding author:

Introduction

The generation of images through photo-induced chemical changes thin filmremains a fertile field for fundamental and applied research. In fact, the prospect of fabricating inmicrooptoelectronic devices has driven the research of new microlithographic resists of even higher resolution, sensitivity, and endurance. Deep UV lithography is one of the most promising technologies for sub-0.5 um features delineation because of its many economics and technical advantages over previous technology. [1,2] Filmsused for photopatterning are many kinds, such as spin-coating film, etc.Ordered super-molecular assemblies based on functional molecul -es has been attracting considerable interest in the application to molecular devices recently. [3, 4]

Langmuir-Blodgett (LB) techniques is one of the most effective ways in preparing nano-assembled ultrathi n films at a molecular level with high molecular orientation on solid substrate. [5] Since the photochemical react ions usually depend on the orientation of the molecules, Langmuir monolayer at air/water interface and the LBf ilms on solid substrate can serve as good modes to investigate application in photopatterning process as phot oresist, photochemical reaction research, and orientation catalytic film for synthesis, nonlinearity film, luminescence film and so on. In this present paper, the research on application of polymer, Porphyrin and derivatives ultrathin films will be presented.

Result and Disscusion

1 Polymer LB Films and its Application

A series ofcopolymers, poly(*N*-dodecylmethacrylamide-*co*-1, 4- dioxaspiro [4, 4] nonane-2-methyl methacrylate) [p(DDMA-DNMMA)], poly (N-dodecylmethacrylamine/ß-naphtylmethacrylate)(pDD-MANPM -A), Poly(N-hexadecylmeth- acrylamide-co- 4-tert-butylphenl methacrylate)[p(HDMA-BPhMA)s] were pre -pared. The properties of these copolymers in Lanmuir film and LB films and photopatterning were al so investigated with π-A isotherm, E_s- π isotherm and AFM method. Results shows that optimum conditions with E_s- π isotherm for LB films deposition of copolymer (p(DDMA-DNMMA)s, s= 10,

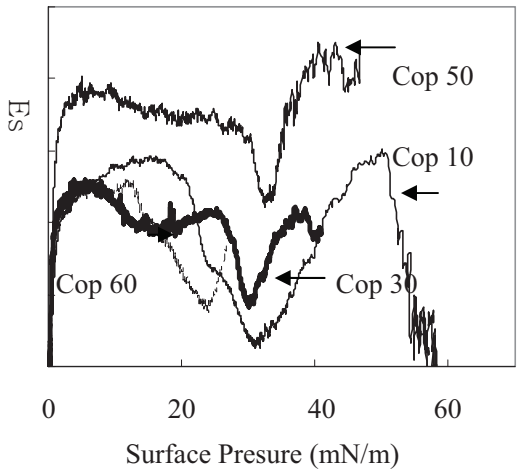

Fig.1 Es-π isotherms of p(DDMA-DNMMA)s

30, 50, 60) is more exact than π-A isotherm (Fig. 1) because of elasticity could give more detailed information on molecular interaction and motion and the monolayer of copolymers(for example, p(DDMA-DNMMA)s, S=50) has high orientation arrangement shown in Figure 2. Upon deep UV irradiation, photopattern images of 0.75 μm can be obtained.

2.Porphyrin derivatives LB films

The film-forming properties of 5, 10, 15-tri (p-chlorophe nyl)-20-oxy-(α-stearic acid) phenyl porphyrin ($TC_{18}PP$) on the air/water interface was studied. The experimental results indicated that $TC_{18}PP$ has good film-forming pe rformance, $TC_{18}PP$ LB films have good stability, homogeneity and periodicity, the long alkyl chains are not stra ight and the porphyrin macro ring in LB films lay on the substrate with a tilted angle 66°.

3.Ferrocence derivatives LB Films

A series of novel amphiphilic ferrocenylimines and their cyclopalladated complexes of general formula [Fe(η^5-C_5H_5)(η^5-$C_5H_4CR_1$=NR_2)] (R_1 = H, CH_3,R_2 = $C_{12}H_{25}$,$C_{16}H_{33}$) were prepared and characterized by ^{1}H NMR, ^{13}C NMR, ^{31} P NMR, IR, HRMS. These amphiphilic cyclopalladated complexes are thermally stable and insens itive to oxygen, moisture and displayed good activity in the Heck reaction of a range of aryl halides with ethyl acylate or styene in bulk solution. They are suitable for formation of LB films which were used for enabling active, selective and recoverable catalysis research.

Acknowledgement

The author expressed sincerely thinks to T.Miyashita group, The Innovation Fund for Outstanding Scholar of Henan Province (0621001100) The Nature Science Foundation of China (20572102) , The Fund for Outstanding Younger Scholar of Henan Province(074100510015) and The Natural Science Foundation of Henan Province (0611020100, 2007150042)

Reference(s)

[1] J-B. Kim, J.-J. Park, and J.-H. Jang, Polym. 41 (2000), pp. 149-153

[2] D. K. Lee, G. Panlowski, J. Photopolym. Sci. Tec., 15 (2002), pp. 427-34

[3] J. Zhao, K. Abe, H. Akiyama, Z.F. Liu, F. Nakanishi, Langmuir 15 (1999), pp. 2543-2550.

[4] A. Ulman, Chem. Rev. 96 (1996), pp. 1533-1554.

[5] A. Aoki, T. Miyashita, Polym. 42 (2001) 7307-7311

IL11

CONTROLLED SYNTHESIS OF NANOSTRUCTURED ZnS BY SOFT-SOLUTION PROCESSING AND ITS APPLICATION TO POLYMER HYBRID MATERIALS

Md. Habib Ullah and Chang-Sik Ha*

National Research Laboratory of Nano-Information Materials, Department of Polymer Science and Engineering, Pusan National University, Busan 609-735
Email: csha@pusan.ac.kr

Colloid-based 'soft-solution' methods are suitable for the synthesis of encapsulated nanocrystals (NCs) because the particle size can be controlled readily upon changing the concentration and the type of organic molecular ligand [1-3]. Functional ligands may be used to coat the surfaces of the particles to allow them to become free standing in solution and prevent their direct aggregation. Such NCs often become soluble in organic solvents or in aqueous solutions when the ligands bind strongly to their surfaces. Water-soluble nanocrystals are used widely for studies in biological systems. NCs that are soluble in common organic solvents are suitable for preparing polymer/inorganic composite materials, which may find applications in high-refractive-index films, tunable light-emitting diodes, optical waveguides, photovoltaic solar cells, and nonlinear optical devices [4-5].

Small, uncapped semiconductor NCs usually form with defective states on their surfaces because of their large surface-to-volume ratios. The state of their surface dramatically affects their degree of luminescence quenching at the crystal surface. Surface defects are also often prominent in capped NCs when the ligands are not anchored suitably onto the surfaces. When the core semiconductor NCs are passivated effectively with appropriate ligands, however, their luminescence and fluorescence intensities can be increased substantially. Such enhanced fluorescence emission results from suppression of nonradiative recombination because of the reduced concentration of surface states that feature dangling bonds and/or unstable surface atoms.

The choice of capping ligand for the NCs is critical because it determines the stability, solubility, reactivity, size, and shape of the NCs during their synthesis. Size-dependent shifts in the absorption onsets and emission maxima to higher energies with decreasing size have been studied widely. Recently, we reported that PDAs are excellent capping ligands for silver nanoparticles, where the ligand-to-metal interaction is extremely strong, and the size, shape and the phase of the colloidal nanoparticles are determined by the isomers of PDA[6,7]. In the first part of present study, we report a simple novel approach for the synthesis of high-quality ZnS NCs capped with either of three isomeric ligands: ortho

(o)-, meta (m)-, and para (p)-phenylenediamines (PDAs). The NCs are of nearly identical size, but the fluorescence emission of the NC was tunable according to the structure of the isomer, i.e. fluorescence emission can be sharply tuned by the same structure molecules with different positioning amine functional groups.

Our synthetic approach was quite simple;. First, Zn^{2+} ions were adsorbed onto the amine of the PDAs. The Zn^{2+}─PDA complex ions were reacted with the S^{2-} ions (in DMAc) that arose from thermal decomposition of thioacetamide. The reacting solutions were then heated under reflux to provide well-passivated, high-quality ZnS NCs. The reaction mixture containing the ZnS NC was then cooled to room temperature. Each of the NC solutions was, however, precipitated in ethanol and washed several times until colorless ethanol was obtained. The NC products were collected through careful decantation. A ZnS NC sample was also synthesized in the absence of PDA, while maintaining all of the other parameters identical to those described above. For convenience, however, we name the NC products passivated with *o*-, *m*-, and *p*-PDA as PNC1, PNC2, and PNC3, respectively, and the bare NC (passivated only with CH_2CNH) as BNC.

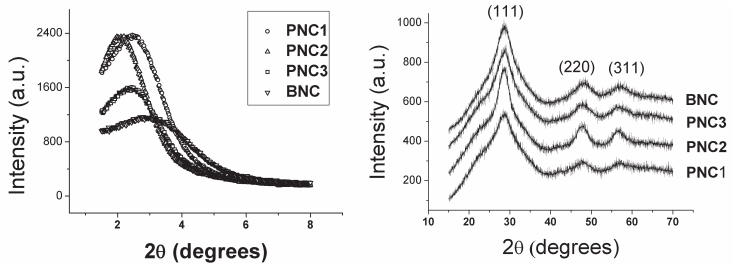

Figure 1 Low- and wide-angle X-ray diffraction of PNC1, PNC2, PNC3, and BNC.

To characterize the NCs morphologically, we studied their low- and wide-angle X-ray diffraction (XRD) patterns. The low-angle XRD peaks (Figure 1, left) of PNC1, PNC2, PNC3, and BNC occurred at 2θ values of 2.5^0, 2.1^0, 2.4^0, and 3.0^0, respectively. The average NC sizes for PNC1, PNC2, PNC3, and BNC, which we determined from the diffraction peak data in the low-angle region, are 3.5, 4.1, 3.6, and 2.8 nm, respectively. Figure 1(right) presents the wide-angle (WA) diffraction patterns of PNC1, PNC2, PNC3, and BNC. Using Debye-Scherrer formula, the diameters of NCs are 3.2, 3.9, 3.3, and 3.0 nm for PNC1, PNC2, PNC3, and BNC, respectively. To verify the morphologies suggested by the low- and wide-angle XRD patterns, we obtained transmission electron microscopy (TEM) images of PNC1, PNC2, PNC3, and BNC. The average sizes for PNC1, PNC2, and PNC3, which we estimated from the size-histograms, were 3.0 ± 0.3, 3.7 ± 0.30, and 3.0 ± 0.5 nm, respectively. Thus, the NC sizes measured

by TEM are consistent with the sizes obtained by XRD. The size histogram for BNC was too broad, and thus its standard deviation was large. The average size-range, however, we estimated to be 2.0–3.5 nm. This broad size distribution reveals that the NCs are unstable in the absence of PDA molecules.

The Fourier transform infrared (FTIR) absorption spectroscopic data of PNC1, PNC2, and PNC3 confirmed that their shell structures consisted dominantly of *o*-, *m*-, and *p*-PDA molecules, respectively, while that of BNC indicated that its NCs contained CH_2CNH molecules. We used X-ray photoelectron spectroscopy (XPS) to reveal the nature of the interfaces between the cores and ligands. Because the amino functional groups coordinated to the surface Zn atoms of the NCs, the N 1s and Zn 2p states provided important information regarding the ligand-to-core interaction.

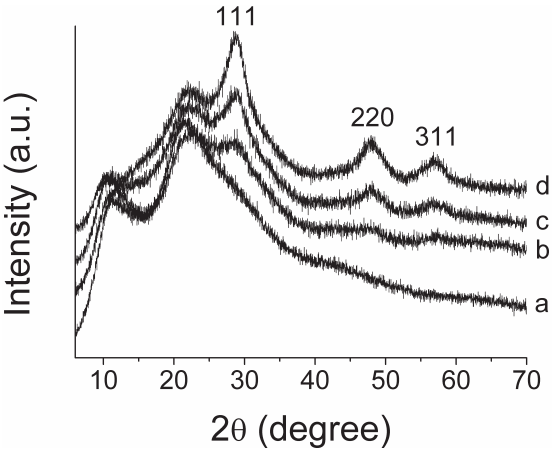

Figure 2 XRD patterns of PVP-ZnS films, for the ZnS contents; a) 0 wt %, b) ~3 wt %, c) ~8 wt %, and d) ~15 wt %.

In the second part of the study, we applied o-PDA functionalized ZnS NCs in poly(vinylpyrrolidone) matrix to make fluoiescent and highly transparent nanocomposite thin films with high refractive index. The nanocomposite films were prepared according to the following procedure.: Solutions of various concentrations of NCs were blended with PVP to control the wt % of ZnS in PVP matrix. Typically, 0.5 g of PVP was added into a solution (6 ml) of NCs. The mixture was stirred magnetically for 8 h at 50 ^{0}C. Very clear transparent solution was obtained, which did not show any phase separation after many months of observation. However, the composite solution was spin coated on the substrates for making thin films. The coated films were dried at 50 ^{0}C for 24 h.

Figure 2 shows the XRD patterns of PVP and PVP─ZnS NC composite films with different ZnS contents. The diffraction peaks at $2\theta = 11.6^0$ and 21.9^0 correspond to PVP crystalline phase (Figure 2a). The diffraction peaks corresponding to the (111), (220), and (311) planes show that the ZnS in the

nanocomposite retains its zinc blend structure. The intensities of these diffraction peaks gradually increase with increasing ZnS content, indicating that the NCs have been successfully incorporated into polymer matrices.

The diameter of the nanocrystals in the composite films (using Debye-Scherrer formula) is estimated to be the same as that of the as-synthesized NCs, indicating no aggregation of NCs in the composite films. AFM images provide detailed information of the surface morphology of the film. From the height analysis of the image of the nanocomposite film, we observed that the average diameter of the NCs is very similar to the diameter measured by TEM. Optical transparency of the nanocomposite films (on quartz substrates) was also compared with that of the pure PVP film. The nanocomposite films can be potentially used as optical thin films or the nanocomposite solutions can be used to fabricate multifunctional devices or optical materials.

Acknowledgements

This study was financially supported by the Korea Science and Engineering Foundation (KOSEF) through the National Research Laboratory Program funded by the Ministry of Science and Technology (MOST; M10300000369-06J0000-36910), the SRC / ERC Program of MOST / KOSEF (grant # R11-2000-070-080020) and the Brain Korea 21 Project.

References

[1] M. H. Ullah, C.-S. Ha, J. Nanosci. Nanotechnol. 5 (2005) 1376

[2] E. C. Scher, L. Manna, A. P. Alivisatos, Phil. Trans. A 361 (2003) 241

[3] J. Joo, H. B. Na, T. Yu, J. H. Yu, Y. W. Kim, F. Wu, J. Z. Zhang, T. Hyeon, J. Am. Chem. Soc. 125 (2003) 11100.

[4] L. L. Beecroft, C. K. Ober, Chem. Mater. 9 (1997) 1302

[5] A. Haryona, W. H. Binder, Small 2 (2006) 600

[6] M. H. Ullah, I. Kim, C.-S. Ha, J. Nanosci. Nanotechnol. 6 (2006) 777

[7] M. H. Ullah, I. Kim, C.-S. Ha. Mater. Lett. 60 (2006) 1496.

IL12

Effect of Silane-Modification of Clay on the Mechanical Properties of Poly(L-lactide)/Clay Composites

Jin San Yoon

Department of Polymer Science and Engineering, Inha University, 402-751 Incheon, Korea

Fax: 82-32-865-5178 E-mail: jsyoon@inha.ac.kr

Biodegradable polymers have been used for numerous niche applications such as surgical implants, sutures, and controlled release drugs. However owing to the formidable recent efforts to develop low cost biodegradable polymers to reduce the solid waste produced by many artificially synthesized polymers, many plastics used for single-use receptacles, fishing tools and packagings of fresh meat and fish have become targets to be replaced with biodegradable polymers. Poly(L-lactide) (PLLA) is one of the most economically competitive biodegradable polymers produced from renewable resources. In this study, an organoclay containing epoxy groups(TFC) was synthesized by reacting (glycidoxypropyl)trimethoxysilane (GPS) with Cloisite®25A (C25A), which had previously been modified with an aliphatic amine compound. This would increase the hydrophobicity of the clay and enhance the wetting properties of the clay layers with PLLA. The chemical reaction between the epoxy groups and the end groups of the PLLA would further improve the interaction between the components of the PLLA/clay composites.

The interlayer spacing, *d*(001), of the C25A (18.46 Å) was almost the same as the *d*(001) of TFC (18.62 Å). The intensity of the *d*(001) peak decreased as the content of C25A in PLLA/C25A composite decreased and shifted slightly toward a lower diffraction angle. The same trend was observed for the PLLA/TFC composites, and the interlayer spacing of the PLLA/TFC composites increased from 30.0 to 30.4 Å as the content of TFC decreased from 10 to 5 wt %. The intensity of the peak of the TFC-based composite was much more attenuated than that of the C25A-based one. The lower intensity of the peak was attributed to the partial disruption of parallel stacking or layer registry of the TFC to give rise to some exfoliation of the clay platelets. TEM image of PLLA/TFC demonstrated the presence of individual layers as well as a few packets of silicate consisting of 2-3 layers, and a higher degree of exfoliation of the silicate layers was obtained for the PLLA/TFC composite than for the PLLA/C25A composite. This is despite the fact that the XRD pattern of the neat TFC was almost identical to that of the neat C25A.

Not only tensile modulus and strength but also elongation at break of the PLLA/ TFC composites increased considerably as a result of the incorporation of TFC. In many cases, the increase in the tensile modulus of the polymers by compounding with clay sacrifices the elongation at break. The higher degree of exfoliation and the improved tensile properties of the PLLA/TFC composites are believed to be associated with the epoxy

functional groups of the TFC, which promoted an interaction between the clay and the polymer via a chemical reaction.

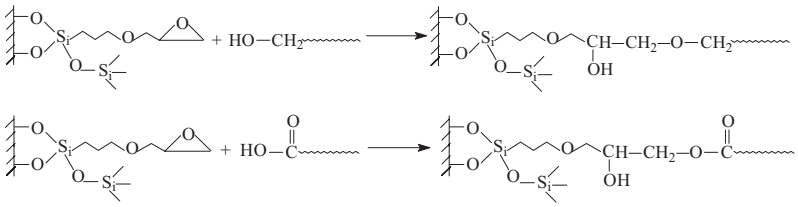

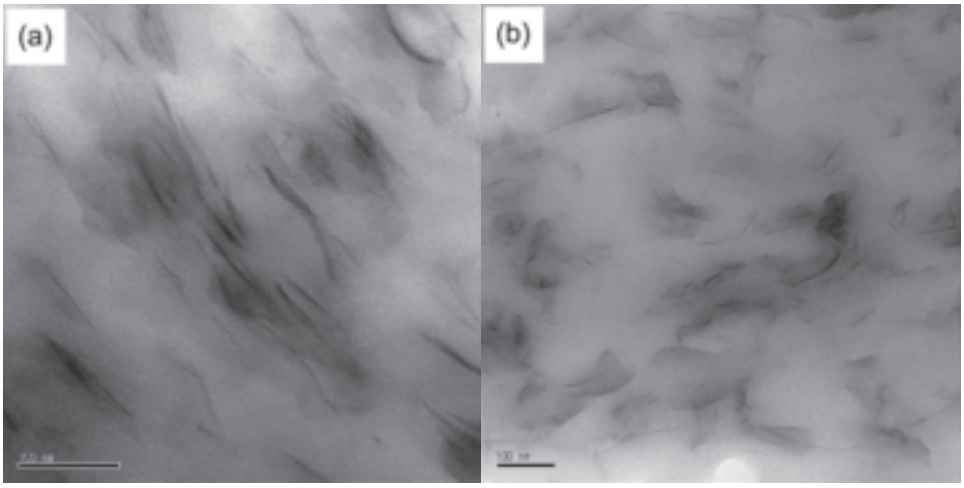

TEM images of PLLA composites with the two clays. (a) PLLA/C25A, (b) PLLA/TFC

Samples	Modulus (MPa)	Elongation at break(%)	Strength(MPa)
PLLA	1583.8	7.5	59.3
PLLA/C25A2	1799.3	5.44	58.4
PLLA/C25A5	1956.1	4.95	57.5
PLLA/C25A10	2204.0	1.24	25.5
PLLA/TFC2	2099.6	6.1	68.6
PLLA/TFC5	2670.4	8.2	74.5
PLLA/TFC10	2805.3	12.9	81.9

Tensile properties of the PLLA/clay composites at room temperature

OL11

FACIL SYNTHESIS OF FREE-STANDING PMO FILMS WITH AMORPHOUS AND CRYSTAL-LIKE WALL STRUCTURE

Sung Soo Park and Chang-Sik Ha*

Department of Polymer science and Engineering, Pusan National University, Busan 609-735, Korea

Surfactant-templated binuclear alkoxysilane precursors, $(R'O)_3Si\text{-}R\text{-}Si(OR')_3$, allow the assembly of periodic mesoporous organosilica (PMO) nanocomposite materials with bridge-bonded organic groups housed inside the channel walls.[1,2] These PMO materials facilitate chemistry of the channels and provide new opportunities for controlling the chemical, physical, mechanical, and dielectric properties of the materials.[3] The morphology of PMO materials often controls their function and utility. In this sense, the film type of PMO material with a crystal-like wall and amorphous wall structure was synthesized at the air-water interface and liquid-bottle interface during hydrothermal reaction.

Free-standing and oriented periodic mesoporous organosilica (PMO) films with variable pore size have been synthesized at the air-water interface using cationic alkyltrimethylammonium surfactants (alkyl chain length from 12 to 18 carbon atoms) as structure-directing agent and 1,2-bis(triethoxysilyl)ethane as organosilica precursor.[4] After hydrothermal reaction at 95 ^oC for 8 h, C_{12}TA-PMO, C_{16}TA-PMO, and C_{18}TA-PMO films grown at the air-water interface have uniform thickness of ca. ~350 nm, ~670 nm, and ~400 nm, respectively. The films are continuous over the entire bulk depending on the size of the reaction bottle. From XRD pattern and TEM image, the PMO films with hexagonal symmetry were identified. It was confirmed by ^{29}Si and ^{13}C CP MAS NMR experiments that the organic-inorganic moiety (-Si-CH_2-CH_2-Si-) is the basic structural unit in the films. The pore diameter and the surface area of surfactant-extracted PMO films, e.g. C_{12}TA-, C_{16}TA-, and C_{18}TA-PMO films, obtained from the N_2 sorption isotherms were to be determined to be 24.3 Å, 26.4 Å, and 32.8 Å and 890.3, 917.7, and 811.0 m^2g^{-1}, respectively.

On the other hand, the synthesis and characterization of PMO film with a crystal-like wall structure has been very important task for more diverse applications. The films with molecular-scale (*i.e.* 7. 6 Å) periodical pore walls have been synthesized by surfactant templating at the liquid-reaction bottle interface.[5] The films have a high-quality well-ordered hexagonal mesostructure, benzene moiety inside the channel wall and are continuous over the entire bulk depending on the size of the reaction bottle and the amount of the reactant solution. The film–forming process works well under static conditions at 95

°C from 2 h to 24 h. Free–standing and benzene–bridged PMO films, with a thickness of 1.6 μm to 3.5 μm have been grown at the liquid–reaction bottle interface. The pore diameter and surface area of the film obtained from an N_2 sorption isotherm were to be determined to be 37.6 Å and 863 m^2g^{-1}, respectively.

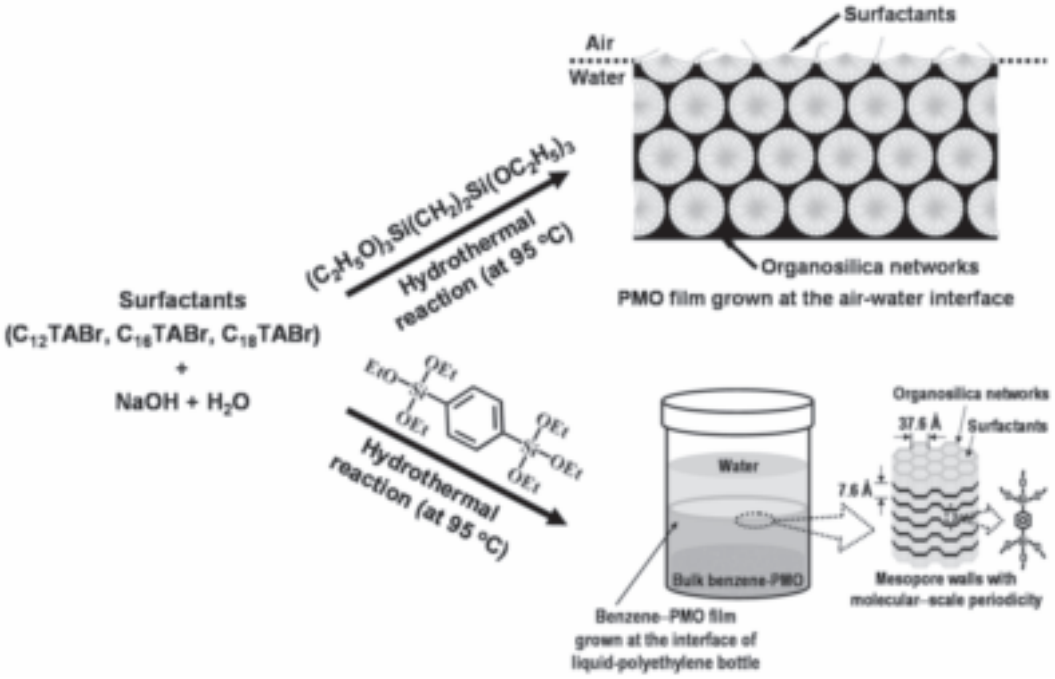

Scheme 1. Illustration for the synthesis process of the free-standing and oriented PMO films.

Acknowledgments

This work was supported by Korea Science and Engineering Foundation (KOSEF) through the National Research Laboratory Program funded by the Ministry of Science and Technology (MOST; No.M10300000369-06J0000-36910), the SRC/ERC program of MOST/KOSEF (Grant #R11–2000–070–080020), and the Brain Korea 21 Project.

References

1. S. Inagaki, S. Guan, Y. Fukushima, T. Ohsuna and O. Terasaki, *J. Am. Chem. Soc*., 1999, **121**, 9611–9614.
2. W. Guo, J. Y. Park, M. O. Oh, H. W. Jeong, W. J. Cho, I. Kim and C. S. Ha, *Chem. Mater*., 2003, **15**, 2295–2298
3. A. Bhaumik, M. P. Kapoor and S. Inagaki, *Chem. Commun.*, 2003, 470–471.
4. (a) S. S. Park and C.-S. Ha, *Chem. Commun*., 2004, 1986-1987. (b) S. S. Park and C.-S. Ha, *Chem. Mater*. 2005, **17**, 3519–3523.
5. S. S. Park, D. H. Park and C.-S. Ha, *Chem. Mater*., 2007, **19**, 2709-2711.

OL12

Preparation of hybrid material of polymer-grafted carbon micro-coils and thermo-sensitive polymer gel

Takeshi YAMAUCHI[1,3,4], Shigenori SATO[1], Norio TSUBOKAWA[2,3,4], Kenji KAWABE[5], Yukio HISHIKAWA[5], and Seiji MOTOJIMA[6]

[1]Graduate School of Science and Technology, Niigata University; [2]Faculty of Engineering, Niigata University; [3]Center for Transdisciplinary Research, Niigata University; [4]Center for Education and Research on Environmental Technology, Materials Engineering, and Nanochemistry, Niigata University; [5]CMC Technology Development Co. Ltd.; [6]Faculty of Engineering, Gifu University

〔Introduction〕

Carbon micro coil (CMC) is a carbon fiber with helical structure and has high grade mechanical and electrical properties. It has also reported that CMC was generated heat with electromagnetic irradiation. For the high-grade composite material of CMC and polymer matrix, it has required that modification of CMC surface with polymer. In this study, we demonstrated the surface modification of CMC with grafting polymers onto CMC and prepared composite material of poly(*N*-isopropylacrylamide) (PNIPAM) gel as thermo-sensitive polymer gels containing CMC by photo-polymerization. The properties of the material such as content of carbon micro-coils, swelling ratio, breaking strength, and thermo-sensitivity, and its function as drug carrier were evaluated.

〔Experimental〕

Poly(vinyl ferrocene (VFE)-*co*-methyl methacrylate (MMA)), polyethylene glycol (PEG), and PNIPAM were grafted onto CMC with ligand-exchange reaction or silane coupling reaction. The composite gels were prepared by photo-polymerization with irradiation of ultraviolet light. *N*-isopropylacrylamide, monomer, *N,N'*-methylenebisacrylamide, crosslinker, 2,2'-Azobis(2-amidinopropane)dihydrochloride, and initiator were dissolved in water. Untreated CMCs, Poly(vinyl ferrocene (VFE)-*co*-methyl methacrylate (MMA))-grafted CMC, PEG-grafted CMC, and PNIPAM-grafted CMC were added this solution with stirring, respectively. The gelation was carried out by irradiating with ultraviolet light for several hours. Content of CMC was calculated with thermogravimetric analysis (TGA). Swelling ratio was calculated from weight of swollen gel and that of dry gel. Breaking strength was evaluated by compression test. Thermo-sensitivity and function as drug carrier were evaluated by relationship between temperature and volume alteration modulus**.**

〔Results and Discussion〕

The amount of grafting polymers onto CMC was increased with polymerization time until 24hours and dispersion of CMC in water and organic solvent was significantly improved by grafting polymer onto CMC. The black colored composite gel membranes were prepared by this method, and polymer-grafted CMC were uniformly dispersed in PNIPAM gels. It was estimated that grafted polymers augmented hydrophilic of CMC, and CMCs were dispersed in the polymer network which contained water solution. Composite gels had slightly larger swelling ratio and smaller breaking strength than normal PNIPAM gel. Composite gels were changed their volume with temperature alternation as same as normal PNIPAM gel, and showed phase transition temperature at 35 ℃. During the shrinking process of composite gels, no CMC was eluded from composite gels. These results suggested that CMC was entrapped polymer matrix very well and the composite gels maintained its thermo-sensitivity to shrink with heat.

〔Acknowledgement〕

This study is supported by Grant for Promotion of Niigata University Research Projects.

OL13

DIELECTRIC STUDY of MISCIBILITY in POLYMER BLENDS

Kazunori Se* and Ryuusuke Shimaguchi

Faculty of Engineering, Fukui University
Bunkyo 3-9-1, Fukui 910-8507, Japan
Phone: 0776-27-8957 Facsimile: 0776-27-8767 e-mail: se@matse.fukui-u.ac.jp

In order to examine the miscibility in polymer blends, dielectric study of polystyrene (PSt) / *cis*-polyisoprene (PIs) polymer blends was carried out. Three polymer blends of PSt12 (M_n=1260, M_w/M_n=1.0$_7$) / PIs31 (M_n=3100, M_w/M_n=1.0$_4$), PSt9 (M_n=930, M_w/M_n=1.0$_9$) / PIs31, and PSt7 (M_n=720, M_w/M_n=1.0$_7$) / PIs31 were employed. They show UCST phase diagrams whose critical solution temperatures are 74.1°C for PSt12/PIs31, 35.6°C for PSt9/PIs31 and 4.6°C for PSt7/PIs31.

PSt and PIs exhibit each dielectric loss peak ($\varepsilon''_a{}^{PSt}$ and $\varepsilon''_a{}^{PIs}$) due to each segmental mode relaxation, and PIs exhibits a dielectric loss peak ($\varepsilon''_n{}^{PIs}$) due to a normal mode relaxation caused by fluctuation of the end-to-end distance of PIs. The PSt/PIs blends exhibit two ε''_a which are the same as $\varepsilon''_a{}^{PSt}$ and $\varepsilon''_a{}^{PIs}$. However, as shown in Figure 1, the PSt31/PIs7 blend exhibits $\varepsilon''_n{}^{Blend}$ which was observed at a different frequency and a different temperature with those of $\varepsilon''_n{}^{PIs}$.

The $\varepsilon''_n{}^{Blend}$ of PSt7/PIs31 was found to be calculated from the corresponding two $\varepsilon''_a{}^{PSt}$ and $\varepsilon''_n{}^{PIs}$ as follows:

$$\varepsilon''_n{}^{Blend}(\omega) = w_{PSt}\varepsilon''_a{}^{PSt}(\omega\zeta_{PSt}/\zeta_{Blend}) + w_{PIs}\varepsilon''_n{}^{PIs}(\omega\,\zeta_{PIs}/\zeta_{Blend})$$

where ζ and w are friction coefficients and weight fractions of the corresponding polymers, respectively. By comparing the observed $\varepsilon''_n{}^{Blend}$ with the calculated $\varepsilon''_n{}^{Blend}$, two shift factors ($\zeta_{PSt}/\zeta_{Blend}$ and $\zeta_{PSt}/\zeta_{Blend}$) were estimated.

A lot of shift factors of the three polymer blends having different weight fractions were determined at different temperatures to be plotted against T/T_c, where T_c is a temperature at a cloud point of each polymer blend. As shown in Figure 2, the two shift factors were classified into four regions: (I) a phase separated region, (II) a weakly phase separated region, (III) a weakly miscible region, and (IV) a miscible region.

Plots of reliability factors ($[\varepsilon''_n{}^{obs} - \varepsilon''_n{}^{cal}]/\varepsilon''_n{}^{obs}$) and half-widths of the normalized dielectric frequency dispersions against T/T_c are also classified into the same four regions as those for the shift factors. Dynamic structure of the PSt/PIs polymer blends will be discussed at the symposium.

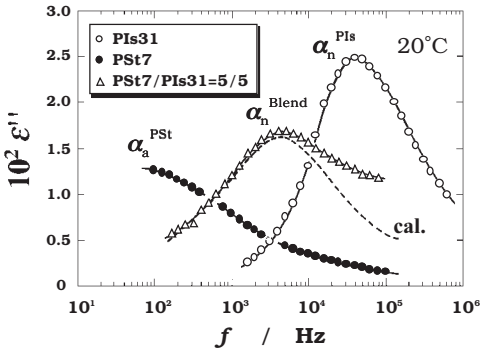

Figure 1 Frequency dependence of $\varepsilon''_n{}^{PIs}$, $\varepsilon''_a{}^{PSt}$ and $\varepsilon''_n{}^{Blend}$, and the calculated $\varepsilon''_n{}^{Blend}$ for PSt7/PIs31 = 5/5 at 20°C.

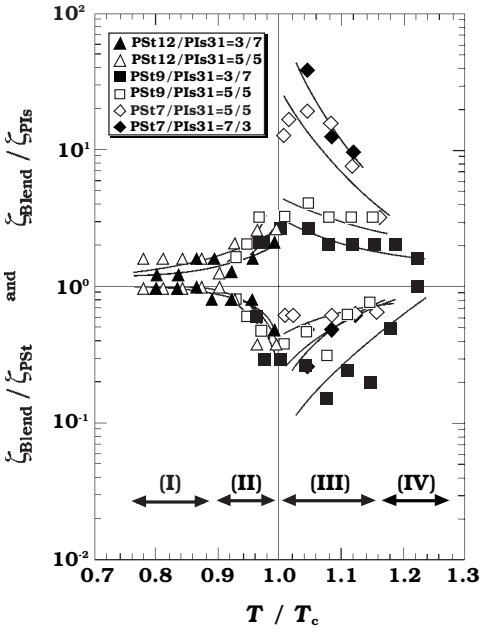

Figure 2 Plots of shift factors ($\zeta_{PSt}/\zeta_{Blend}$ and $\zeta_{PSt}/\zeta_{Blend}$) against T/T_c.

OL14

Crosslinking Points of Natural Rubber Vulcanizates

Seiichi Kawahara*, Jinta Ukawa and Yoshimasa Yamamoto
Department of Chemistry, Faculty of Engineering,
Nagaoka University of Technology, Nagaoka, Niigata 940-2188, Japan

INTRODUCTION

Crosslinking points of natural rubber vulcanizates is a principal constitutive unit that governs mechanical properties of the rubber, *i.e.* tensile strength, tear strength, and so forth; hence, it has been of importance to elucidate the crosslinking points. It may be characterized by nuclear magnetic resonance (NMR) spectroscopy, since NMR spectrum depends on a chemical environment of individual atoms. Previous works on the characterization of the crosslinking points, thus, have been made mainly by high-resolution solid-state ^{13}C-NMR spectroscopy, as natural rubber is insoluble in organic solvents after vulcanization. However, since pulse sequences applicable to the characterization were limited for the solid-state NMR spectroscopy due to high power decoupling, magic angle spinning and high speed spinning, signals appearing after vulcanization were assigned with predicted chemical shifts of plausible crosslinking points, which were estimated by empirical correlations with shift factors[1,2]. Mori and Koenig[1,2] assigned signals at 44ppm and 57ppm of the natural rubber vulcanizates to C_4 attached with mono-sulfide in *trans*-1,4 configuration and C_1 attached to mono-sulfide in *trans*-1,4 configuration, respectively, in which subscripts 1 and 4 of C atom belong to IUPAC nomenclature. In spite of the reported crosslinking points, such as the C_4 attached with mono-sulfide in *cis*-1,4 configuration and C_1 attached to mono-sulfide in *trans*-1,4 configuration, however, there is other possibility for crosslinking points, i.e. secondary and quaternary carbons. Thus, we have to distinguish positively the secondary and quaternary carbons from the reported tertiary carbon as a crosslinking point. In previous papers[3,4], we proposed high-resolution latex-state NMR spectroscopy to characterize rubber vulcanizates. Furthermore, we determined suitable conditions to obtain high-resolution spectrum through latex-state ^{13}C-NMR spectroscopy, being 10 w/w% in dry rubber content, less than 1 w/w% in surfactant concentration, T_g+70K in experimental temperature and no-spinning of sample tube. In this paper, the crosslinking points of natural rubber vulcanizates are characterized by high-resolution latex-state ^{13}C-NMR spectroscopy with various pulse sequences. The assignment of the signals appearing after vulcanization is supported with model compounds such as low molecular weight *cis*-1,4-polyisoprene by high-resolution solution-state NMR spectroscopy.

EXPERIMENTAL

Natural rubber latex used in this study was a commercial high ammonia natural rubber latex of 60 w/w % dry rubber content (DRC). Liquid *cis*-1,4-polyisoprene, whose number average molecular weight and polydispersity were 1.0×10^3 and 1.10, respectively, was a standard *cis*-1,4-polyisoprene useful for size exclusion chromatography, which is purchased from Polymer Source Inc. Vulcanization of natural rubber was made in latex stage. First, natural rubber latex (*ca.* 1,000ml) was prevulcanized with 88.5g of 20w/v% KOH solution, 17.5g of 30%S/15%ZnO suspension and 99.5g of 50 w/v% sodium di-n-butyldithiocarbamate solution at 40^{o}C for 4 hours. Second, vulcanization of the prevulcanized natural rubber latex was carried out at 90^{o}C for 1 – 72 hours, after dilution of the prevulcanized latex with water to adjust 20 w/w% DRC followed by adding 1 w/w% sodium dodecyl sulfate (SDS). The resulting vulcanized latex was filtered with 40 μm mesh followed by centrifugation at 10,000*g*. Cream fraction of the latex was re-dispersed in 1 w/w% SDS solution to make 30 w/w%DRC latex and was washed by centrifugation, again. The washed cream fraction was redispersed in 0.1 w/w% SDS solution with deuterium dioxide to make 50 w/w%DRC.

NMR measurements were carried out with a JEOL ECP-400 FT-NMR spectrometer. The vulcanized natural rubber latex with deuterium dioxide was used for the measurements without further treatment, whereas the vulcanized liquid *cis*-1,4-polyisoprene was dissolved into deuteriated chloroform without TMS. ^{1}H-NMR, ^{13}C-NMR, DEPT and APT

measurements were carried out at 323K at pulse repetition times of 7 sec and 5 sec, respectively. Two-dimensional ^{1}H-^{1}H, ^{1} H-^{13}C and heteronuclear multiple bond correlation measurements were made to collect two-dimensional hyper complex data. After weighting with shifted sine-bell function, the data was Fourier-transformed in the absolute value mode.

RESULTS and DISCUSSION

Figure 1 shows the expanded aliphatic region of the latex-state ^{13}C-NMR spectra for unvulcanized natural rubber and its vulcanizates. Two signals appeared at about 44 ppm and 58 ppm after vulcanization of the rubber latex, and their intensities depended on the vulcanization time; the longer the crosslinking time, the higher is intensity of the signals. It is possible to consider that the two signals may link to S atom, as reported by Mori and Koenig[1,2].

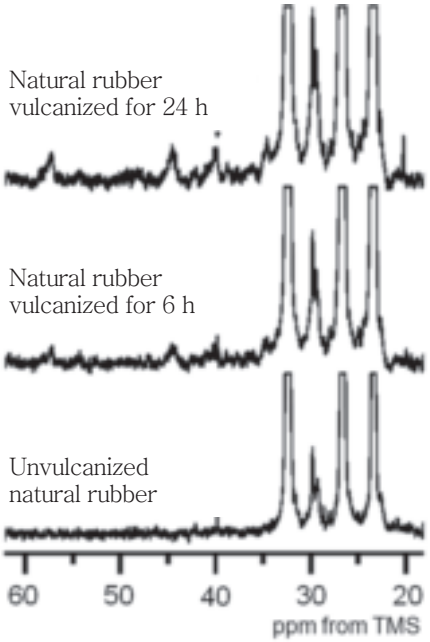

Fig.1 Aliphatic region of Latex-state ^{13}C-NMR spectra.

To assign the two signals, we applied DEPT at 135^{o} pulse (DEPT135) and APT measurements to the vulcanizates. Figure 2 shows DEPT135 and APT spectra for the vulcanizates prepared by vulcanization of natural rubber latex for 24 hours, together with complete decoupling spectrum. Signals at 24, 26 and 32 ppm characteristic of *cis*-1,4 isoprene units were shown to be upward, downward and downward in DEPT135 spectrum, while they were downward, upward and upward in APT spectrum, respectively, reflecting C5 methyl, C4 methylene and C1 methylene groups. Methylene group of fatty acids was shown to be downward signal in DEPT135 spectrum, while it was upward signal in APT spectrum. Thus, the pulse width used for DEPT135 and APT measurements were proved to be correct to assign the small signals at 44 and 58 ppm. As is clearly seen, the signal at 44 ppm was assigned to methylene group linking to S atom due to not only downward signal in DEPT135 spectrum but also upward signal in APT spectrum. In contrast, the signal at 58 ppm was assigned to methine group due to not only upward signal in DEPT135 spectrum but also downward signal in APT spectrum. Thus, in the present work, we assigned the signals at 58 ppm in ^{13}C-NMR spectrum to C1, C3, and C2 of the isoprene units linking to S atom. The signals at 44 ppm in ^{13}C-NMR spectrum were assigned to not only C5 and C1 of the isoprene units but also the secondary carbon adjacent to C1, C3, and C2 of isoprene units linking to S atom.

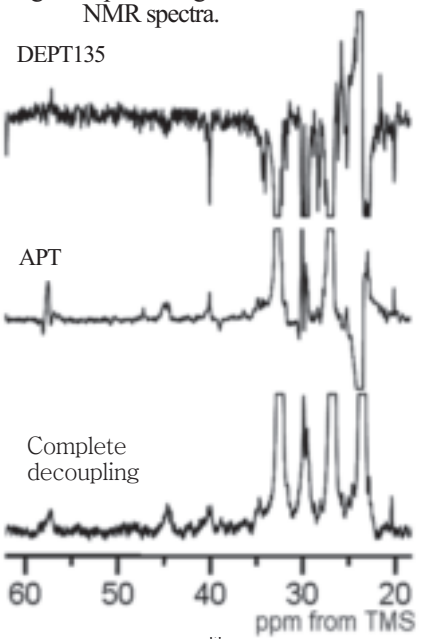

Fig.2 Latex-state ^{13}C-NMR spectra for natural rubber vulcanized for 24 h.

CONCLUSION

The crosslinking points of natural rubber vulcanizates were characterized by high-resolution latex-state ^{13}C-NMR spectroscopy. The signals at 58 ppm in ^{13}C-NMR spectrum were assigned to C1, C3, and C2 of the isoprene units linking to S atom. On the other hand, the signals at 44 ppm in ^{13}C-NMR spectrum were assigned to not only C5 and C1 of the isoprene units but also the secondary carbon adjacent to C1, C3, and C2 of isoprene units linking to S atom.

References

1 Mori, M., Koenig J. L.: Rubber Chem. Technol., 70, 671 (1997).

2 Mori, M.: Rubber Chem. Technol., 76, 1259 (2003).

3 Kawahara, S., Bushimata, S., Sugiyama, T., Hashimoto, C. and Tanaka, Y.: Rubber Chem. Technol., 72, 844 (1999).

4 Kawahara, S., Washio, K., Morita, T., Tanaka, Y., Isono, Y.: Rubber Chem. Technol., 74, 295 (2001).